AIRCRAFT ACCIDENT REPORT 2/2015

Report on the serious incident to Boeing B787-8, ET-AOP London Heathrow Airport on 12 July 2013

AIRCRAFT ACCIDENT REPORT 2/2015

Air Accidents Investigation Branch

Report on the serious incident to Boeing B787-8, ET-AOP London Heathrow Airport 12 July 2013

This investigation has been conducted in accordance with
Annex 13 to the ICAO Convention on International Civil Aviation,
EU Regulation No 996/2010 and
The Civil Aviation (Investigation of Air Accidents and Incidents) Regulations 1996.

The sole objective of the investigation of an accident or incident under these Regulations is the prevention of future accidents and incidents. It is not the purpose of such an investigation to apportion blame or liability.

Accordingly, it is inappropriate that AAIB reports should be used to assign fault or blame or determine liability, since neither the investigation nor the reporting process has been undertaken for that purpose.

© *Crown Copyright 2015*

This report contains facts which have been determined up to the time of publication. This information is published to inform the aviation industry and the public of the general circumstances of accidents and serious incidents.

Extracts may be published without specific permission providing that the source is duly acknowledged, the material is reproduced accurately and it is not used in a derogatory manner or in a misleading context.

Published 19 August 2015

Printed in the United Kingdom for the Air Accidents Investigation Branch

Department for Transport
Air Accidents Investigation Branch
Farnborough House
Berkshire Copse Road
Aldershot
Hampshire GU11 2HH

July 2015

The Right Honourable Patrick McLoughlin
Secretary of State for Transport

Dear Secretary of State

I have the honour to submit the report on the circumstances of the serious incident to Boeing B787-8, registration ET-AOP at London Heathrow Airport on 12 July 2013.

Yours sincerely

Keith Conradi
Chief Inspector of Air Accidents

© Crown Copyright 2015

Contents

© Crown Copyright 2015

© Crown Copyright 2015

Appendices

GLOSSARY OF ABBREVIATIONS USED IN THIS REPORT

^{o}C, F, K	degrees Celsius, Fahrenheit, Kelvin
ΔG	electrical energy
ΔH	enthalpy
ΔT	adiabatic temperature rise resulting from 1 Amp discharge (Kelvin)
Δt	discharge time (seconds)
A	Amp (Ampere)
AAIB	Air Accidents Investigation Branch
ACO	Aircraft Certification Office
AD	Airworthiness Directive
Ah	Ampere-hours
AIM	Aircraft Identification Module
APU	auxiliary power unit
ARC	Accelerating Rate Ccalorimeter
ARFF	Airplane Rescue Fire Fighting
AWG	American Wire Gauge
CCV	Closed Circuit Voltage
CFR	Code of Federal Regulations
CFRP	carbon-fibre reinforced polymer
cm	centimetre
CMM	Component Maintenance Manual
CNSATM	Communication, navigation and surveillance air traffic messages
CO	carbon monoxide
CO_2	carbon dioxide
Cp	specific heat capacity
CT	computed tomography
DC	direct current
dT/dt_{max}	maximum heating rate up to 80^{o}C
DTP	Destructive Test Procedure
EAFR	Enhanced Airborne Flight Recorder
EASA	European Aviation Safety Agency
ECS	Environmental Control System
ELT	Emergency Locator Transmitter
ETSO	European Technical Standard Order
FAA	Federal Aviation Administration
FAM	Flight Attendant Manual
FAR	Federal Aviation Regulation
FDS	Fire Dynamics Simulator
FHA	Functional Hazard Analysis
FMEA	Failure Mode and Effects Analysis
FTIR	Fourier transform infrared
g	gram
HCN	hydrogen cyanide
I	current
ICAO	International Civil Aviation Organisation
J	Joule
kJ	kiloJoule
kt	Knots
L	left
Li-MnO_2	Lithium-Manganese Dioxide
mA	milliAmp
mins	minutes
mm	millimetre
MOM	Multi-Operator Message
MSDS	Material Safety Data Sheet
NDT	non-destructive testing
NO_2	nitrogen dioxide
NRS	Navigation Radio System
NTSB	National Transportation Safety Board
OCV	Open Circuit Voltage
OFAR	overhead flight attendants rest
PE	Polyethylene
P_{max}	heat in Watts generated by battery
PP	Polypropylene
ppm	parts per million
P_{PTC}	Power dissipated in PTC
PTC	Positive Temperature Coefficient
QRH	Quick Reference Handbook
R	right
RFFS	Rescue and Fire Fighting Services
R_{LOAD}	load resistance
R_{PTC}	PTC resistance
RTCA	Radio Technical Commission for Aeronautics
R_{TOT}	Total circuit resistance
SB	Service Bulletin
secs	seconds
SEM	scanning electron microscope
TSO	Technical Standard Order
TTU	Through-Transmission Ultrasonic
TU	Transmitter Unit
V	Volt
W	Watt
XRD	X-ray diffraction

© Crown Copyright 2015

Aircraft Accident Report No: 2/2015 (EW/C2013/07/01)

Registered Owner and Operator: Ethiopian Airlines

Aircraft Type: Boeing B787-8

Nationality: Ethiopia

Registration: ET-AOP

Place of Accident: London Heathrow Airport

Date and Time: 12 July 2013 at 1534 hrs

Introduction

On the afternoon of Friday 12 July 2013 the Air Accidents Investigation Branch (AAIB) was notified of a ground fire in a parked and unoccupied Boeing 787-8 on Stand 592 at London Heathrow Airport. The circumstances surrounding the occurrence did not fall within the definitions of an accident or serious incident as defined in ICAO Annex 13. However, the Chief Inspector, in exercise of his powers under the Civil Aviation (Investigation of Air Accidents and Incidents) Regulations 1996, initiated an investigation, treating the occurrence as a serious incident and invoking the protocols of ICAO Annex 13 with regard to the participation of other interested States. An investigation was commenced immediately and a team of AAIB Inspectors was deployed.

The AAIB were assisted in the investigation by Accredited Representatives from the National Transportation Safety Board (NTSB) (representing the State of Design and Manufacture), the Civil Aviation Authority of Ethiopia (representing the State of Registry and the Operator) and the Transportation Safety Board of Canada (representing a State of component manufacture), with technical advisors from the Federal Aviation Administration (FAA), the operator and the aircraft and component manufacturers.

Summary

The aircraft suffered extensive heat damage in the upper portion of the aircraft's rear fuselage, in an area coincident with the location of the Emergency Locator Transmitter (ELT). The absence of any other aircraft systems in this area containing stored energy capable of initiating a fire, together with evidence from forensic examination of the ELT, led the investigation to conclude that the fire originated within the ELT.

© Crown Copyright 2015

The ground fire on ET-AOP was initiated by the uncontrolled release of stored energy from the lithium-metal battery in the ELT. It was identified early in the investigation that ELT battery wires, crossed and trapped under the battery compartment cover-plate, probably created a short-circuit current path which could allow a rapid, uncontrolled discharge of the battery. Root Cause testing performed by the aircraft and ELT manufacturers confirmed this latent fault as the most likely cause of the ELT battery fire, most probably in combination with the early depletion of a single cell.

Neither the cell-level nor battery-level safety features prevented this single-cell failure, which propagated to adjacent cells, resulting in a cascading thermal runaway, rupture of the cells and consequent release of smoke, fire and flammable electrolyte.

The trapped battery wires compromised the environmental seal between the battery cover-plate and the ELT, providing a path for flames and battery decomposition products to escape from the ELT. The flames directly impinged on the surrounding thermo-acoustic insulation blankets and on the composite aircraft structure in the immediate vicinity of the ELT. This elevated the temperature in the fuselage crown to the point where the resin in the composite material began to decompose, providing further fuel for the fire. As a result, a slow-burning fire became established in the fuselage crown and this fire continued to propagate from the ELT location, even after the energy from the battery thermal event was exhausted.

Fourteen Safety Recommendations have been made during the course of the investigation. In addition the ELT manufacturer carried out several safety actions and is redesigning the ELT unit taking into account the findings of this investigation. Boeing and the FAA have also undertaken safety actions.

The following causal factors were identified in the ground fire:

a) A thermal runaway failure of the lithium manganese dioxide battery in the ELT resulted in the uncontrolled release of stored energy within the battery cells.

b) The location and orientation of the ELT, and the compromised seal on the battery cover-plate, allowed the resulting hot gas, flames and battery decomposition products to impinge directly on the aircraft's composite fuselage structure, providing sufficient thermal energy to initiate a fire in the rear fuselage crown.

c) The resin in the composite material provided fuel for the fire, allowing a slow-burning fire to become established in the fuselage crown, which continued to propagate from the ELT location even after the energy from the battery thermal runaway was exhausted.

© Crown Copyright 2015

d) The Navigation Radio System safety assessment conducted in support of the ELT certification, did not identify any ELT battery failure modes which could represent a hazard to the aircraft, and therefore these failure modes were not mitigated in the ELT design or the B787 ELT installation.

The following factors most likely contributed to the thermal runaway of the ELT battery:

a) The trapped ELT battery wires created a short-circuit condition, providing a current path for an unplanned discharge of the ELT battery.

b) The ELT battery may have exhibited an unbalanced discharge response, resulting in the early depletion of a single cell which experienced a voltage reversal, leading to a thermal runaway failure.

c) The Positive Temperature Coefficient (PTC) protective device in the battery did not provide the level of external short-circuit protection intended in the design.

d) There was no evidence that the reset behaviour, and the implications of the variable switching point of the PTC, had been fully taken into account during the design of the ELT battery.

e) The absence of cell segregation features in the battery or ELT design meant the single-cell thermal runaway failure was able to propagate rapidly to the remaining cells.

© Crown Copyright 2015

1 Factual information

1.1 History of the event

The Boeing 787-8 aircraft landed at London Heathrow Airport at 0527 hrs on 12 July 2013 after an uneventful flight from Addis Ababa and arrived on Stand 326 at about 0540 hrs. The flight crew did not report or record any technical defects. After passenger and crew disembarkation, the aircraft was towed to Stand 592 to await its next service later that day. Before leaving the aircraft the engineer, on the flight deck, instructed the ground handling agent to remove ground electrical power. The ground handling agent accordingly turned off ground power at the stand's control box but left the power umbilical cables attached. The engineer confirmed on the flight deck that ground power was no longer available. He then secured and left the aircraft, shortly after 0730 hrs.

At approximately 1534 hrs an employee in the air traffic control tower noticed smoke emanating from the aircraft and activated the crash alarm. The Rescue and Fire Fighting Service (RFFS) arrived on scene at 1535 hrs and discharged water and foam onto the outside of the aircraft. One fire fighter removed the power umbilical cables from the aircraft as a precaution.

Fire fighters equipped with breathing apparatus entered the aircraft at 1537 hrs via the L2 door and encountered thick smoke. As they moved to the rear of the aircraft the smoke became denser so they opened further cabin doors to clear the smoke. At the rear of the passenger cabin they observed indications of fire in a gap between two overhead luggage bins. They were unable to use a hose-reel as the gap was too small and discharged a handheld 'Halon' extinguisher through the gap, about 20 minutes after entering the cabin. This was ineffective, so they removed some ceiling panels to expose the area and to get better access. At this point a small amount of flame was visible. This was extinguished with several pulses of water spray from their hose-reel, about 25 minutes after entering the cabin. A thermal-imaging camera was used to identify affected areas requiring further cooling.

1.2 Injuries to persons

Not applicable.

1.3 Damage to aircraft

The aircraft structure sustained fire damage to a section of the rear fuselage crown skin and fuselage frames. The damage extended over an area of approximately 9.5 square metres, bounded by frame nos. 1644 to 1794 and stringers 7L to 3R (Figure 1). In this area the fuselage insulation blankets had been destroyed or severely damaged. The structural damage was most severe

© Crown Copyright 2015

in the area adjacent to the location of the ELT, with significant resin loss and ply disbonding in the fuselage skin and frames. The cabin interior tie-rods in this area had sustained damage to their upper portions and the Environmental Control System (ECS) ducts in the region of the fire had been damaged.

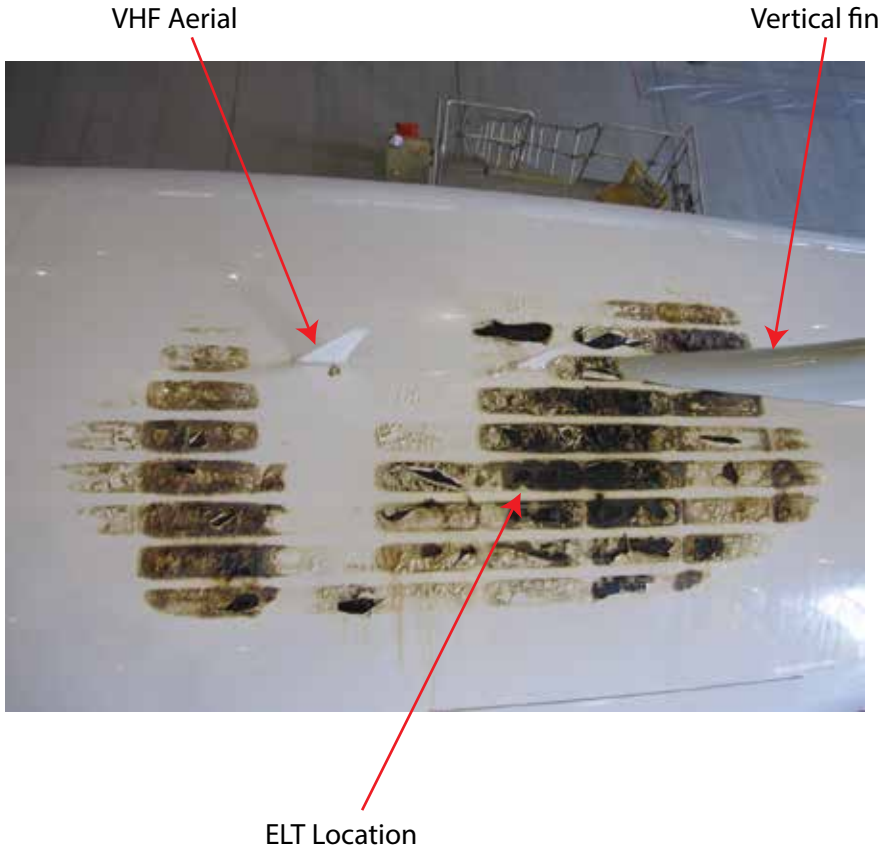

Figure 1

External view of fuselage damage

In addition to the fire damage, soot deposits were found over large areas of the crown skin. Large quantities of soot contamination were also found behind all of the rear cabin sidewall structure and in the lower fuselage, extending from the central equipment bay to the rear pressure bulkhead.

1.4 Other damage

There was no other damage.

1.5 Personnel information

The aircraft was unoccupied.

1.6 Aircraft information

1.6.1 General information

Manufacturer:	Boeing Aircraft Company
Type:	B787-8
Aircraft Serial No:	34744
Year of manufacture:	2012
Total airframe hours:	1,865 hours
Total airframe cycles:	357 flight cycles
Last Maintenance Check:	1A/2A check, 11 July 2013
Certificate of Registration No:	R-427
Certificate of Airworthiness:	A-427
Issuing Authority:	Ethiopian Civil Aviation Authority
Date of issue:	20 November 2012

1.6.2 Aircraft description

The Boeing 787 Dreamliner is a long-range twin-engine aircraft with a conventional twin-aisle layout. Approximately 50% of the aircraft's primary structure is constructed using composite materials, including the fuselage and the wings. The B787 programme was awarded Federal Aviation Administration (FAA) type certification in August 2011.

During the development of the B787, Boeing contracted with Honeywell Aerospace to design the Navigation Radio System (NRS) for the B787, which includes the Emergency Location Transmitter (ELT). Honeywell subcontract the manufacture of the ELT to Instrumar Limited.

The incident aircraft, ET-AOP, entered service on 20 November 2012. The aircraft was grounded on 16 January 2013 as part of a B787 fleet-wide grounding for modifications to the B787 main and APU batteries and returned to service on 27 April 2013. There were no defects or maintenance entries in the aircraft technical records relevant to this incident.

1.6.3 Emergency Locator Transmitter (ELT) information

An ELT is a radio location device, designed to notify rescue authorities of an aircraft's location in the event of an emergency. ET-AOP was equipped with a Honeywell RESCU 406AFN Automatic Fixed ELT, part number 1152682-2, serial number 05055.

The RESCU 406AFN system includes a transmitter unit (TU), an external fuselage-mounted antenna, a flight deck remote control panel with a three-position 'ON/ARMED/RESET' switch, a DIP switch containing the aircraft's

© Crown Copyright 2015

unique identification address, an Aircraft Identification Module (AIM) which programmes the TU with data stored in the DIP switch and associated system wiring.

The RESCU 406AFN ELT can be activated automatically by an internal acceleration sensor, manually by the flight crew, or via a three-position 'TX/OFF/ARM' toggle-switch on the transmitter unit. Once activated it transmits three emergency signals, which include digitally encoded bursts of data on 406.028 MHz and continuous analogue signals on 121.5 and 243 MHz. When transmitting, the typical current load of the ELT is comprised of a 0.11 Amp (A) continuous current and 2.0A pulses of 0.5 seconds duration (averaging 0.02A continuous). Unless activated, the ELT operates in 'ARMED' mode, with a current draw of less than 1 microamp.

On the B787 the ELT transmitter unit is installed in the aft fuselage crown above the passenger cabin ceiling. It is mounted on a composite 'intercostal' bracket, or mounting plate, suspended between two fuselage frames (Figure 2). With the exception of its inboard face, the ELT is surrounded by thermo-acoustic insulation blankets (Figure 3).

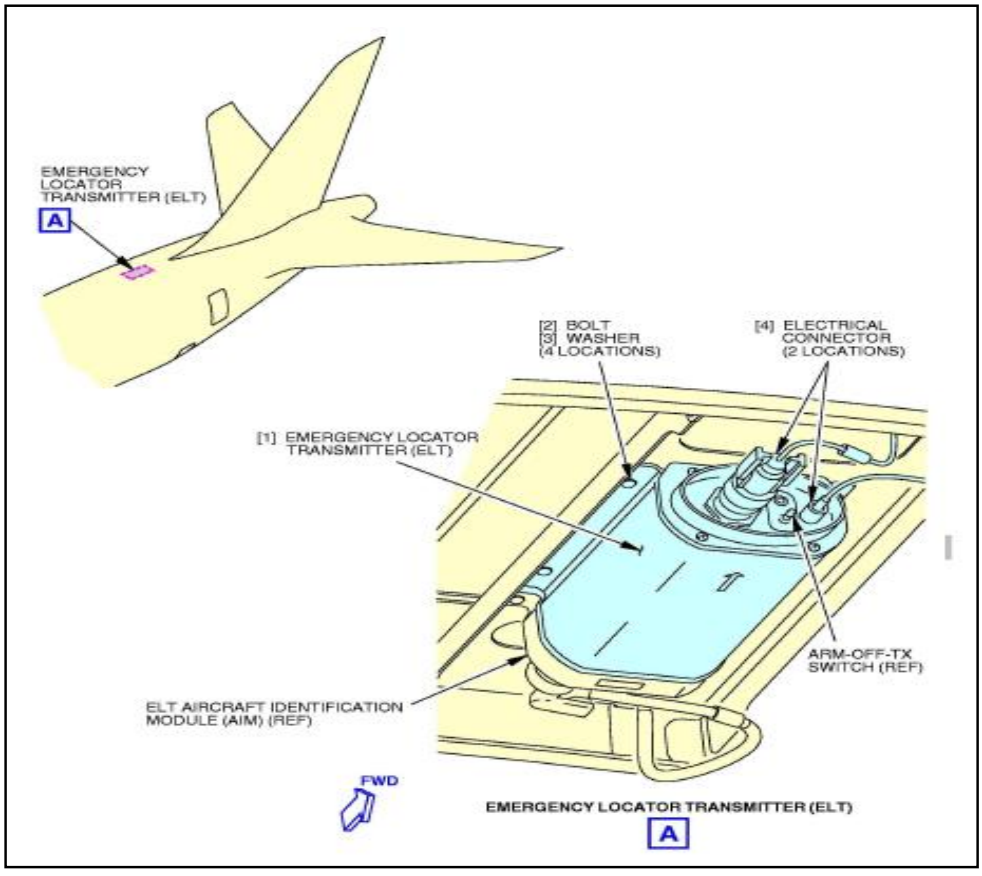

Figure 2

ELT location on B787

Figure 3

ELT installation on B787

1.6.4 ELT battery information

1.6.4.1 General

The ELT is powered by a non-rechargeable 'lithium-metal'[1] battery, comprised of five Lithium-Manganese Dioxide (Li-MnO_2) 'D-cells'[2] and installed in the transmitter unit (Figure 4). The ELT battery, part number S00130, was developed, designed and manufactured by Ultralife Corporation of Newark, New York, under contract to Instrumar Limited. The battery involved in this incident was assembled in November 2010 using five cells, part number UBI-3356, from the same lot produced in June 2010. The battery was delivered to Instrumar Ltd in November 2010 and installed in ELT serial number 05055, which was shipped to Boeing in April 2011.

The design of this battery is unique to the Honeywell RESCU 406AF and 406AFN ELTs, although the constituent cells are used in a number of other applications. Each cell has a nominal voltage of 3V, although this is typically closer to 3.3V. The five cells are connected in series to provide a battery pack with a nominal Open Circuit Voltage[3] (OCV) of 16.5V. The battery is rated to a maximum continuous discharge current of 3.3A, and has a capacity of 11.1 ampere-hours (Ah). The operating temperature range of the cells is -40°C to 72°C. Two wires, terminated in a plastic connector, allow connection of the battery to the ELT. The battery has a design life of 12 ½ years and a service life of 10 years.

1 A battery is a stored energy device consisting of one or more electrochemical cells that convert chemical energy into electrical energy. A 'lithium-metal' battery, also known as a 'lithium-primary' battery, is a non-rechargeable battery in which the anode is made from a layer of metallic lithium.

2 A 'D-cell' is a cylindrical cell with a nominal diameter of 33.2 mm and a length of 61.5 mm.

3 Open Circuit Voltage is the difference in electrical potential between the positive and negative terminals of a cell or battery when it is disconnected from any electrical circuit.

© Crown Copyright 2015

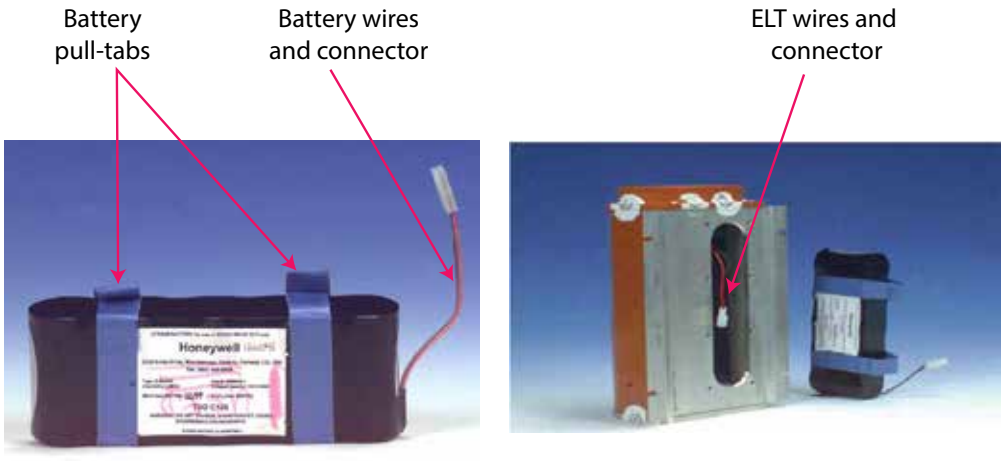

Figure 4

ELT battery pack and ELT transmitter unit, showing battery compartment

1.6.4.2 Battery pack construction

Figure 5 shows the design of the ELT battery. The cells are numbered 1 to 5, from the most positive to the most negative. Nickel tabs welded between the positive terminal of one cell and the negative header of the adjacent cell, provide the series connection. The positive wire is connected to Cell 1 and the negative wire, which also incorporates a Positive Temperature Coefficient (PTC)

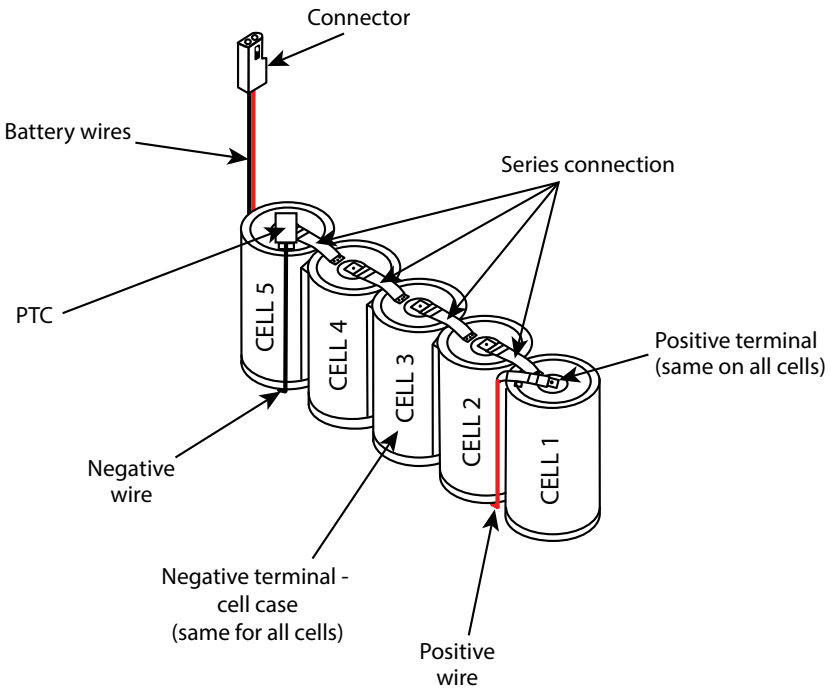

Figure 5

Battery pack illustration
(outer shrink-wrap and insulation omitted for clarity)

protective device, to Cell 5. The wires consist of multi-strand copper wire, coated in silver and covered in PTFE[4] insulation. Hot-melt glue provides mechanical attachment of the cells. Cardboard insulator strips and foam padding, profiled to the shape of the cells, provide electrical insulation and protect the tops and bottoms of the cells, while an outer film of shrink-wrap provides mechanical support, environmental protection and electrical insulation.

1.6.4.3 Positive Temperature Coefficient (PTC) protective device

The RESCU 406AF/AFN ELT battery circuit contains a single polymeric PTC device, part number LR4-380F, manufactured by the TE Circuit Protection business unit of TE Connectivity Ltd. The PTC is a resettable temperature-sensing device intended to protect the battery from excessive current caused by 'external short-circuit'[5] conditions. In normal operation the PTC has a very low resistance. However if the temperature exceeds the device's switching temperature, either as a result of high current through the device or an increase in ambient temperature, the PTC will 'trip', transitioning to a high-resistance state. This increased resistance protects the battery circuit by substantially reducing the amount of current that can flow to a steady-state 'leakage current.'

The PTC consists of two nickel tabs and a semi-crystalline polymer core which contains conductive particles. At normal temperature the conductive particles form low-resistance networks in the polymer. However, above the switching temperature, the crystallites in the polymer melt and become amorphous. As the crystallites melt the PTC swells, causing the conductive particles to separate. This results in a large non-linear increase in the electrical resistance of the device.

The PTC will latch in the tripped (high-resistance) state until the fault is removed or the power to the circuit is removed. The device can then cool and recrystallize, returning to a low-resistance state. The full specification for the PTC is shown in Appendix A, however some of the key electrical characteristics are presented in Table 1.

[4] Polytetrafluoroethylene.

[5] An 'external short-circuit' is a short-circuit which occurs outside the battery cells, for example in the battery wiring or the circuit to which it is connected.

Parameter	Description	Nominal value for LR4 380F PTC
Holding current I_H @20°C	The maximum current the device can sustain without tripping.	3.8A
Trip current I_T @20°C	The minimum current at which the device will trip.	8.3A
Switching temperature	Temperature at which the device will transition from the low resistance state to the high resistance state.	125°C
Maximum operating voltage V_{MAX}	The maximum voltage the device can withstand without damage at the rated current.	15Vdc
Maximum operating current I_{MAX}	The maximum fault current the device can withstand without damage at the rated voltage.	100A
Power dissipated P_D @20°C	The power dissipated by the device when in the tripped state	2.5 W

Table 1

Electrical characteristics of LR4-380F PTC,
based on data from manufacturer's specification

The rated hold and trip currents for the PTC are specified in still air at 20°C, however, as it is a thermally activated device, any change in ambient temperature will affect the performance of the PTC. As the ambient temperature increases, less energy is required to trip the device and therefore the hold current and time-to-trip will reduce. Figure 6 has been created from the thermal de-rating curves in the manufacturer's specification, to show how the hold and trip currents vary with ambient temperature.

© Crown Copyright 2015

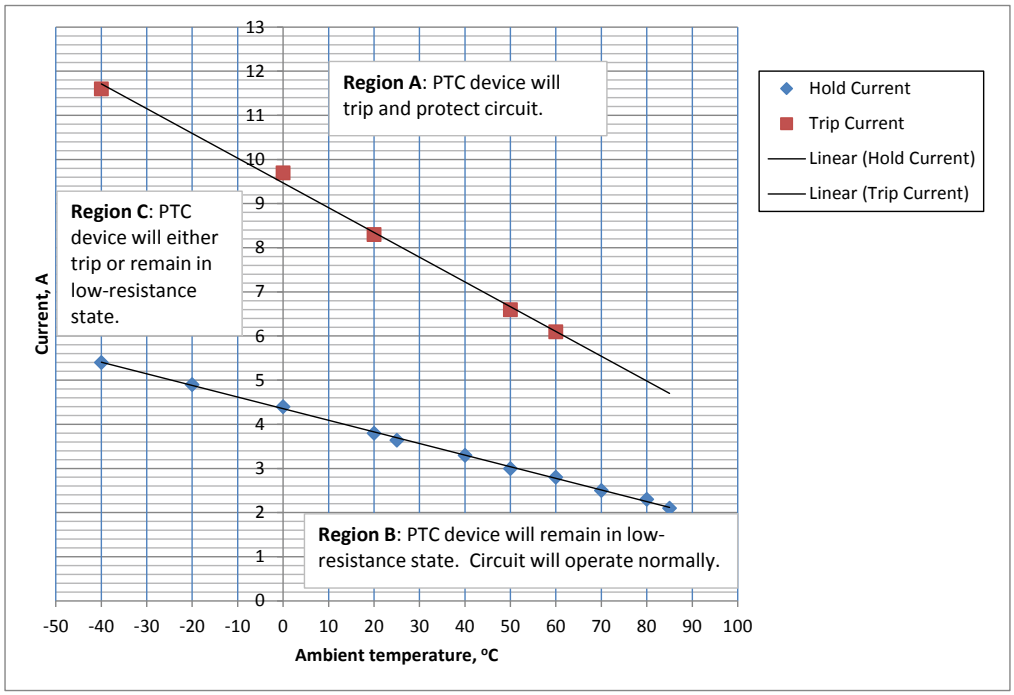

Figure 6

Effect of temperature on Hold / Trip current for LR4-380F PTC, based on data from manufacturer's specification

1.6.4.4 Cell construction

Each of the Li-MnO_2 cells contains a 'jelly roll' electrode winding comprised of a metallic lithium anode (negative electrode), a manganese-dioxide cathode (positive electrode) and two layers of separator membrane (Figure 7).

The anode, which provides the 'fuel' for the electrochemical reaction, is a layer of extruded lithium metal[6] foil. A copper strip embedded along its length acts as a current collector and ensures all of the lithium is evenly consumed during discharge. The anode tab is a nickel strip that is welded to the end of the anode during the winding process, and then welded to the rim of the negative cell can.

The cathode material[7] is 'calendared' onto an aluminium mesh, and rolled to form a solid strip. The aluminium mesh acts as current collector for the cathode; an aluminium tab welded to the mesh at the centre of the strip, acts as the cathode tab, joining the current collector to the positive terminal of the cell.

6 Lithium metal is highly reactive and flammable.

7 The cathode material is made from a mixture of heat-treated MnO_2, 'carbon black' and a liquid Teflon suspension which is mixed into a paste.

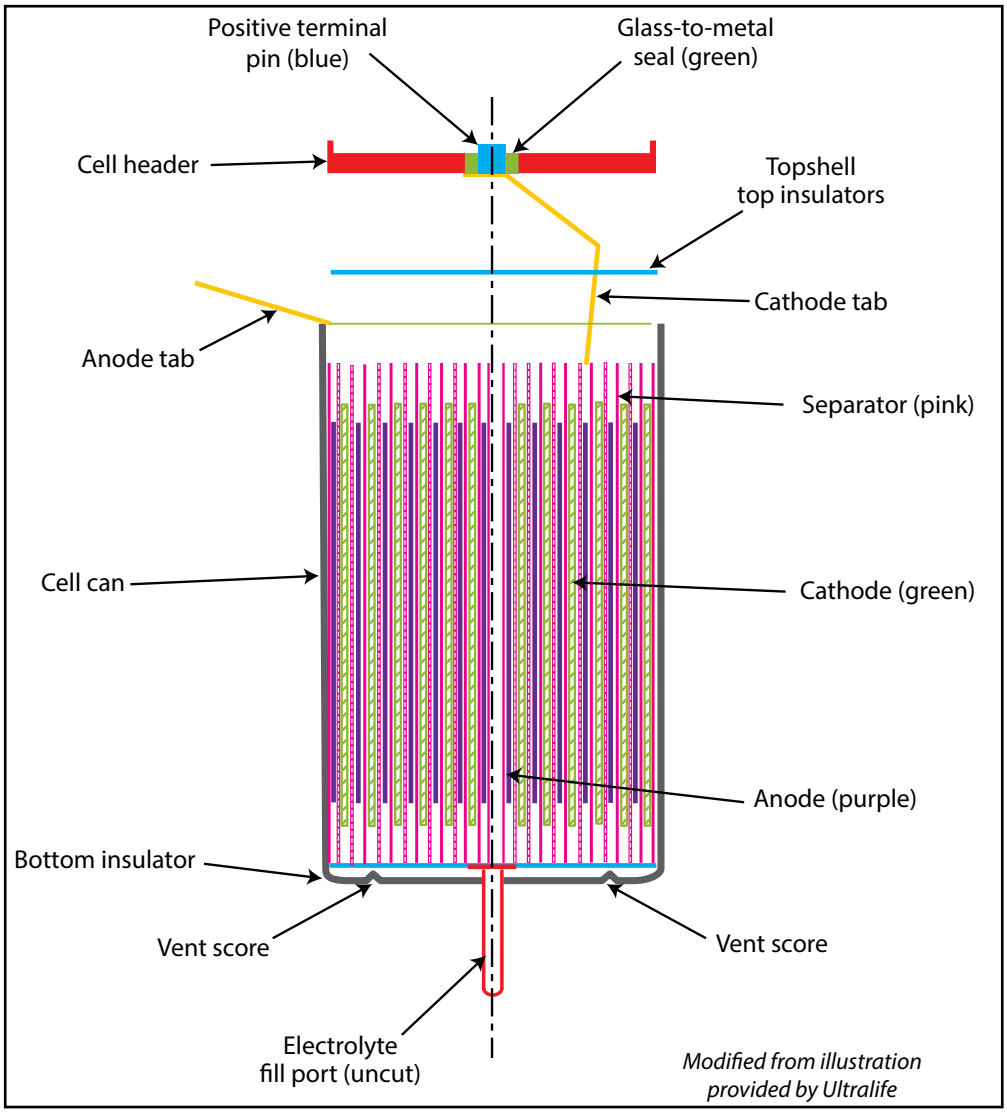

Figure 7

Cell construction – cross-section through a Li-MnO_2 spiral-wound cell

Liquid electrolyte[8] provides electrical connection between the electrodes by allowing the transport of ions between the anode and the cathode.

The cell can is made from nickel-plated cold-rolled steel, and acts as the negative terminal of the cell. The base of the cell contains two scored safety vents, designed to rupture if the cell pressure exceeds 350 – 500 psi, which may occur if the cell temperature exceeds 140 - 150°C. A molybdenum pin centred on the top of the cell forms the positive terminal and is insulated from the rest of the cell case by a glass-to-metal seal.

[8] The electrolyte is a mix of propylene carbonate, tetrahydrofuran and dimethoxymethane solvents and a lithium perchlorate salt. The electrolyte is flammable.

© Crown Copyright 2015

1.6.4.5 Cell separator

The cell separator is a tri-layer micro-porous polymeric membrane consisting of a Polyethylene (PE) layer, sandwiched between two Polypropylene (PP) layers. It provides physical separation between the cathode and anode and between the cathode and cell can. During normal cell operation, the micro-porous structure of the separator allows ions to flow between the electrodes.

However, in the case of excessive cell temperatures above 132°C, the PE inner layer will melt and clog the pores in the PP layers. This leads to a substantial reduction in the flow of ions between the electrodes and a corresponding increase in the cell's electrical resistance. Reducing the flow of ions in this manner causes the electrochemical reactions in the cell to shut down, and allows the cell to cool.

If the cell temperature exceeds 160°C (the melting temperature of the outer PP layers), the separator will start to shrink and melt, losing its ability to insulate the electrodes and protect the cell from an 'internal short-circuit'[9].

1.6.5 Aircraft structure

The B787 fuselage primary structure is manufactured primarily from laminated carbon fibre reinforced polymer (CFRP). The fuselage is comprised of six semi-monocoque barrel sections, which are produced as one-piece assemblies. These include CFRP stringers, which are co-cured on the interior surface of the fuselage sections during production. Mechanically fastened CFRP frames secured to the fuselage sections by shear ties provide additional load-carrying capability. These frames and shear ties are designed with cut-outs to allow them to be fitted over the integral stringers. One of the advantages of using CFRP in aircraft structure is that the strength of a continuous component or panel can be 'tailored' to carry the required loads. This usually takes the form of variations to the number of plies or layers within the structure, changes in the orientation of the ply direction and the use of different ply 'weaves'. The fuselage loads in the region of the ELT are such that the fuselage skin in this region is thinner than in other areas of the crown skin.

The ELT is mounted on a CFRP mounting plate between adjacent fuselage frames 1719 and 1744, in the upper rear fuselage, to the left of the aircraft centreline.

[9] An 'internal short-circuit' is a short-circuit which occurs inside a cell, if the positive and negative electrodes come into contact. An internal short-circuit can occur if the integrity of the cell separator is compromised by physical or thermal abuse or by a manufacturing defect. An internal short-circuit may result in an uncontrolled high-rate discharge of the cell.

© Crown Copyright 2015

Thermal and acoustic insulation

Acoustic dampers are bonded to the fuselage skin in each 'bay' formed by the stringers and frames. These consist of a sandwich-type structure made up of an inner and an outer carbon fibre tile bonded to a sound-absorbing polymer filler.

The cabin ceiling fittings, baggage bins and other items are secured by CFRP and metal tie-rods which attach to nodal brackets on the upper sections of the frames and shear ties.

To minimise heat loss from the fuselage and to suppress noise, two layers of thermal insulation blankets are fitted. These consist of a glass-fibre 'batting' material enclosed in a fire retardant polymer envelope. The first layer is a 'bay blanket' which is a thick blanket approximately 2 feet wide, and is installed in the bays formed by adjacent frames. The second layer consists of a thinner 'over-blanket', approximately 4 feet wide, which is installed over the frames and covers two bay blankets and a central frame. The edges of the over-blankets are lapped to form a continuous layer of insulation over the frames. The over-blankets are shaped to allow them to fit tightly around the ends of the cabin tie-rods where they attach to the frames. There is a cut-out in the over-blanket to allow access to the ELT.

1.6.6 Cabin environment

The B787 maintains, by design, a higher humidity level in the cabin environment than previous aircraft types. As in other pressurised aircraft, in-flight condensation may collect in the fuselage crown and side walls, behind the thermo-acoustic insulation blankets.

1.7 Meteorological information

When ET-AOP landed at 0527 hrs the weather was CAVOK with a light wind from 040-050°, varying between 340° and 070°, at 5 kt. The temperature was 12°C.

While the aircraft was parked on Stand 592 the weather was predominately CAVOK and the wind remained light, generally from the north-east. At the time the fire was first noticed, at 1533 hrs, the wind was from 050° varying between 280° and 090° at 4 kt and the temperature was 25°C.

1.8 Aids to navigation

Not applicable; the aircraft was parked.

1.9 Communications

Not applicable; the aircraft was parked and unoccupied.

1.10 Aerodrome information

Not applicable.

1.11 Flight recorders

The aircraft was fitted with two Enhanced Airborne Flight Recorders (EAFR) which recorded flight data, audio data and communication, navigation and surveillance air traffic management (CNSATM) messages. Both recorders were attached to the fuselage structure in the ceiling area, one at the front of the aircraft and one at the rear.

Both recorders were recovered and successfully downloaded at the AAIB. The rear EAFR was positioned such that there was some sooting on the outer casing from the fire.

Each EAFR independently recorded the same parameter-set and ceased recording flight data at 05:51:09 hrs, ten minutes after engine shutdown, as designed. There were no ELT parameters recorded. The front and rear recorders received electrical power from the aircraft left and right 28V DC buses respectively. This electrical power supply to both recorders ceased at 07:36:22 hrs, coincident with the routine APU shutdown, or removal of ground power.

© Crown Copyright 2015

1.12 Aircraft examination

1.12.1 Initial aircraft examination

After removal of the aisle ceiling panels, a visual examination of the interior of the rear fuselage crown skin was carried out. All the bay blankets and over-blankets between frames 1644 and 1794, and stringers 2R and 7L, had been severely damaged or destroyed (Figure 8). The remaining blankets between frames 1605 and 1835 showed varying degrees of thermal exposure and damage but had remained attached to the crown skin.

Insulation blankets

There was evidence of the remains of several insulation blanket envelopes on the upper surface of a number of cabin baggage bins.

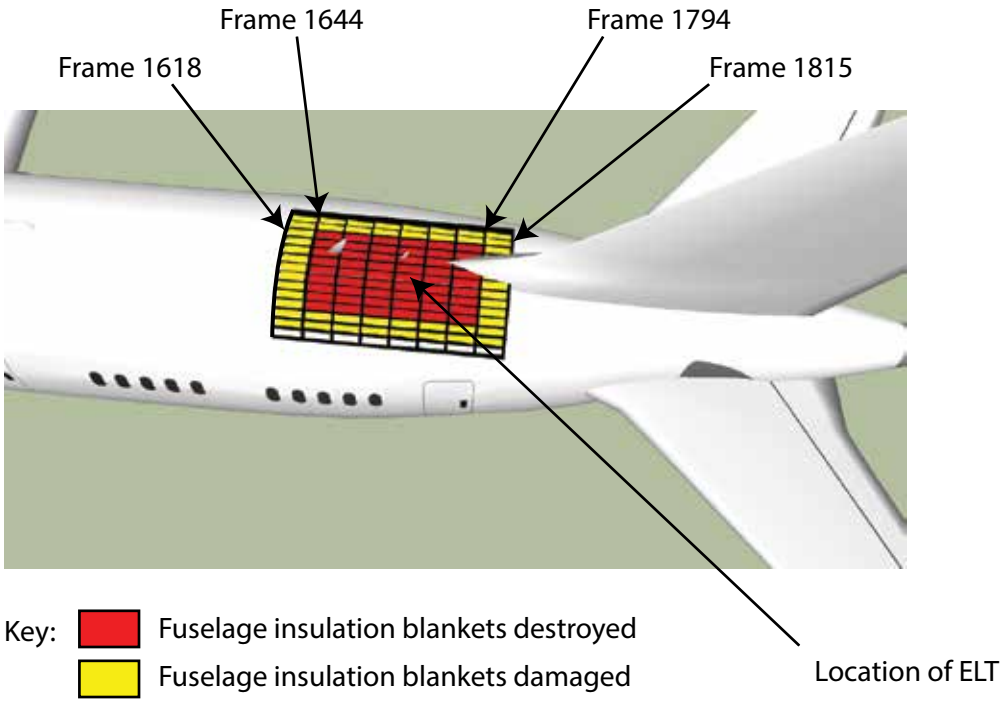

Figure 8

Fuselage frame diagram

Structural damage

The ELT, its mounting plate and sections of the frames to which it was attached, had suffered severe thermal damage. The ELT forward frame attachment point had failed and the ELT was supported only by its rear attachment point and the coaxial cable (Figure 9).

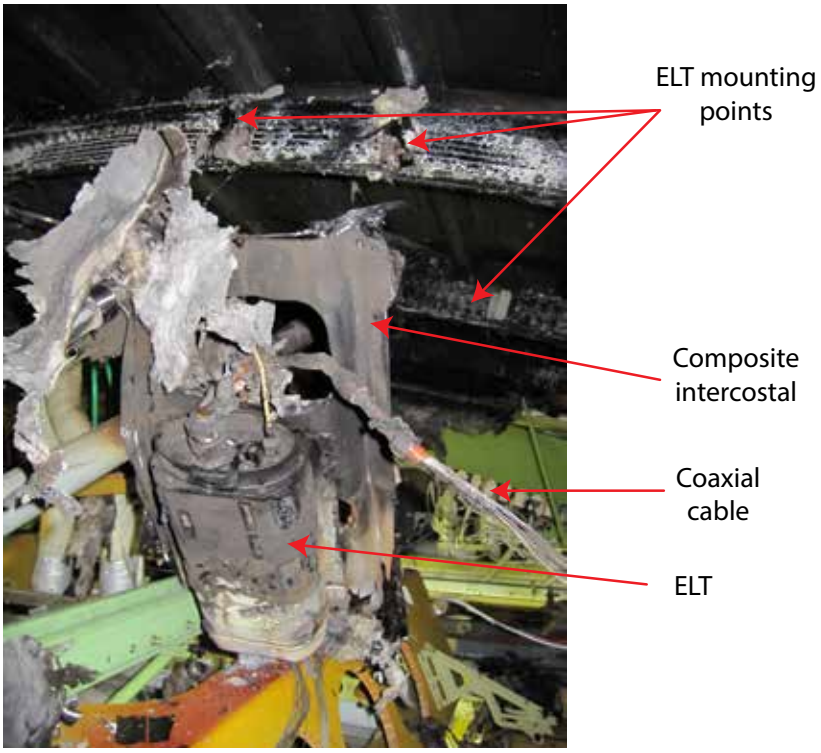

Figure 9

ELT and ELT mounting plate, view on forward end, looking aft

Fire damage was found on the interior of the fuselage skin between stringers 4R and 7L, which extended forward to frame 1618 and rearwards to frame 1815. This damage appeared more severe in the region of the ELT mounting structure. The external fuselage skin showed clear evidence of heat damage in the location of the ELT and its surrounding area (Figure 10). Despite the degree of damage observed, the fuselage skin had not been breached by the fire.

The cabin interior tie-rods had been damaged in this region. The damage was generally restricted to the portions of the rods within 12 cm of the damaged fuselage crown skin. The cabin environmental control system (ECS) ducts in the rear crown skin area had also been damaged. There was no evidence that the fire had progressed to any other area of the fuselage.

© Crown Copyright 2015

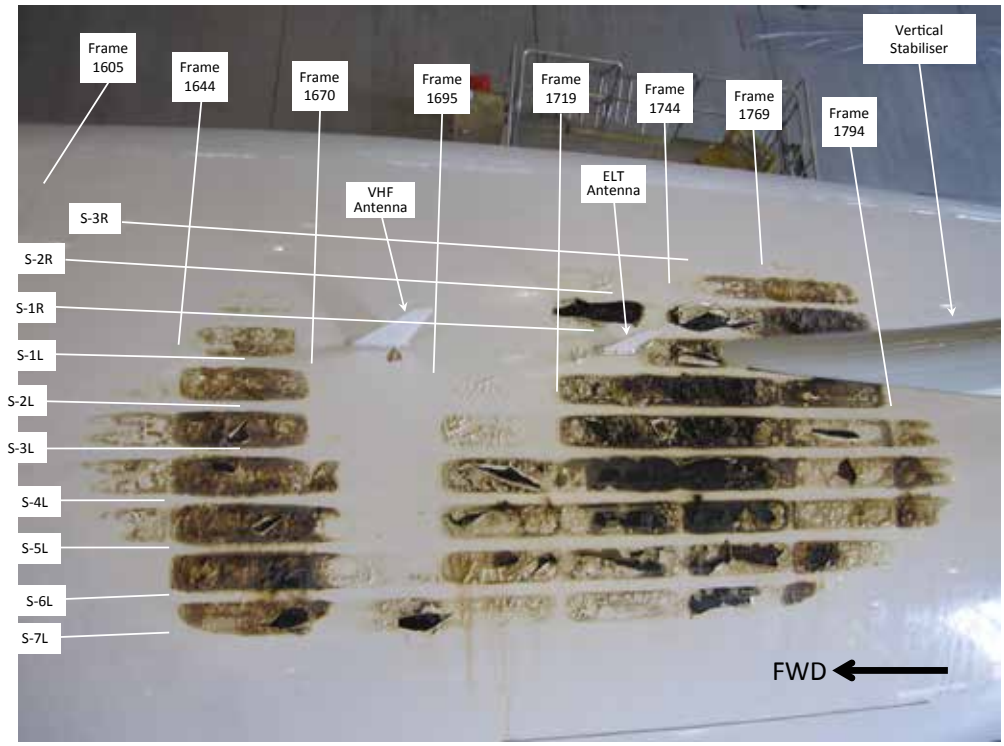

Figure 10

Photograph of external skin damage with frame and stringer numbers super-imposed

Soot contamination

Removal of the cabin sidewalls confirmed that soot had been deposited behind the cabin sidewalls from the rear of the cabin to a position just forward of the wing root. Removal of the rear freight bay interior showed heavy soot deposits on all surfaces. The central equipment bay was also heavily contaminated with soot.

1.12.2 Aircraft structural examination

1.12.2.1 Initial examination

A visual inspection of the aircraft structure was carried out after removal of the remains of the thermal insulation blankets. This identified an area bounded by stringers 2R and 7L, and frames 1644 and 1794, which had suffered significant fire damage. All the acoustic dampers in this area had been destroyed. The ECS duct and cabin tie-rods in this area also exhibited the most severe damage.

Varying levels of damage were observed to the skin and frames beyond this area extending from stringer 8R to 9L and between frames 1605 and 1836. Generally

© Crown Copyright 2015

the damage appeared to become less severe the greater the distance from the ELT. The damage to the acoustic dampers in this area also varied. Those dampers closest to the outer edges of the damaged zone had lost the outer carbon tile, exposing the polymeric damper material. The damage, particularly the distortion and charring of the polymeric material, increased the closer they were to the severely damaged zone, resulting in the complete destruction of the polymeric material.

The frames and skin in the most damaged section had suffered a large degree of resin loss with the carbon fibre layers visible. This was particularly apparent on fuselage frames 1719 and 1744 close to the ELT, where the plies on the frame edges had begun to separate.

The ELT was removed from the aircraft for examination, together with its mounting plate and the sections of frames 1719 and 1744 to which it was attached. When the mounting plate was separated from the ELT it was found to have suffered almost total resin loss, with all the carbon fibre laminations separating readily (Figure 11). Both frame sections had also suffered from resin loss but remained substantially intact.

Figure 11

ELT composite mounting plate

The ELT mounting plate was examined in a laboratory to assess the temperature to which it had been exposed and the duration of the exposure. However, the loss of resin within the structure was almost total and no estimation could be

made. Examination of the CFRP plies in a scanning electron microscope (SEM) identified numerous areas where material associated with lithium manganese dioxide batteries had penetrated the plies following their separation after heating.

1.12.2.2 Detailed examination

An ultrasonic survey of the external surface was carried out by a team of Boeing engineers at London Heathrow to identify the extent of the damage to the rear fuselage crown. The ultrasonic survey identified areas of skin which had voids present or showed evidence of disbonding. The survey results were combined with the visual inspection of the interior surface of the crown skin to produce a plot of the extent of the skin damage (Figure 12).

During the course of the aircraft repair, a large section of the rear crown skin was replaced, together with all the damaged frame sections. This included all the areas identified as being damaged or discoloured in Figure 12. To facilitate removal the damaged section was cut into six pieces which, together with the damaged frame sections and the remains of the insulation blankets, were transported to the AAIB headquarters for further investigation.

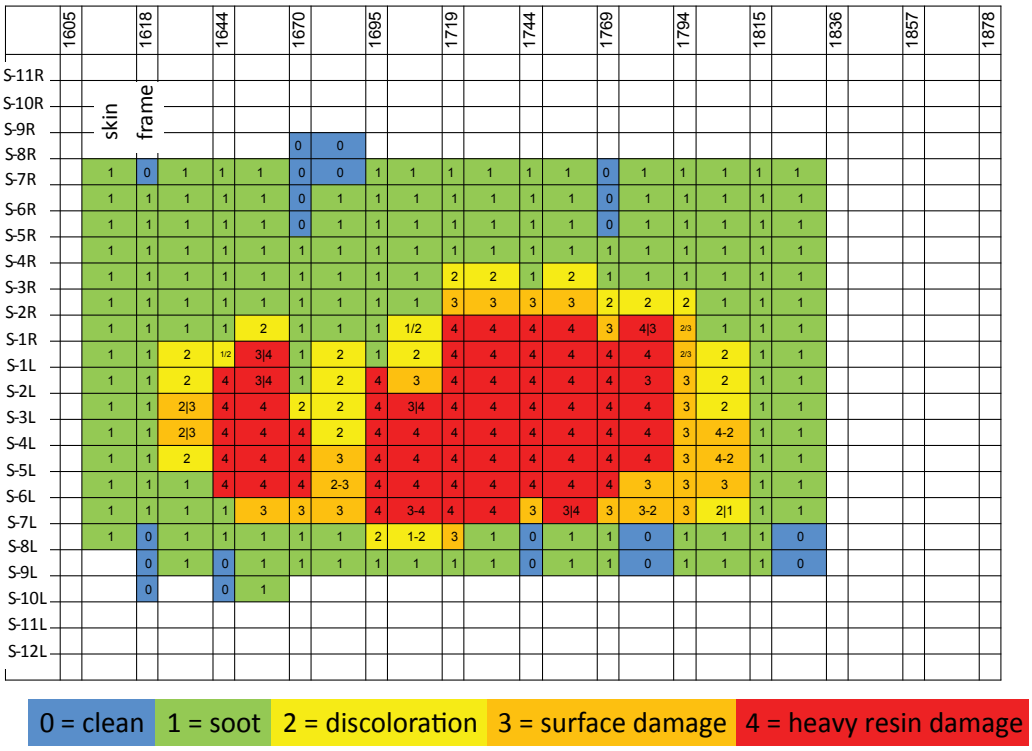

Figure 12

Plot of interior skin damage (viewed from above)

Examination of the removed skin confirmed that the areas showing large amounts of resin damage had lost a significant amount of rigidity and the exposed layers of carbon fibres readily separated. The frames exhibited varying degrees of damage. There was evidence of significant loss of resin to frames 1719, 1744 and 1769 between stringers 2R and 6L which resulted in a loss of rigidity in the affected areas. Additionally, the carbon fibre layers had begun to separate at the edges of the frame (Figure 13).

The sections of frame 1719 and 1744, which had been removed with the ELT mounting plate, were subject to laboratory analysis, to determine the temperature to which they had been exposed. The examination confirmed that all the resin had been lost from the frame sections closest to the ELT and that significant resin loss had occurred in the surrounding sections of the frame. However, it was not possible to determine the maximum temperature or duration of heat exposure.

Figure 13

Damage to frame 1719 in the region of the ELT mounting plate (looking aft)

1.12.3 Examination of the ELT

1.12.3.1 Initial examination

Initial examination of the ELT, after removal from the aircraft, showed that the ELT case was badly heat damaged and all of the orange paint had burnt off. Heavy sooting and carbon deposits were evident on the forward two-thirds of the ELT TU. There was no sooting on the rear third of the TU or the AIM, indicating that temperatures on this portion of the ELT had been sufficiently high to burn off the soot deposits (Figure 14). A small gap was evident between the AIM and TU.

© Crown Copyright 2015

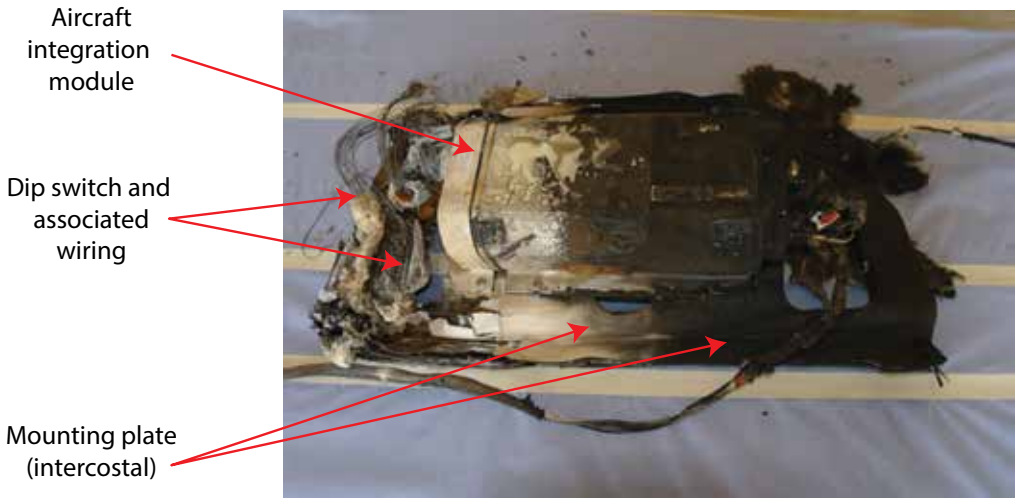

Figure 14

View of lower surface of ELT after removal from the aircraft

1.12.3.2 Computed tomography (CT) examination of ELT

The AAIB conducted a computed tomography (CT) examination to document the internal configuration of the ELT and its battery before disassembly. The forward and rear halves of the ELT were scanned separately, due to its size. The images produced from the CT scans were examined for evidence of missing or damaged components, foreign objects or other anomalies.

The CT images of the ELT showed large breaches in the cell walls of Cells 1 and 2, on the outboard side, and ruptures in the base of Cells 1, 3, 4 and 5. The CT scans also showed that the positive terminal pins on all five cells had been displaced from the cell headers, and that there was a substantial amount of debris in the ELT battery compartment. Significantly, as shown in Figure 15, the ELT battery wires appeared to be crossed and flattened, adjacent to one of the fasteners for the battery cover-plate. The scans also showed that this fastener was not fully inserted in its fastener hole.

© Crown Copyright 2015

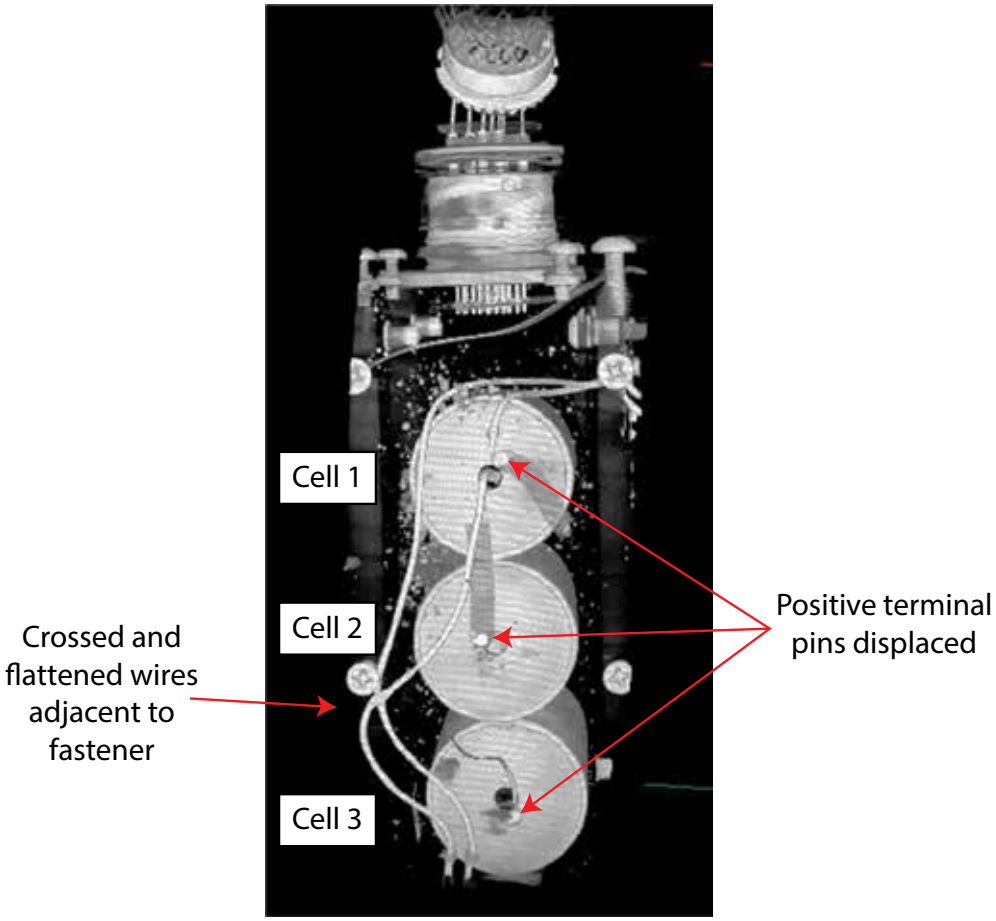

Figure 15

CT image showing top-down view of ELT battery cells 1 to 3

1.12.2.3 Removal of ELT battery

Further examination of the ELT was conducted at the AAIB facilities. The upper surface of the ELT (in the installed orientation) and the battery cover-plate were covered in combustion products and deposited material. In particular, there was a distinct brown deposit matching the shape and position of the lightening hole in the ELT mounting plate.

The battery cover-plate was bulged in one location. On removing the cover-plate it was evident that the ELT battery wires were crossed and trapped under the cover-plate in this location (Figures 16 and 17). The battery had experienced severe disruption, exhibiting evidence of a high-energy thermal event, consistent with the cell's having experienced a thermal runaway[10].

[10] In the case of lithium batteries, the term 'thermal runaway' refers to a self-sustaining, uncontrollable increase in temperature and pressure. It is an exothermic reaction, releasing more heat energy during the reaction than was absorbed to initiate and maintain the reaction. Thermal runaway can culminate in a cell exhibiting violent venting of toxic or flammable gases or electrolyte, decomposition, fire and explosion. The heat released by the affected cell can also heat adjacent cells, such that the failure propagates to other cells in the battery.

© Crown Copyright 2015

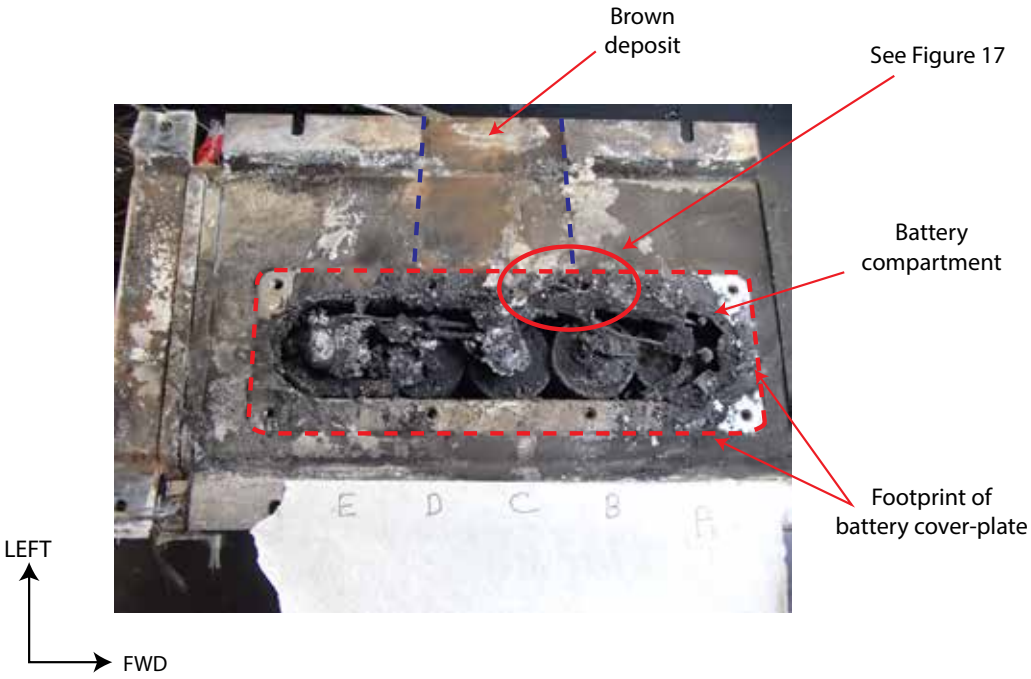

Figure 16

Upper surface of ELT with battery cover-plate removed; tops of battery cells visible

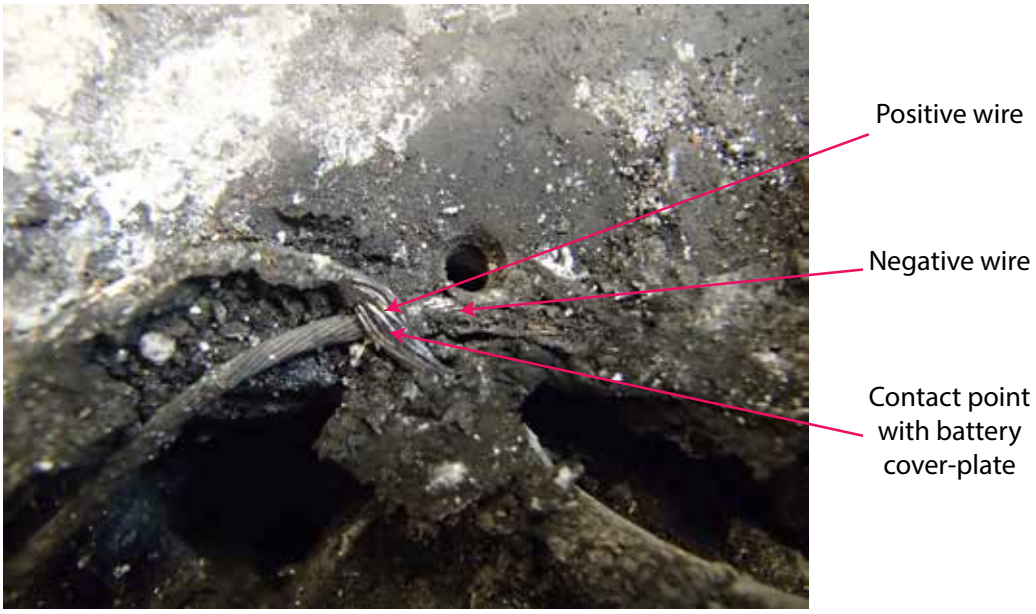

Figure 17

Zoomed-in view of crossed ELT battery wires, identified in Figure 16

The presence of charred, encrusted debris above the battery, around the battery wires and under the footprint of the cover-plate, was consistent with ejected battery decomposition products. The foam gasket which normally sits between the cover-plate and ELT case, was absent, most likely having been consumed in the fire. It was therefore not possible to determine the pre-incident condition of the gasket at the location of the trapped wires.

Upon removal of the battery it was confirmed that all five cell cases had been breached and battery material had been ejected into the battery compartment. The cells were burnt and blackened and encrusted in charred debris (Figure 18). The remains of the PTC were evident on the negative wire, where it normally terminates on the Cell 5 header, but due to thermal damage it was not possible to determine its pre-incident condition or electrical connection.

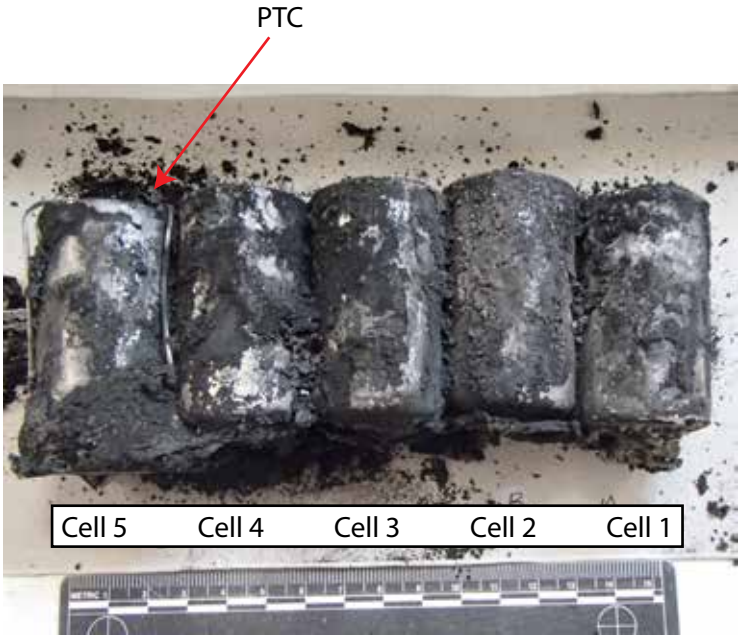

Figure 18

View on inboard side of ELT battery, immediately after removal from ELT

1.12.3.4 Detailed teardown examination of ELT

A teardown examination of the ELT was undertaken at a Honeywell facility in Phoenix, Arizona, under AAIB direction. The AIM module and connector were removed. Both of these exhibited significant heat distress and evidence that hot gas had exited the ELT through the AIM.

The upper surface of the ELT case was cut out to allow access to the ELT and to preserve fragile evidence at the location of the trapped wires. Inside the ELT there was extensive evidence of heat damage and sooting.

© Crown Copyright 2015

The three printed circuit cards from the ELT were examined and CT-scanned. They had suffered severe thermal damage and had been exposed to temperatures hot enough to cause the solder to re-flow and many components to become detached from the cards. No pre-existing conditions were identified with the circuit cards and there was no evidence that the thermal event had originated at the circuit cards.

The battery cover-plate was CT-scanned and the resulting imagery was compared with a digital model of the cover-plate. This confirmed that it had sustained permanent deformation during the event, consistent with the observed bulging.

1.12.3.5 Forensic examination

General

A section from the upper surface of the ELT case, the battery cover-plate, the battery compartment walls and the battery wires were subject to detailed forensic analysis at QinetiQ facilities, in Farnborough, UK. This included visual and optical microscope examination, analysis of the components in a scanning electron microscope (SEM) and the use of Fourier transform infrared (FTIR), x-ray diffraction (XRD) and energy dispersive x-ray spectroscopy techniques to identify and characterise material and deposits on the component.

Fragments of attached debris along the wire path, on both the cover-plate and the ELT case, exhibited imprints from wire strands and were consistent with the wire insulation material.

Deposits on the cover-plate and the ELT case were determined to be rich in manganese oxide, chlorine, bromine and aluminium oxide, consistent with ejected battery material and corrosion product. In general these deposits had a mud-cracked appearance, indicative of having been wet at some point.

Lower surface of battery cover-plate

Two adjacent contact locations were identified along the path of the trapped wires (Figure 19). These were consistent with having been made by two separate wire strands from the positive (upper) conductor. A very thin layer of material rich in copper and silver, consistent with the battery wire material, had been transferred to the cover-plate at these locations. There was no evidence of arcing, melting or fretting.

© Crown Copyright 2015

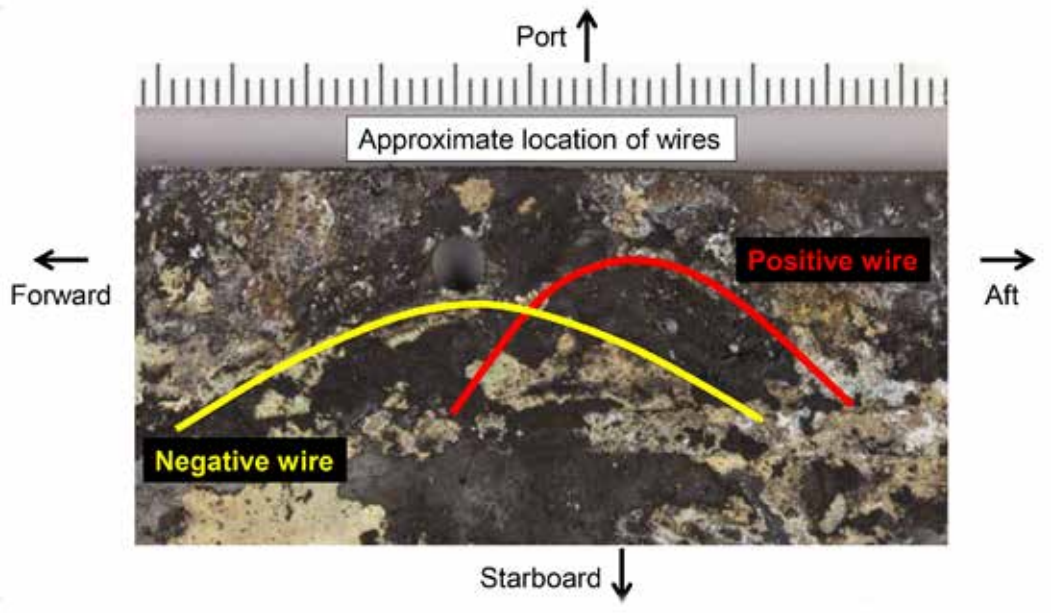

Figure 19

Zoomed-in view of ELT cover-plate,
showing approximate path of trapped wires

ELT case and upper surface of battery cover-plate

Examination of the upper surface of the ELT case revealed no evidence of metal-to-metal contact between the conductors of the battery wires and the ELT case.

After removing the encrusted debris from the ELT case, a large corrosion pit was observed, immediately adjacent to the fastener hole at the wire cross-over location and numerous small corrosion pits were observed nearby. Micro-sections taken through the ELT case in the area of the brown deposit showed the presence of corrosion pitting and significant amounts of aluminium oxide corrosion product, underneath the brown deposit. The most prevalent corrosion was observed in those areas where the brown deposit had been thickest, although comparatively little surface disruption existed in regions where the brown deposit was thinner.

The observed corrosion pitting and the nature of the corrosion product on the ELT case was consistent with an ambient temperature aqueous corrosion[11] process. Such pitting is associated with the presence of chloride or fluoride, both of which were present in the surface deposits, most probably from lithium salts in the battery electrolyte.

[11] Aqueous corrosion is an electrochemical reaction of materials due to a wet environment, resulting in the deterioration of the material and its properties.

Had corrosion existed on the ELT case prior to the incident, the corrosion product would be expected to contain sodium or potassium, however none was detected during this examination. The absence of sodium in the small corrosion pits indicate that the corrosion was probably caused after the battery failure, by reactions with electrolyte residues. Large volumes of water were sprayed into the fuselage crown area of ET-AOP by the RFFS when they were fighting the fire and this is likely to have contributed to the post-incident corrosion.

ELT battery wires

All the insulation was absent from the battery wires, consistent with exposure to high temperatures. It was therefore not possible to determine the pre-incident integrity of the wire insulation at the location of the trapped wires.

The cross-over of the wires was on the ELT side of the electrical connector, rather than the battery side. The positive (upper) wire exhibited some untwisting of the strands at the wire cross-over location and two strands of the wire exhibited visible flattening (Figure 17). Some transfer of aluminium cover-plate material onto the wires had occurred at the contact location, as well as localised removal of the silver coating, exposing the copper wire. The size, shape and alignment of the features on the positive wire corresponded with those on the cover-plate. No evidence of melting was observed.

There was no evidence of contact between the lower (negative wire) and the ELT case.

Deformation of wire strands was evident at the mating face between the upper and lower wires, and there was some localised removal of the silver coating on both wires. Fine copper-rich particulates on the surfaces of both wires could be attributed to fretting debris, indicating possible relative movement between the wires.

ELT battery compartment walls

The outer surface of the battery compartment walls exhibited discolouration consistent with heat damage, and the inner surfaces were covered in combustion debris. Battery combustion products had adhered to the inner surface of the left wall, adjacent to the approximate position of the Cell 1 and 2 side-wall ruptures. There was also some localised melting in this area. In the corresponding location on the external surface, a dark heat-tinted region indicated a hot spot adjacent to the boundary of Cells 1 and 2.

© Crown Copyright 2015

1.12.4 Examination and disassembly of ELT battery and cells

1.12.4.1 General

Following removal from the ELT, the battery was CT-scanned and examined by the AAIB at the QinetiQ facilities at Farnborough. The battery was then disassembled and additional CT scans were performed, individually on Cell 4 and Cell 5 and together on Cells 1, 2 and 3 which could not be separated. The AAIB, with assistance from QinetiQ, then conducted a teardown of each individual battery cell and examined the cell contents and structure. This included weighing the cells, disassembling the cell cans, removing the remains of the electrode windings, and separating, identifying and weighing the individual components.

1.12.4.2 CT examinations of ELT battery and cells

Examination of the CT scans showed that the cell walls in the vicinity of the large sidewall ruptures on Cell 1 and 2, had melted and re-solidified, fusing the two cells together (Figure 20). The melting point of the steel cell-can material is approximately 1,500°C. Solidified debris had accumulated around the sidewall ruptures between Cells 1 and 2, both inside and outside the cells. Smaller ruptures in the sidewalls of Cells 2 and 3 were evident and these had caused localised fusing of the cell walls in two locations. A bulge in the upper half of Cell 3 protruded into Cell 2, causing deformation of the Cell 2 sidewall (Figure 21). The cells were not vertically aligned, particularly Cell 2, which had shifted upwards from the rest of the pack. This suggested some relative movement between the cells during the battery fire. Some horizontal misalignment between the cells was also evident.

All the positive terminal pins were absent from the cell headers, however the positive pin of Cell 2 remained attached to the nickel series-connection strap, which was still welded to the header of Cell 1.

All of the cells were bulged, indicating they had experienced very high internal pressures. The CT scans showed that the nickel anode tab was present, adjacent to the sidewalls, in all five cells.

Corrosion pits were evident on the surface of a number of the cells.

© Crown Copyright 2015

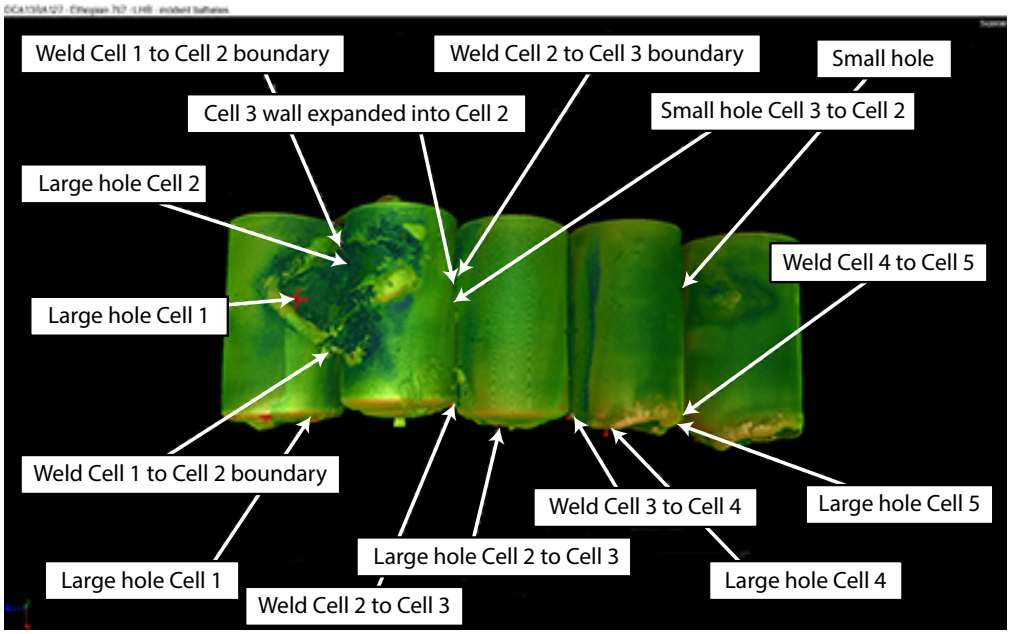

Figure 20

Rendered image from CT scan of battery, showing Cell 1 to Cell 5 (left to right)

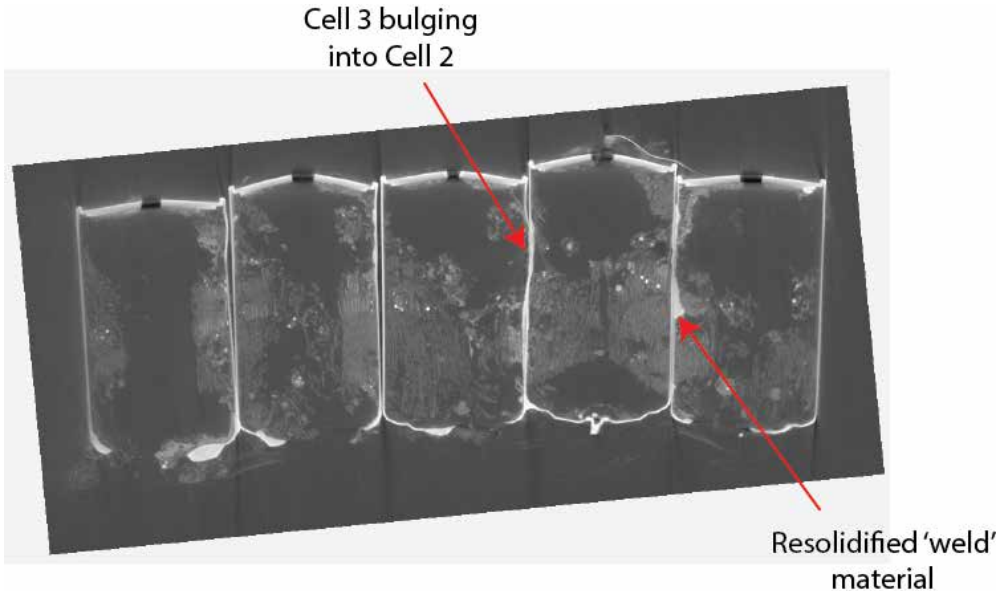

Figure 21

Slice through battery from CT scan showing Cell 5 to Cell 1 (left to right)

1.12.4.3 Visual examination of the battery and cells

General observations

Substantial amounts of brown surface oxidation were evident on the external surfaces of all the cells. This was not visible when the battery was first removed from the ELT, indicating a rapid post-incident degradation in the surface condition of the cells. The weight of the battery pack, prior to disassembly, was 347 g. The weight of a new battery is approximately 610 g. The cell headers on all the cells were intact, with the exception of the glass-to-metal seal which normally holds the positive terminal pin in place. This was consistent with the glass having been exposed to temperatures above its melting temperature (860°C) or excessive pressure within the cells.

Observations on individual cells

Cells 1 and 2 appeared to have sustained the greatest thermal damage, particularly in the area of the sidewall ruptures. The base of Cell 1 was ruptured and distinctly bulged. One of the vents in Cell 1 was partially open; the other was obscured by the rupture in the base.

The base of Cell 2 was bulged but was otherwise completely intact. It was the only cell where the fill port was still present. One of the two vents was partially open, the other was obscured by deposited material.

Cell 3 had a small rupture on the base. One of the vents was closed and the other was obscured by the rupture.

Cell 4 had a large aperture in the base. One of the vents was open, the other was obscured by the rupture. There was considerable build-up of solidified debris between the base of Cells 4 and 5. Embedded in this was a short section of battery wire.

Cell 5 had a large aperture in the base and exhibited the most extensive pooling of molten material around the base.

1.12.4.4 Disassembly of battery pack

Cells 4 and 5 had been joined by a small area of fused cell-wall material close to the base, so Cell 5 was detached using a scalpel. This resulted in a small hole in Cell 4 and some extra ‘weld’ material remaining on Cell 5. Cell 4 detached easily from Cell 3, having been held together only by encrusted debris. The cell cans of Cells 1, 2 and 3 were fused together and could not be separated.

© Crown Copyright 2015

1.12.4.5 Disassembly of cells

General observations

The cell windings in all cells had been heavily damaged as a result of the incident. All of the cells were dry and there was no liquid electrolyte remaining and this was consistent with the electrolyte having evaporated or burned during the battery failure. The boiling point of the electrolyte is 85°C. There was no evidence of any remaining lithium foil (anode) in the cells. This may be explained by the lithium-metal being physically consumed as the cells discharge, by thermal exposure above the melting point of lithium-metal (180°C), or by a combination of both. However, some fragments of copper foil current collector were retrieved from all cells. The melting point of the cooper foil is 1,085°C. Fragments of aluminium mesh, melting point 660°C, were found in all cells, although the size and amount varied by cell. There was no separator material remaining in any cell, consistent with exposure to temperatures above the separator melting point (165°C).

The cathode windings had sustained severe thermal damage in all cells. Much of the cathode winding material had been reduced to dry, powdery debris, which appeared consistent with the electrode material having been exposed to very high temperatures. The decomposition temperature of manganese dioxide is 535°C. The ruptures in the cell bases and sidewalls meant that much of this disintegrated cell winding material had escaped into the ELT battery compartment or fell out of the cells during handling. Some cells retained portions of cathode that still exhibited the winding structure of the 'jelly roll'. These were very fragile and it was not possible to unwind the remnants of the windings without them disintegrating. Both the debris and remaining cathode windings were black with a distinctive green hue.

No gross anomalies or inclusions were noted within the cells. However, the level of damage sustained during the incident meant it was not possible to determine whether any pre-incident defects had existed within the cell windings.

Cell 5

Removal of external debris revealed that there were, in fact, two separate apertures in the base of Cell 5. A pipe-cutter was used to open the cell, with some difficulty as the cell was no longer perfectly cylindrical. Large fragments of aluminium mesh (cathode current collector) were present in the upper half of the cell. A few coils of copper foil (anode current collector) were present at the expected position, around the 'equator' of the cell, but they were in a fragile condition (Figure 22). The lower half of the cell contained debris, some of which was solidified.

© Crown Copyright 2015

Figure 22

Cell 5 disassembly showing remaining cell winding components

Cell 4

Cell 4 was opened with relative ease using a pipe cutter, being more rounded than Cell 5. Remnants of the cell winding structure were present in the upper half of the cell. The copper current collector in Cell 4 was largely intact and was recognisable as copper, appearing less burnt or oxidised than the fragments retrieved from other cells. This was the only area of the cell which exhibited any remaining integrity and the copper foil appeared to be holding the remaining cell winding material together. The lower half of the cell contained many fragments of aluminium mesh, the largest of which was approximately 3.5 cm long. Overall, Cell 4 seemed to contain more material, and was more intact, than any of the other cells. Some solidified debris was present on the inside cell wall, on the Cell 3 side.

Cell 1

The Cell 1 can was cut lengthwise to open the cell. The outer-most half of the cell can was detached; the other half remained attached to Cell 2. There was much solidified debris on the internal and external surfaces, in the region of the sidewall ruptures. The rupture in Cell 1 was larger than that in Cell 2. Some fragments of copper current collector were retrieved, much smaller than those in Cell 4 and some were very burnt. Small fragments of aluminium mesh were also retrieved. The nickel anode tab was not visible but had been identified on the CT scan; it was most likely embedded in the solidified debris around the sidewall rupture.

Cell 2

Cell 2 was cut lengthwise, avoiding the area of the sidewall rupture. Half of the cell can remained attached to Cell 3, the other half to Cell 1. Cell 2

© Crown Copyright 2015

contained the least amount of cell winding material and that which remained was largely dust, comprised mostly of green powdery debris, with distinctive red particles. Portions of aluminium mesh were visible but appeared smaller and less numerous than in other cells. Only one small strand of copper current collector was present at the Cell 1 side, with a few more small fragments at the Cell 3 side. Much of the debris within Cell 2 had solidified on the internal cell walls, particularly around the sidewall ruptures on both sides, and it was not possible to remove this. The nickel tab was evident at the Cell 2-3 interface.

Cell 3

Cell 3 was cut lengthwise. The half on the Cell 4 side was detached, the other half remained attached to Cell 2. The internal debris was solid on the side nearest to Cell 2, and could not be removed, but the debris was more powdery on the Cell 4 side. Larger fragments of aluminium mesh were present, and a few coils of copper current collector, some embedded in the solidified debris. The nickel tab was not visible, likely embedded in the solidified material.

Summary

The following table summarises the findings of the cell disassembly and provides a comparison with the expected findings for a new cell.

	Cell 1	**Cell 2**	**Cell 3**	**Cell 4**	**Cell 5**	**New cell**
% of base missing due rupture	30%	0%	20%	60%	60%	0%
Nickel strip (anode tab)	Present	Present	Present	Present	Present	Present
Amount of Copper foil (anode) remaining	0.16 g 22% 130 mm	0.06g 8% 40 mm	0.29 g 40% 255 mm	0.5 g 68% 505 mm	0.41 g 56% 340 mm	0.73 g 100% 695 mm
Amount of Aluminium mesh (cathode) remaining	0.11 g 2.5%	0.08 g 1.8%	0.34 g 7.7%	0.15 g 3.4%	0.25 g 5.7%	4.4 g 100%
Weld	To Cell 2	To Cell 1 and 3	To Cell 2	Spot Weld to Cell 5	Spot Weld to Cell 4	N/A
Cell weight	210.41 g			68.08 g	67.67 g	114 g

Table 2

Summary of cell disassembly findings

1.12.4.6 Forensic examination of cell cans

Micro-sections taken through the Cell 1 and 2 sidewalls showed thinning of the sidewall close to the rupture, as material was consumed by melting, and thickening where the cell walls had re-solidified. The fused cell wall material consisted primarily of iron and manganese, with small quantities of nickel, copper and aluminium.

There was no clear evidence from analysis of the cell cans to indicate which cell initiated the event.

The oxidation and corrosion pitting observed on the external cell walls was consistent with post-incident electrochemical or aqueous corrosion processes, where galvanic coupling between the nickel plating and iron substrate had led to localised pitting.

1.13 Medical and pathological information

Not applicable.

1.14 Fire

1.14.1 General

The damage to the aircraft showed that a fire had broken out in the rear fuselage crown skin and, as the aircraft was unoccupied, the time taken from the initiation of the fire to its detection could not be determined. The only source of stored energy within the fire-affected area of the crown was the ELT and the severity of the damage to the ELT and its mounting structure confirmed that it was the source of the fire.

1.14.2 Propagation of the fire

Certification

Prior to certification, Boeing were required to meet FAA Issue Paper CS-14 'Fuselage Post-Crash Fire Survivability of Boeing Model 787 Series Aircraft'. This confirmed that the fuselage structure of the B787 would provide the same resistance to fire penetration as a conventional aircraft.

Thermal properties of CFRP

When exposed to elevated temperatures the chemical bonds within the CFRP resin weakens and, at higher temperatures, the resin begins to degrade, and then vaporise from the structure. If a sufficiently high temperature is reached, the resin vapours will ignite. Tests conducted by Boeing demonstrated that

vaporisation of the B787 CFRP typically occurs at approximately 300°C and ignition could occur when the temperature reaches 330°C to 360°C. Figure 23 illustrates a typical cross-section of a CFRP skin panel after exposure to fire. Typically in 'open air' conditions, after ignition has occurred and the heat source is removed, CFRP will self-extinguish. Sustaining combustion within CFRP requires a combination of sustained elevated temperatures and sufficient thermal input to cause adjacent CFRP to reach ignition temperature.

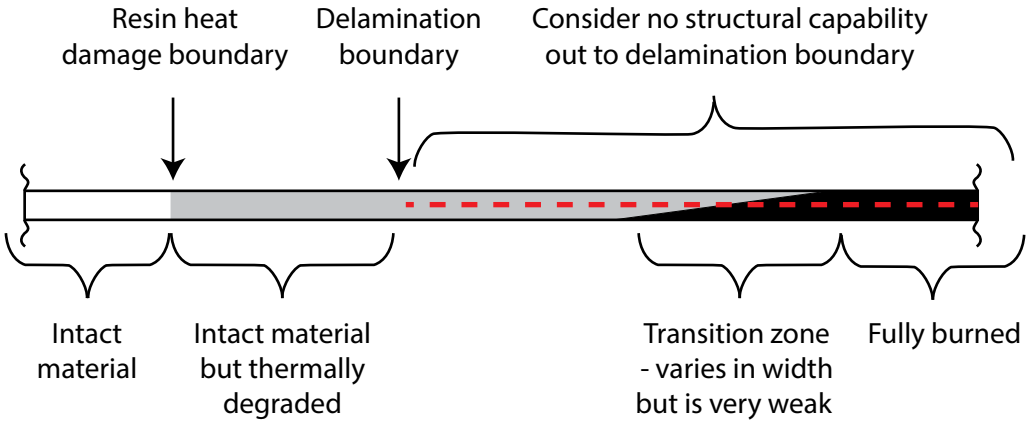

Figure 23

Typical cross section of burned CFRP (Boeing)

Tests carried out by the FAA[12] confirmed that epoxy carbon composites behave like a 'charring' material. As the epoxy resin (typically 35% of the laminate) vaporises and burns it leaves behind an insulating layer of carbon fibres, which is essentially inert. This causes a continual reduction in the internal heating of each subsequent layer of composite, which results in a decreasing burn rate with time.

Fuselage insulation

The insulation blankets installed in the fuselage comply with the requirements for flame resistance defined by Code of Federal Regulations (CFR) 14 CFR 25.856(a). As a function of their design, the insulation blankets have minimal potential to provide an additional source of fuel for fire propagation. The low thermal conductivity of the blankets also provide an effective barrier between the attic airspace and the space between the insulation and the crown skin. In the event of a fire in this space, the insulation blankets will minimise heat loss to the 'attic' airspace. Whilst the insulation blankets are designed to be fire resistant they are not fireproof; continued exposure to fire will result in the burning of the polymer envelope and the release of the insulation material.

[12] Quintiere, J, Walters, R and Crowley, S: *'Flammability Properties of Aircraft Carbon - Fiber Structural Components'* FAA report DOT/FAA/AR-07/57, Oct 2007.

Structural fire progression

Inspection of the remains of the insulation blankets showed that the heaviest soot was found on the outer face (the side facing fuselage skin) of the bay blankets. Lesser amounts of soot were observed on the inner faces of the bay blankets and both faces of the over-blankets. This suggested that once the fire had become established in the CFRP, it progressed within the air gap between the bay blankets and the skin. In this situation the fuselage frames and shear ties would have acted as temporary barriers to fire progression. While the insulation blankets remained intact, the cut-outs in the shear ties would have provided a path for the fire to progress from bay to bay. In areas where the insulation blankets were held tightly against the skin, the damage to the CFRP was less than in adjacent areas. Two such areas were between frames 1670 and 1695, where the VHF aerial is installed (Figure 10), and in areas around the periphery of the burn damage, where the insulation blankets made contact with the top of the 'hat-section' stringers.

The fire damage to the composite tie-rods in the crown area had a discrete transition from damaged to undamaged material; the location of this transition point coincided with the point where the tie-rods protruded through the insulation blankets. There was little or no discolouration or damage to the tie-rods inboard of the insulation blankets. This indicated that the ambient temperature within the attic space was too low to sustain combustion of the tie-rods.

1.15 Survival aspects

1.15.1 General

A fire within the fuselage of a passenger aircraft can present significant survivability issues. These relate to the heat of the fire, the toxicity of the gases released, the reduction in visibility to both passengers and crew, and the time taken for the presence of a fire to be detected by the occupants. When the RFFS entered ET-AOP they reported that the visibility within the aircraft cabin was extremely limited due to the presence of dense smoke throughout the cabin. In addition they were unable to detect the fire with thermal imaging equipment.

Given the location of the ELT fire, in the attic area, had this event occurred on an occupied aircraft, the fire would not have been visible to either passengers or crew, nor would any heat effect from the fire have been apparent to the occupants. The noise produced by the ELT battery failure may have provided some indication of a problem in the area, but it is not known whether it would have been identified as a fire.

In view of this, the most likely method for the crew to detect the presence of a fire in the attic area would be the smell of the combustion products and the presence of smoke/soot distributed by the ECS system. It is not known how long it may take for such a fire to be detected and the location of the ELT could prolong the time taken to locate the source. The noise produced by an ELT battery failure may provide some indication as to the location of the fire.

In these circumstances the main issues regarding survivability are the flame propagation, the actions that the flight and cabin crew take after detecting the presence of a fire, and the toxicity of the combustion products produced by the fire and distributed by the ECS system.

1.15.2 Cabin crew and flight crew fire fighting

1.15.2.1 Firefighting equipment

The operator's B787s are equipped with three Halon fire extinguishers located in the forward galley, midgalley and rear galley, and have a throw of about 2.5 m. They also have two water fire extinguishers, one located in the forward galley and one at the crew station at Door 3 Left. In addition they are also equipped with 14 constant-flow portable oxygen bottles located throughout the cabin, for use by the crew. There are also five smoke hoods; two in the forward galley, one in the mid-galley, one at the crew station at Door 3 Left and one in the rear galley. There is also a crash axe located in the flight deck (Figure 24).

The aircraft operator specifies the type of extinguishers to be installed. Some B787s may be fitted only with Halon extinguishers and others only with water extinguishers. Additionally, on B787s fitted with an overhead flight attendants rest (OFAR), a Halon fire extinguisher and a smoke hood are located in the OFAR.

© Crown Copyright 2015

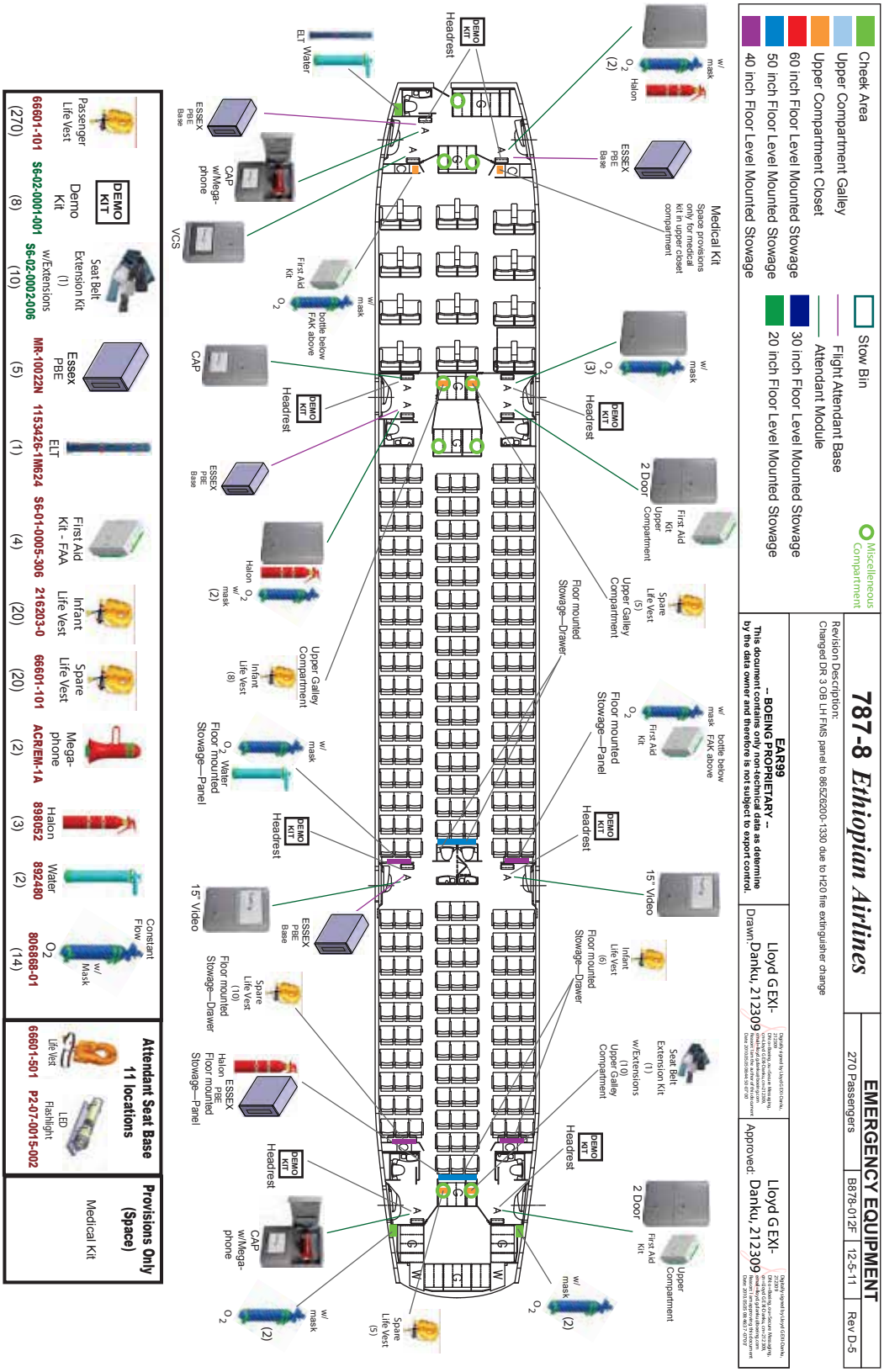

Figure 24

Ethiopian Airlines B787 emergency equipment layout

1.15.2.2 B787 Flight Attendant Manual

The manufacturer's B787 Flight Attendant Manual (FAM) provides general guidance on fighting an aircraft cabin fire. It also has a section on specific types of fire; this includes a section '*Lithium Battery Fires*', which was incorporated in May 2014, after the ET-AOP incident. The FAM states:

> *'Cabin Fire Fighting.*
>
> *Immediately attack the fire with the nearest appropriate type fire extinguisher. Direct the extinguishing agent at the base of the flames at the near edge and bottom of the fire first…*
>
> *Immediately notify the flight deck. Request help from other crew members…*
>
> *Remove electrical power from the affected area.*
>
> *Bring additional fire fighting equipment to the fire scene as necessary:*
>
> - *portable oxygen bottle with smoke mask attached and/or smoke hood with oxygen*
> - *crash axe…'*

and:

> *'Lithium Battery Fires:*
>
> *If there is a fire involving lithium batteries:*
>
> - *Relocate passengers away from the device.*
> - *Notify the flight deck and call for assistance*
> - *Fires may occur behind floor or ceiling panels (such as fixed ELT above the flight attendant rest area) or in equipment compartments. Signs of fire may include odor, hot spots or visible smoke.*
> - *Attempt to locate the source of the fire. Feel suspected area(s) with the back of hand to prevent injury.*
> - *Use the crash axe if necessary to access a lithium battery fire behind a panel. A small hole can initially be made in a panel and Halon or Halon replacement fire extinguishers can be discharged through the hole to knock down the fire before opening a panel and exposing the fire zone to cabin air.*

- *Use care to avoid damaging primary structure and windows, and injuring personnel.*
- *Utilize a Halon, Halon replacement, or water fire extinguisher to extinguish the fire and prevent the spread of the fire to adjacent battery cells and materials.*
- *After extinguishing the fire, douse the device with water or other non-alcoholic liquids to cool the device and prevent additional battery cells from reaching thermal runaway.'*

1.15.2.3 ELT battery fire fighting

In the event of an ELT battery fire, in an aircraft configured like ET-AOP, a ceiling panel at the rear of the passenger cabin would have to be lowered to access the ELT. The cabin crew would then have to stand on a seat, or an arm-rest, to aim a fire extinguisher at the source of the fire. For aircraft with an OFAR, an access panel in the ceiling permits access to the ELT.

For in-flight cabin fires, cabin crew are trained to identify the source of the fire, and to don a smoke hood and gloves, if time permits. However, it may be difficult to locate the source of a non-visible fire, because the aircraft's environmental control system (ECS) would distribute the smoke and fumes.

In the event of a cabin fire the flight crew would action the *'Smoke, Fire or Fumes'* checklist from the Quick Reference Handbook (QRH). This includes the possibility of initiating a diversion and if directed, action the *'Smoke or Fumes Removal'* checklist. The objective of the *'Smoke, Fire or Fumes'* checklist is to remove electrical power from the ignition source and if required, to land the aircraft as soon as possible. However, the ELT is independent of the aircraft's electrical network and, in the event of an ELT battery fire, the checklist actions related to removing electrical power from the ignition source will be ineffective.

1.15.2.4 Rescue and Fire Fighting Service (RFFS) information

The aircraft manufacturer published '*Airplane Rescue and Fire Fighting (ARFF) Information'* for the B787 on the internet. This included information about how fires on composites compare to aluminium aircraft. It also included a diagram showing the locations of the main and APU large-format lithium-ion batteries on the aircraft; however, the ELT lithium-metal battery was not included (Figure 25).

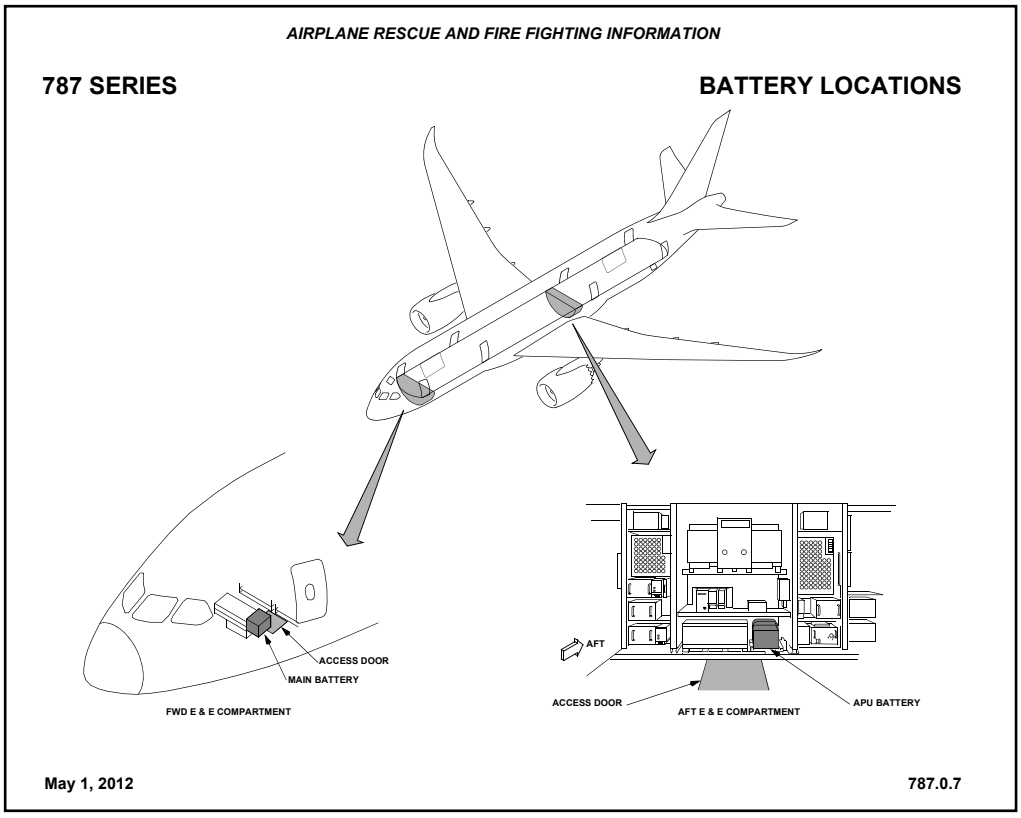

Figure 25

B787 Battery Locations

1.15.3 Toxicity

The burning of CFRP can produce large quantities of dense smoke containing soot particles and combustion products. During the B787 design and certification process Boeing and the FAA conducted tests to evaluate the flame propagation performance of composite fuselage structure when samples representative of B787 fuselage skin were exposed to fire. In these tests a sheet of CFRP was exposed to a flame source, typically an ignited heptane-soaked foam block to confirm flame propagation resistance. The results of these tests demonstrated that the materials used in the manufacture of the B787 met the requirements of FAA Special Condition 25-07-09-SC 'Composite Fuselage In-Flight Fire/ Flammability Resistance'.

The combustion products produced in these tests may be considered typical of gases and particles released by the combustion process. In practice, the products of combustion are dependent on a number of variables[13], for example, the decomposition rate of the polymer matrix increases with the temperature of the fire. This can result in higher quantities of carbon monoxide (CO), carbon dioxide ($CO_{2)}$, hydrogen cyanide (HCN) and nitrogen dioxide (NO_2) in the smoke

[13] A.P. Mouritz, A.G. Gibson: '*Fire Properties of Polymer Composite Materials*' ISBN 978-1-4020-5355-9.

and a reduction in the level of heavier volatile organic compounds. In addition, the production of lighter gases, CO and CO_2, is dependent on the specific type of combustion. For example, a smouldering burn of a composite material may produce 50 parts-per-million (ppm) of CO and 300 ppm of CO_2. When the same material is burnt in an open flame, the concentrations can increase to 100 ppm CO and 5,000 ppm CO_2, due to the higher rate of decomposition of the resin matrix. This variability in combustion compounds, and the influence of the aircraft ECS system on the distribution of the smoke, make it difficult to quantify the nature and toxicity of the smoke produced during a composite fire.

As a result of the ET-AOP incident, Boeing carried out a review of the existing toxicity data relating to B787 CFRP and cabin interior materials. This confirmed that the data complied with Boeing's internal and industry-accepted requirements. The data confirmed that the materials used in the manufacture of the B787 met the current FAA requirements.

The Boeing ECS group has commenced development of an airflow model to evaluate how a functioning aircraft ECS system would disperse combustion products from an ELT fire. The ECS model will analyse the dispersion of the gases released by an ELT battery during failure (Section 1.16.3.6) and will reflect operation of the ECS system in both the 'normal' and 'cabin smoke procedure' modes.

As part of their ongoing test process, the FAA will carry out a re-evaluation of the current flammability testing of aircraft materials to ensure the test methodology remains appropriate to evaluate flame propagation properties of composite fuselage structure. In addition the FAA have undertaken to investigate additional test methods to produce more representative flammability data for aircraft certification.

1.16 Tests and research

1.16.1 ELT fault tree

Following the ET-AOP ground fire, Boeing and Honeywell performed a 'Fault Tree Analysis[14]' to identify all potential root causes that could lead to an ELT battery thermal event. The analysis grouped the failures into three categories: electrical overheat, chemical overheat and physical overheat. The following potential root causes were identified within each failure mode category:

[14] Fault tree analysis (FTA) is a deductive technique in which an undesired state of a system is analysed, to understand the ways in which the system can fail.

- Electrical overheat – battery harness short-circuit (pinched wire), PTC unable to protect circuit, resistive short from ELT circuit card, cell voltage depletion / reversal;
- Chemical overheat – drying out or loss of electrolyte, cell case corrosion due to the presence of moisture;
- Physical (mechanical and thermal) overheat – latent damage / cell manufacturing flaw, mechanical damage, internal short circuit, lightning strike, external fire or heat source.

Examination of the aircraft had revealed no evidence of a lightning strike having occurred on the ELT antenna. Similarly, no external heat or ignition sources were identified in the vicinity of the ELT. Therefore these failure modes were eliminated.

Some failure modes were considered possible but no evidence existed to support them so these were eliminated. These included the failure modes in the chemical category and all the remaining failure modes in the physical category.

All the failure modes within the electrical overheat category were considered to be plausible. Testing and analysis were conducted to validate or eliminate potential root causes.

For reference, generic information on lithium-metal battery failure modes is included in Section 1.18.1.

1.16.2 ELT circuit analysis

Honeywell, Instrumar and Boeing conducted an analysis to determine whether any ‘sneak paths’ exist within the ELT, which could provide an unintended short-circuit path to charge or discharge the ELT battery. The power-supply card within the ELT is the only component which directly interfaces with the battery, however it has a protective diode which prevents reverse current through the battery and therefore prevents battery charging from any source.

A sustained continuous high battery current through the power-supply card would result in overheating of circuit-card components which would fail in open circuit, and was therefore considered highly improbable.

The analysis found no external sneak paths between the ELT battery and the external aircraft interfaces. It also identified that no single-point component failure inside the ELT could result in a continuous high load on the battery. This was therefore ruled out as a possible failure mode.

© Crown Copyright 2015

1.16.3 Manufacturers' Root Cause testing

1.16.3.1 General

Based on the outcome of the fault tree analysis, parallel and coordinated test programmes were undertaken by Boeing and Honeywell in support of the AAIB investigation, with input from Ultralife and Instrumar. The tests were performed in test facilities at the manufacturers' respective sites and the results of the tests were documented in a jointly produced Boeing/Honeywell 'B787 ELT Incident Root Cause Report[15]' provided to the AAIB in April 2014.

Tests were performed on individual cells from an ELT battery and on complete ELT battery packs, either in isolation or while installed in a RESCU 406AFN ELT. Since the battery pack wires on ET-AOP were found to have been crossed and pinched together, an external short-circuit condition was considered to be a highly plausible root cause of the battery fire and much of the testing therefore focused on this failure mode, in isolation and in combination with other failure modes. Some of the relevant tests performed and documented in the Root Cause Report, are described in the subsequent sections of this report.

1.16.3.2 Single-cell tests

1.16.3.2.1 Single-cell thermal abuse tests

While external thermal abuse of the ELT battery had been eliminated as a possible cause, Honeywell conducted a number of thermal abuse tests to verify the expected effect of exposing individual Li-MnO_2 cells to excessive temperatures. In these tests, discrete cells were mounted in a variety of orientations and exposed to excessive temperatures ranging from 350 to 500°F (177 to 260°C). In all cases the cells decomposed under thermal runaway, violently venting gas, flames and sparks. The time to failure reduced as the temperature increased.

1.16.3.2.2 Single cell corrosion tests

Honeywell performed a number of corrosion tests in which individual cells where exposed to varying conditions which might be expected to induce corrosion, to determine whether corrosion could lead to a thermal event.

One cell was subjected to tap water being dripped on the top of the cell, and another to salt water. The cells fully discharged over a period of 80 hours. Some corrosion was noted but the cell case was not breached, and no venting or temperature excursions occurred.

[15] Boeing Document No. D613Z037-01; Honeywell Document No. 21-15433.

In a second test one cell was placed in a closed high-humidity environment, while another was partially submerged in a salt-water solution. After six months in this condition, the voltage of the partially submerged cell had dropped to 0.9 V, while the voltage of the other cell remained unaffected. The exposed portion of each cell exhibited extensive corrosion but no evidence that the cell had been breached or that a thermal event had occurred.

Cell corrosion as a precursor to a thermal event was eliminated as a possible root cause. However, the tests identified that moisture on the top of a cell could bridge the glass-to-metal seal, which insulates the positive terminal from the negative cell case, causing a short across the cell terminals and leading to depletion of the cell.

1.16.3.3 Battery-level external short-circuit tests

1.16.3.3.1 General

A number of sample ELT batteries were discharged under a variety of short-circuit conditions. The tests included 'hard[16]' short-circuit and 'resistive[17]' short-circuit conditions. The batteries were instrumented to measure individual cell voltages, battery voltage, discharge current and cell temperatures.

In the following three tests the battery circuit was modified to bypass the PTC, in order to understand the behaviour of the battery without this protective device in place.

1.16.3.3.2 Honeywell Test 7: Battery pack external short-circuit, low resistance

The intent of this test was to simulate a low-resistance short-circuit path by placing a 1 ohm resistor in the battery circuit, giving an approximate 15A discharge current. Additional 18 AWG[18] wire (the same gauge used in the battery leads) was used to allow the circuit to be completed manually outside the test chamber. The negative wire was resistance-welded to the terminal tab on Cell 5, where the PTC is normally installed.

Soon after the short circuit was applied, the battery pack voltage dropped to zero indicating an open circuit. Examination of the battery pack revealed that the high current had resulted in a failure of the resistance-weld where the

16 In this context a 'hard' short-circuit implies any contact which would provide a minimal resistance current path, permitting a high discharge current. Direct metal-to-metal contact between the conductors of the trapped battery wires or between the positive conductor and the ELT case, could theoretically create a 'hard' short-circuit.

17 In this context a 'resistive' short-circuit refers to a short-circuit condition with some degree of electrical resistance, which could limit the discharge current. Partial contact between the ELT battery wires, or between the positive conductor and the ELT case, could create a 'resistive' short-circuit.

18 American Wire Gauge.

negative wire was terminated to Cell 5, causing an open circuit. The battery pack was undamaged. Although this test was terminated early, the failure of the test equipment is relevant because it indicated that high discharge currents, in the order of 15 A, could cause the wiring in the battery circuit to fail.

1.16.3.3.3 Honeywell Test 9: Battery pack external short-circuit, moderate resistance

Test 9 was similar to Test 7, with the exceptions that heavier gauge wire (14 AWG) was used to route the battery leads outside the test facility and a 3.3 ohm resistor was used to simulate a moderate-resistance short circuit and reduce the discharge current to 4A.

The battery discharged over a 3 hour period, before the cells depleted one-by-one in a benign manner. As each cell depleted there was a small temperature increase of 5 to 8°C but none of the cell temperatures rose above 52°C. There was no rupture, flame, sparks, venting or leakage.

1.16.3.3.4 Honeywell Test 10: Battery pack external short-circuit, low resistance

Test 10 was similar to Test 9, but with a 1 ohm resistor to increase the discharge current. The pack voltage, measured as 15.2V before the test, dropped to just under 12V when the short-circuit was applied, giving a discharge current of 10.8A.

Twenty three minutes after the battery pack was shorted, Cell 2 experienced a 'voltage reversal'[19] to -10V, becoming resistive (Figure 26). Approximately 2½ minutes later, Cell 2 experienced a rapid rise in temperature and decomposed under thermal runaway, exhibiting violent venting of gas, sparks and flames. The failure propagated to the remaining four cells, which all failed in a similar manner.

Post-test examination of the cells revealed they were burned and blackened and a number of the cells had been breached at the base of the cells. The maximum cell temperature was approximately 1,300°F (704°C), while the air temperature above Cell 2 peaked at approximately 2,300°F (1,260°C).

[19] 'Voltage reversal' or 'cell reversal', is a term used to describe a change in polarity experienced by a cell. This phenomenon is often associated with cell imbalance, where one cell in a pack discharges more rapidly than the others, due to minor variations in cell capacities. A voltage reversal is often associated with a large increase in the cell's electrical resistance. More information on voltage reversal and cell imbalance is included in Section 1.18.1.4.

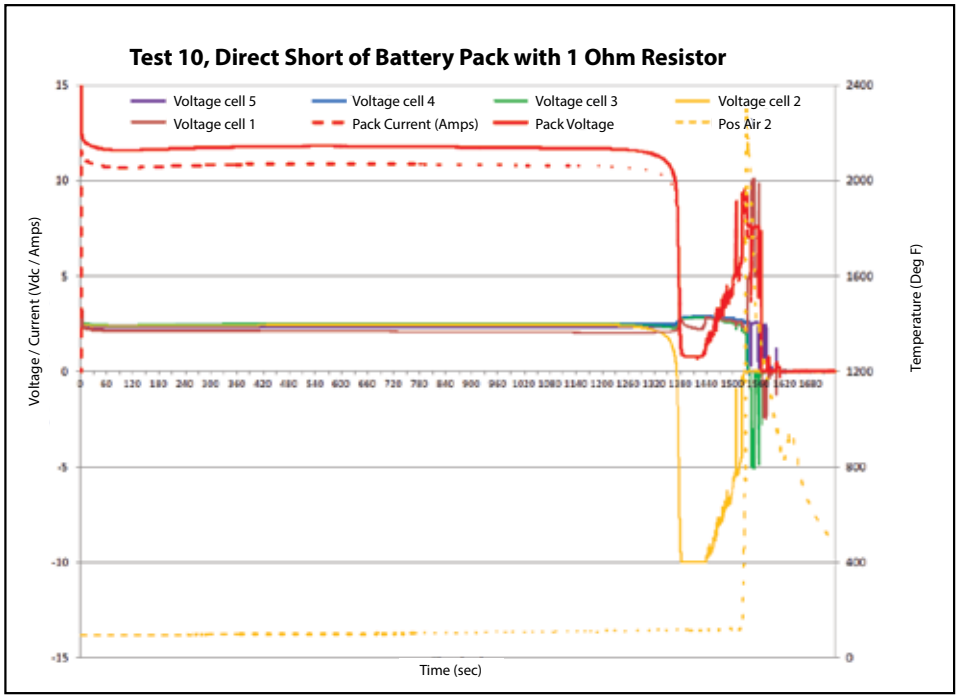

Figure 26

Honeywell Test 10, low resistance short of ELT battery pack with 1 ohm resistor (PTC bypassed)

1.16.3.4 External short-circuit test on batteries installed in an ELT

1.16.3.4.1 General

A number of discharge tests were performed on sample ELT batteries installed in an ELT, to model the equipment installation more closely. The batteries were discharged under a variety of short-circuit conditions. The PTC was bypassed in one test, but was included in the battery circuit for the remainder. Instrumentation was added to measure voltages, current, temperatures and in some cases, pressure.

1.16.3.4.2 Boeing Destructive Test Procedure (DTP) DTP-1: Hard short-circuit test

This test was performed to benchmark the behaviour of an installed ELT battery when the battery leads were directly shorted together. Three ELTs were tested concurrently and were warmed to 40°C, to approximate the thermal conditions in the fuselage crown prior to the ET-AOP event[20].

In all three cases, the PTC tripped soon after the wires were shorted, rapidly reducing the current to a very low level, between 137 and 154 mA. This current

[20] ET-AOP was parked for a number of hours in temperatures of up to 25°C. Boeing estimated that in these conditions, the ambient temperature in the fuselage crown would have been approximately 40°C.

© Crown Copyright 2015

was not sufficiently high to elevate the cell temperatures to a dangerous level and the batteries discharged gradually, over a three-day period. The maximum cell temperatures were achieved as the cells reached their end of life and their internal impedance began to rise, but did not rise above 80°C. PTC temperatures between 105 and 115°C were recorded. The cells failed in a benign manner.

A hard short-circuit arising from direct contact between the positive and negative battery wires was ruled out as a possible cause of the ET-AOP event, as the high resulting current would trip a functioning PTC, to protect the circuit.

1.16.3.4.3 Boeing DTP-2: Variable resistance short-circuit test

This test was conducted to understand the behaviour of the ELT battery in a partial, or moderate-resistance, short-circuit condition. The test set-up (Figure 27) was the same as DTP-1, except that two resistors were installed in the circuit to provide discharge currents of 3.2A (High), 2.1A (low) or 5.3A (both). The resistors were located outside the ELT and were switched in and out of the circuit to provide an adjustable current. The objective was to keep the discharge current high, without tripping the PTC, by monitoring the PTC temperature to keep it just below the threshold temp (118°C). Two ELTs were tested.

During the discharge, Cell 5 in ELT 1 experienced a voltage reversal and high internal heating rate, peaking at a temperature of 122°C after 5 ½ hrs. In ELT 2, Cell 4 experienced a voltage reversal after 5 hrs and Cell 3 shortly after, peaking at 125°C. At this point in the discharge there was considerable remaining energy within the batteries but the PTC tripped, preventing further discharge.

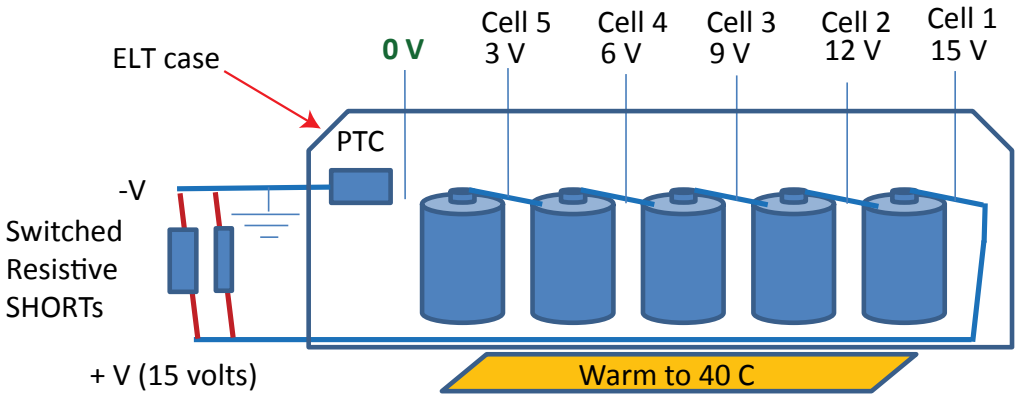

Figure 27

Illustration of Boeing DTP-2 test set-up;
variable resistance short-circuit of battery pack installed within ELT at 40°C

1.16.3.4.4 Boeing DTP-3: Fixed resistance short-circuit test

This test was conducted with the aim of creating a fixed-resistance short-circuit to heat the cells during discharge, without tripping the PTC. The test set-up was the same as DTP-2 except that a single fixed resistor was installed in the circuit. Three ELTs were tested concurrently. A 15 ohm resistor was used in ELT 1, to give a 1A discharge current, and a 6.8 ohm resistor was used in ELTs 2 and 3, for a 2A discharge current. The batteries in ELT 1 & 2 were fully charged, while that in ELT 3 had the Cell 1 voltage reduced by 10% to simulate an unbalanced pack, with one weaker cell.

In ELT 1, Cell 1 experienced a voltage reversal to -7 V after 3¼ hrs, when its temperature reached 124°C. This was probably due to partial shutdown of the cell separator. The discharge current dropped to 650 mA. The battery then discharged until all its energy was expended. The remaining cell temperatures did not rise above 90°C.

In ELT 2, Cell 2 experienced a voltage reversal to -9V, after 40 mins, at a temperature of 82°C. The discharge current dropped to around 0.5A, then recovered to approximately 1.75A. The cell temperatures continued to increase after this event, but at a slower rate. Cell 1 reached a maximum temperature of 138°C, before exhibiting a sharp reduction in temperature, probably as a result of the cell shutdown separator activating. Coincident with this, Cell 3 experienced a voltage reversal. The discharge current dropped briefly to 0.5A before recovering to 1.5A. The temperature of all the cells then dropped and continued to reduce as the battery discharged to depletion.

The ELT 3 results were very similar to ELT 2 with a Cell 1 voltage reversal after about 45 mins. After 6½ hrs Cell 1 exhibited sharp cooling, and it is likely that Cell 1 vented liquid electrolyte at this point.

The PTC did not trip in any of the tests and the maximum PTC temperature recorded was just over 100°C. Examination of the batteries revealed that slow venting had occurred on Cell 1 in ELT 2 and 3, with one vent on each cell having ruptured. These results indicate that at 2A, the temperatures in the vented cells had exceeded 140°C, and therefore that the cells were possibly close to a more significant failure mode.

1.16.3.4.5 Honeywell Test 11: Low-resistance short-circuit test with PTC bypassed

The PTC was bypassed and a 1 ohm resistor was placed in the circuit (but outside of the ELT) to allow a low-resistance short of the battery pack. The ELT was modified to route the battery instrumentation outside of the ELT and the ELT was mounted in a configuration and orientation broadly representative of its installation in a B787.

© Crown Copyright 2015

Approximately 27 minutes after the short was initiated, Cell 4 experienced a voltage reversal leading to thermal failure with violent venting of gas, sparks and flames. The failure propagated to the remaining cells and pressure pulses were recorded as each cell vented. These breached the seal on the battery cover-plate, resulting in the escape of smoke and fumes from the ELT, but no flames or sparks.

1.16.3.4.6 Honeywell Test 31: Moderate-resistance short-circuit test with unbalanced pack

In some of the preceding tests, one or more cells discharged more rapidly than the other cells, leading to a voltage reversal and in some cases, thermal failure. To examine the relevance of early depletion of a cell, an 'unbalanced'[21] battery pack was intentionally created by replacing a single cell (Cell 1) in a new battery pack, with a cell that had been depleted in an earlier test. The PTC remained in the circuit and a 3 ohm resistor was used to provide a moderate-resistance short and a discharge current of approximately 3.1A. The objective was to drive a high current through the depleted cell, without tripping the PTC. The resistor was mounted inside the ELT so that the resistive heating from the short-circuit remained within the ELT. The ELT was mounted in a configuration and orientation representative of the ELTs installation in a B787 and an insulation blanket was wrapped around 4 sides of the ELT, to simulate the aircraft's thermo-acoustic blankets.

Immediately after initiating the short, the depleted Cell 1 voltage reversed to -2V. One hour later, Cell 1 voltage dropped further to -5.5V and it then experienced a significant thermal event, which cascaded to the other cells over a 15 minute period (Figure 28). Cell 1's maximum temperature at failure (260°C) was noticeably lower than the temperature of the remaining four cells during their subsequent failures (426 – 649°C), most likely because it had been depleted prior to the test.

[21] An unbalanced battery is one in which one of cells depletes more rapidly than the others, due to minor variations in cell capacities. More information about unbalanced batteries is included in Sections 1.18.1.4 and 1.18.1.5.

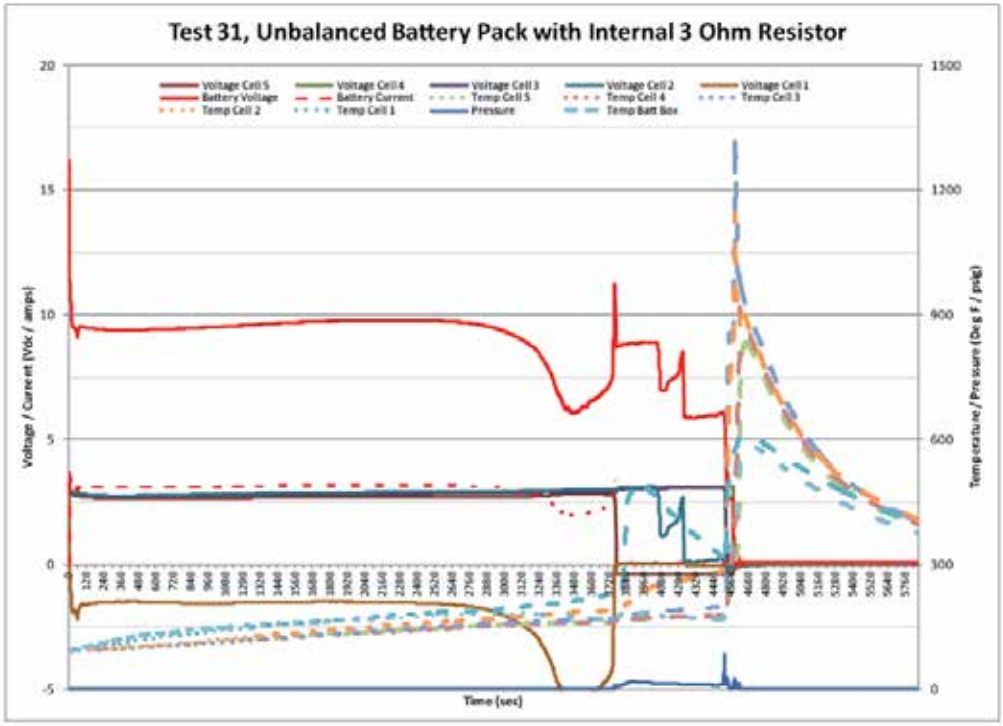

Figure 28

Honeywell Test 31 results,
moderate-resistance short of unbalanced battery pack installed in ELT

1.16.3.4.7 Honeywell Test 32: Moderate-resistance short-circuit test

A 4 ohm resistor installed inside the ELT was placed in the circuit with a fresh balanced battery pack, providing a 2.7 to 2.8A discharge current. The test set-up was the same as Test 31. The cell temperatures rose during the discharge until after 38 minutes the PTC tripped, dropping the current to 0.1A. The cell temperatures then decreased and the circuit remained shorted for 4 hours, until the test terminated.

1.16.3.4.8 Honeywell Test 33: Moderate-resistance short-circuit test with PTC manual reset

The test set-up was similar to Test 32, except that the resistance was increased to 5 ohms, giving a discharge current of 2.7 – 2.9A. The PTC tripped after 64 minutes dropping the current to 0.1A.

With the high resistance of the tripped PTC in the circuit, the battery pack voltage dropped to approximately 12V (Figure 29). 22 minutes after the PTC tripped the circuit was manually opened, resetting the PTC to its low resistance state. The circuit was then reconnected to re-create the short circuit. After a short period the PTC tripped again. This process of opening and closing the circuit was repeated; the time required to trip the PTC decreased with each cycle.

© Crown Copyright 2015

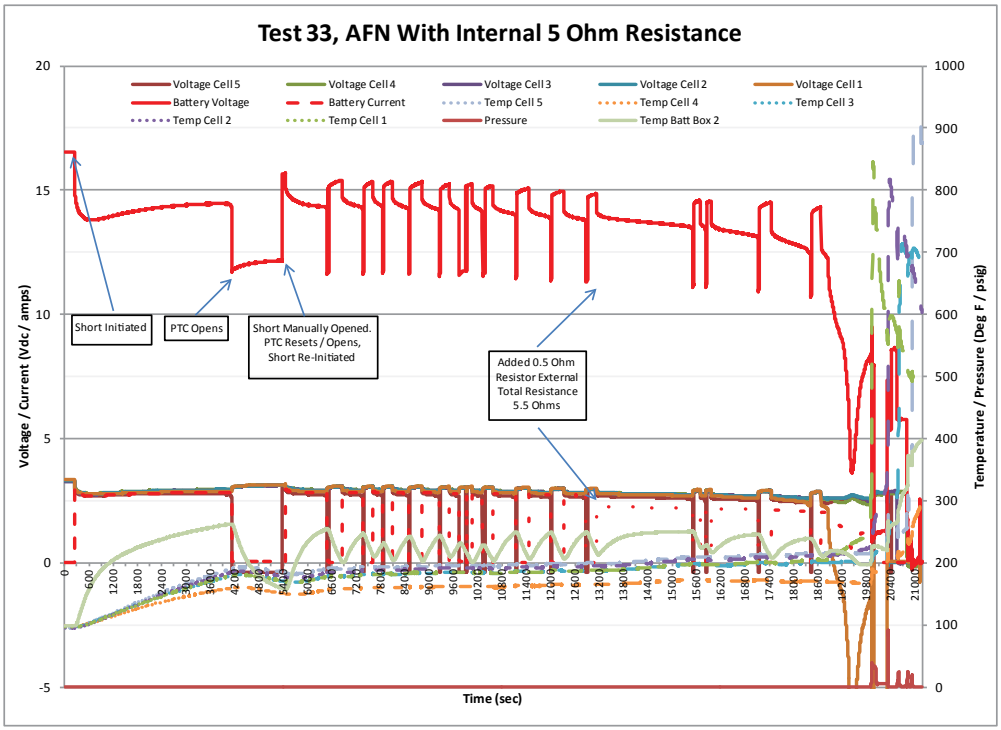

Figure 29

Honeywell Test 33 results, moderate-resistance short of balanced battery pack installed in ELT with manual PTC resets

After 11 cycles of opening and closing the circuit as a means of getting the PTC to reset, an additional 0.5 ohm resistor was added, outside the test chamber. This reduced the current to 2.2A and increased the time between PTC trips. After a total of 16 cycles, Cell 1 experienced a voltage reversal (Figure 30) and decomposed under thermal runaway. This propagated to the neighbouring cells in a cascading thermal runaway, over the next 19 minutes.

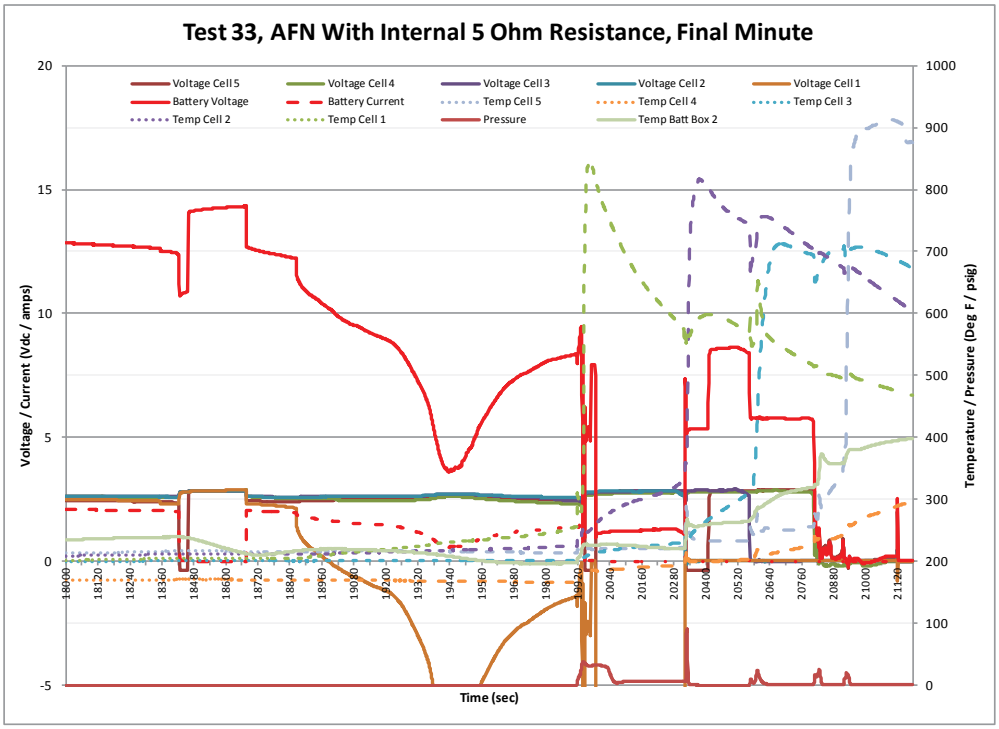

Figure 30

Honeywell Test 33 results, expanded view showing final failure

The cells were found burnt and blackened but most of the decomposition products were retained within the ELT (Figure 31).

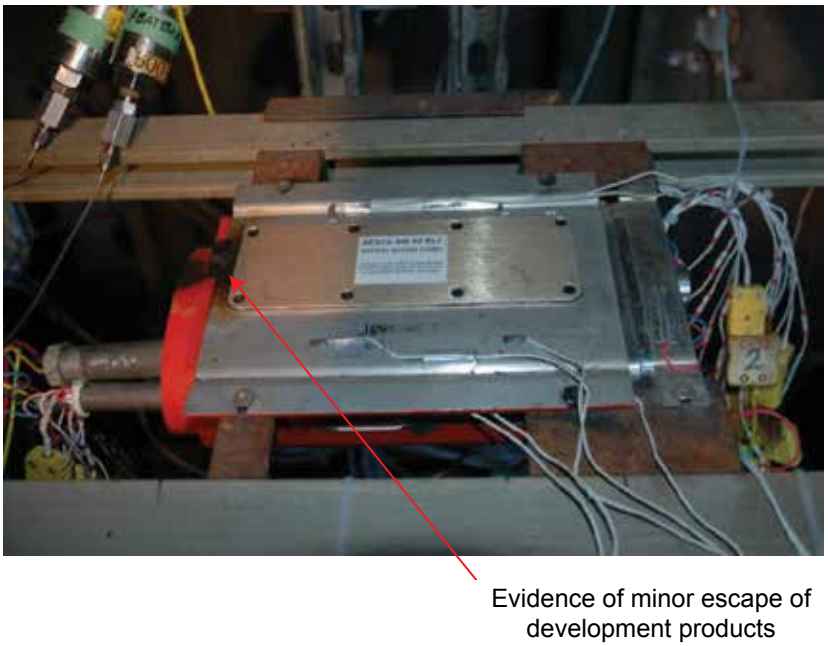

Figure 31

Honeywell Test 33, ELT post-test showing only minor escape of battery decomposition products from battery compartment

1.16.3.4.9 Honeywell Test 35: External short-circuit test at low temperature

This test aimed to evaluate the performance of the battery and PTC at cold temperatures. A fresh battery pack was cold-soaked overnight in a thermal chamber set at 2°C and was partially depleted. A 0.5 ohm resistor was then placed in the circuit and the PTC immediately tripped, limiting the discharge current to approximately 0.25A. The PTC temperature increased to 50°C. The circuit remained connected and after 2 hrs 20 mins one cell experienced a voltage reversal, followed three minutes later by a second cell. Just prior to the second cell reversal, the PTC reset to the low-impedance state. The reset was identified by a rapid decrease in temperature of the PTC and an increase in current. The test did not result in a thermal event because the battery was close to depletion at the time of the PTC reset.

1.16.3.4.10 Boeing DTP-20: Fixed resistance test with intermittent short-circuit

This test was designed to determine whether an intermittent short-circuit, which could occur if there was only partial, or intermittent, contact between the pinched wires, could induce cell damage which might precipitate a thermal event. This situation might occur as a result of sustained aircraft vibration.

The PTC may allow short-duration high-current pulses of 8A or more without tripping, as the time-to-trip can be 10 seconds or more at 8A. An ELT battery pack was therefore connected to a mechanical relay which was repeatedly cycled by a pulse generator to apply the short-circuit. The cell temperatures did not exceed 60°C and no cell failures occurred.

The test concluded that rapid intermittent application of a short-circuit was not likely to lead to cell damage.

1.16.3.5 Battery drain tests

In the discharge tests the battery thermal events were generally precipitated by one or more cells experiencing a voltage reversal. Voltage reversals lead to a substantial increase in a cell's resistance, which increases the overall circuit resistance and is generally accompanied by a corresponding reduction in current. This effect is shown in the results of Honeywell Tests 10 (Figure 26) and 31 (Figure 28). Analysis of these results determined that the resistive cells achieved a maximum resistance of 14 ohms and 11 ohms respectively.

In order to gather more data on the resistance of depleted cells, Instrumar discharged six ELT batteries at a variety of discharge currents between 0.5 and 2.0A. The depleted cells exhibited maximum resistances between 4 and 32 ohms, but typical values were around the 5 ohm level.

© Crown Copyright 2015

1.16.3.6 ELT battery toxicity

During the Root Cause testing both Boeing and Honeywell undertook specific tests to identify the composition and quantity of gases released during an ELT battery or individual cell failure. One of the Honeywell tests involved single D-cells subject to thermal runaway inside a smoke chamber, where the gases emitted were free to mix with air in the chamber. Thermal runaway was initiated using an external heat source. Another test involved a new battery installed in an ELT. The ELT battery cover-plate was modified to include a pressure-relief port, from which the emitted gases were directly sampled, thereby preventing mixing of the gases with ambient air. Single-cell thermal runaway was induced by reverse-charging a single cell.

Carbon monoxide, carbon dioxide and hydrogen cyanide were among the gases detected during these tests. The gases from the ELT test included gaseous emissions from other ELT components consumed during the battery failure, such as the urethane foam padding in the battery compartment and ELT circuit card components. An analysis of the chemical composition of a D-cell compared to the gases released during a failure, indicated that significant chemical changes occur within a cell as it fails.

Boeing performed a variety of tests on two D-cells within a pressure vessel and also on a portable ELT, installed in a cabinet, representative of the portable ELT storage on an aircraft. The portable ELT contained 4 D-cells, similar to those installed in the RESCU 406AFN ELT. The gases emitted included hydrogen, oxygen, argon, nitrogen, carbon monoxide, methane, carbon dioxide, methanol, various hydrocarbons and various sulphur compounds.

The Honeywell and Boeing tests provided useful preliminary information on the gases released during a battery failure, although they did not attempt to classify the exact composition or quantities of gases released during the ET-AOP event. Both sets of tests indicated that the composition and quantity of gas produced varied considerably, depending on the type of combustion and on the amount of oxygen available. In a real environment, the amount of oxygen available to sustain combustion would vary depending on the precise installation of the battery and its location.

The results of the Boeing and Honeywell battery toxicity tests will be used in the Boeing ECS modelling discussed in Section 1.15.3.

© Crown Copyright 2015

1.16.3.7 Instrumar PTC testing

1.16.3.7.1 PTC reset testing - informal bench testing

The results of the Root Cause discharge tests showed that the behaviour of the PTC was a significant factor in determining whether an external short-circuit resulted in a battery thermal event. Honeywell Test 31 showed that a PTC reset, or multiple resets, could theoretically lead to a thermal event.

In order, therefore, to understand the reset behaviour of the PTC, some informal bench tests were performed by Instrumar. An LR4-380F PTC was placed in a simple circuit, in series with a 15V power supply and a load resistor at ambient temperature (20˚C). Three load resistors were chosen to provide either a current just below the PTC trip limit or a current substantially below the trip limit. The circuit was configured so that the resistor could be bypassed or shorted to trip the PTC (Figure 32).

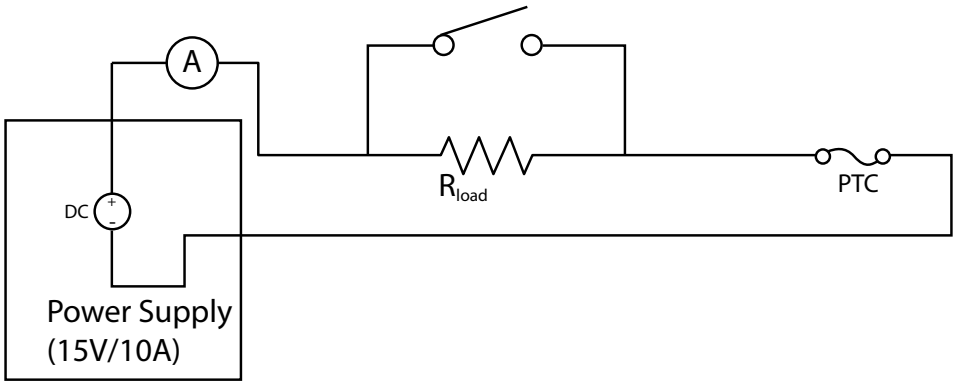

Figure 32

PTC reset test, circuit configuration

In the first test the circuit was shorted across the 5 ohm load resistor; the power supply current was limited to 4A. The PTC did not trip. Heat was applied to the PTC with a heat gun to force it to trip. Once tripped, the PTC stayed in the 'high-impedance mode' even after the heat gun was removed and the short across the load resistor was removed to reduce the current.

A freeze spray was used to cool and reset the PTC. Once reset, the current was limited by the 5 ohm load resistor and therefore the PTC did not go back into high-impedance mode.

The test was repeated with the power-supply current limited to 8A. The PTC tripped within 30 seconds without the application of external heat, due to the higher current. After removing the short across the 5 ohm load resistor to reduce the current, the PTC still remained in the high-impedance mode.

© Crown Copyright 2015

The test was re-run with the 10 ohm and then the 20 ohm load resistors in the circuit, with similar results. Once in high-impedance mode, even after removal of the current, the PTC did not reset until a shot of freeze spray was applied.

These informal tests demonstrated that the PTC did not readily reset upon reducing the current, once it had tripped and was in the high-impedance mode. However, cooling the PTC could cause it to reset.

1.16.3.7.2 PTC reset testing in thermal chamber

Further tests were conducted in a thermal chamber, to allow precise control of ambient temperature. Using a 12V power-supply limited to 10A current and an ammeter to measure current (Figure 33), the load resistance (R_{LOAD}) was switched between a short (zero resistance) and 5 ohms. The chamber temperature was dropped incrementally. Once the temperature had stabilised the chamber was maintained at each temperature point for 5 minutes.

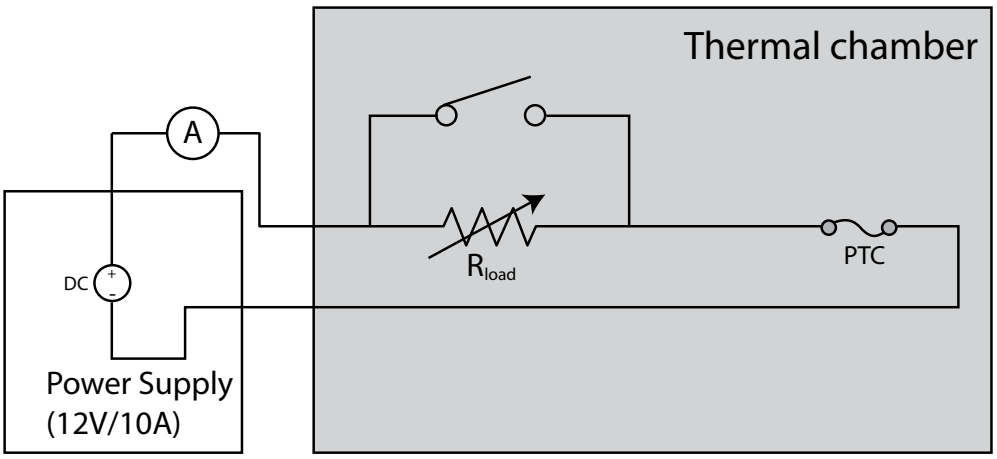

Figure 33

PTC reset test in thermal chamber, circuit configuration

With a 10A current applied the PTC quickly tripped to the high-impedance mode. When the resistive load was switched in to reduce the current, the PTC did not reset, even when the chamber temperature was progressively dropped to -30°C to cool the PTC. The chamber temperature was therefore maintained at -30°C and the power-supply voltage was dropped until the PTC reset. The results, presented in Table 3 show that in the tripped state the PTC resistance varied considerably. The key parameter which seemed to dictate reset behaviour was the power dissipated in the PTC.

© Crown Copyright 2015

Chamber Temp. °C	Power-supply voltage (V)	Current (mAmps)	Load resistance (R_{LOAD}) (Ohms)	PTC resistance R_{PTC} (Ohms)	Total circuit resistance R_{TOT} (Ohms)	PTC power dissipated P_{PTC} (Watts)	
0	12.0	308	0	39.0	39.0	3.70	
0	12.0	360	4.99	28.3	33.3	3.67	
-2.5	12.0	314	0	38.2	38.2	3.77	
-2.5	12.0	370	4.99	27.4	32.4	3.76	
-5.0	12.0	320	0	37.50	37.5	3.84	
-5.0	12.0	380	4.99	26.6	31.6	3.84	
-7.5	12.0	328	0	36.6	36.6	3.94	
-7.5	12.0	385	4.99	26.2	31.2	3.88	
-10.0	12.0	336	0	35.7	35.7	4.03	
-10.0	12.0	395	4.99	25.4	30.4	3.96	
-15.0	12.0	349	0	34.4	34.4	4.19	
-15.0	12.0	418	4.99	23.7	28.7	4.14	
-20.0	12.0	362	0	33.2	33.2	4.34	
-30.0	12.0	480	4.99	20.0	25.0	4.61	
-30.0	12.0	390	0	30.8	30.8	4.68	
-30.0	10.0	730	4.99	8.7	13.7	4.64	
-30.0	10.0	470	0	21.3	21.3	4.70	
-30.0	9.0	1680	4.99	0.36	5.36	1.01	RESET

Table 3

Results of PTC reset test with variable circuit load

A second, similar test was run, with the external load varying between a short and 10 ohms. The results indicated similar PTC behaviour, however the PTC reset at a much higher temperature (+ 2.5°C), due to the reduced current under the higher resistance load. For both PTC reset tests, it was observed that the PTC resistance, R_{PTC}, varied considerably while in the tripped state. Also, as shown in Figure 34, the PTC power value was relatively constant, while in the high-impedance state, and linearly proportional to ambient temperature.

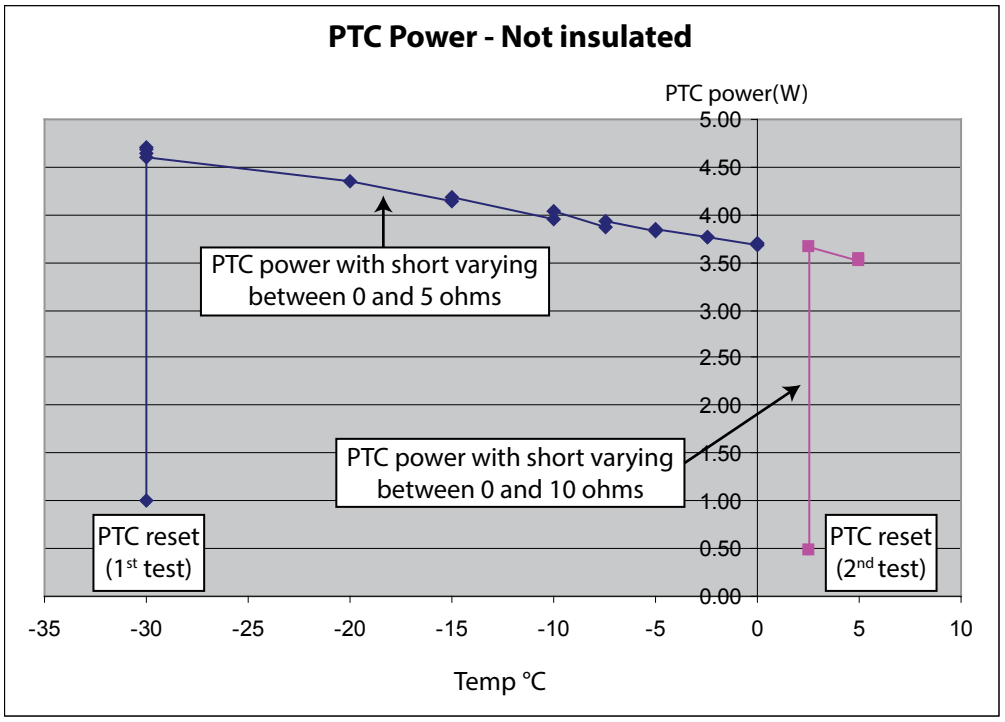

Figure 34

PTC reset test: PTC power versus temperature

A further test was run using a 10 ohm resistor with the PTC wrapped in electrical tape to provide a level of thermal insulation, altering the heat dissipation characteristics of the PTC. As before, the PTC power in the high-impedance state was relatively constant and varied linearly with temperature. However, the power dissipated by PTC was approximately 30% lower due to the effect of the insulation.

1.16.3.7.3 Determination of PTC reset resistance

The PTC reset testing indicated that, once tripped, the PTC would change its resistance as required, to deliver the power necessary to maintain the high-impedance mode. This condition was met for the three PTC reset tests conducted in the thermal chamber. If a change in the electrical circuit or the ambient temperature occurred which made it impossible for the PTC (regardless of its resistance) to maintain the required power, the PTC would reset.

Figure 35 shows a representation of the PTC in high-impedance mode in a typical simple circuit.

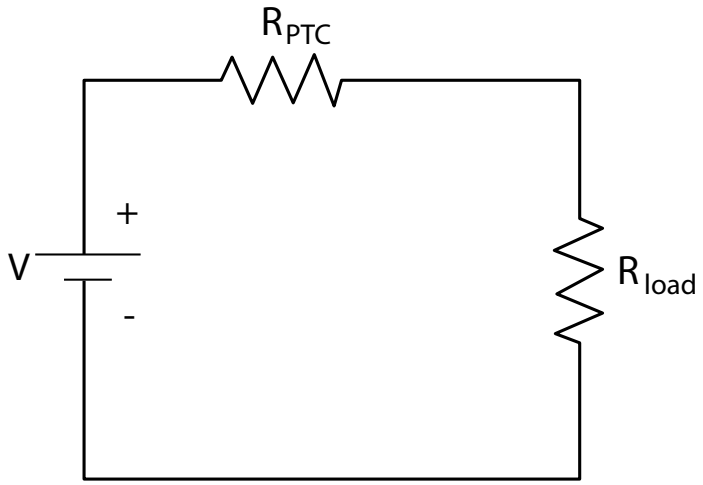

Figure 35

Simple circuit representation of PTC in high-impedance mode

The power dissipated in the PTC can be calculated using the following formula:

$$P_{PTC} = \left(\frac{V}{R_{PTC} + R_{load}} \right)^2 R_{PTC}$$

Maximum power occurs in the PTC when R_{PTC} equals R_{LOAD}. R_{LOAD} would include all other resistive loads in the circuit, so in the case of the ELT battery, R_{LOAD} would include the sum of the individual cell resistances. Maximum power can be calculated using the following formula:

$$P_{PTCMAX} = \frac{V^2}{4} \frac{1}{R_{load}}$$

When in the tripped condition, if P_{PTCMAX} is less that than the power required to maintain the high-impedance mode, at a given temperature, the PTC will reset. This relationship allows the reset behaviour of the PTC to be predicted for a given circuit. To predict the PTC behaviour for the ELT battery, the thermal condition of the PTC in its installed condition must be replicated.

A further PTC reset test was performed with the PTC installed in its normal position in a battery pack. The battery was not electrically connected to the circuit, but was used only to recreate the PTC's normal thermal environment, so that a power-temperature curve could be generated.

Once the power-temperature curve is known, the required external resistance for PTC reset can be calculated. A 12V power-supply was used to represent a battery with one depleted cell and four charged cells. The calculated reset

© Crown Copyright 2015

load resistance (with the 0.4 ohms resistance of four charged cells subtracted) would represent the required depleted cell resistance necessary to cause a PTC reset during an external short-circuit of the battery pack. The test results showed that the required depleted cell resistance to reset the PTC could vary from 10.7 to 17.8 ohms over a temperature range from -20°C to 40°C.

1.16.3.7.2 Instrumar PTC mechanical abuse testing

An LR4-380F PTC was subjected to a range of mechanical abuse, applied in stages, to determine its susceptibility to damage. The PTC, in the un-tripped low-impedance state, was bent to approximately 15° until a break in the polymer was felt; it was then bent to more than 90°; and finally twisted slightly. After each stage of abuse, current was passed through the PTC to try and cause it to trip; the PTC functioned normally.

A current below the trip limit was then passed through the damaged PTC and it was twisted further. The two nickel plates, normally separated, of the PTC came into contact, causing a hot spot that vaporised the plastic coating and some of the polymer core material. The PTC did not recover normal functionality.

These tests demonstrated that it is difficult to damage a PTC in the low-impedance mode to the extent where an electrical short, which bypasses the polymer core, is generated. Only extreme mechanical abuse could cause such a failure. In the high-impedance mode however, it is relatively easy to induce such damage. In this state, the polymer core has changed phase to a much softer material. Compressing the device can cause the metal plates, normally separated by the polymer core, to contact each other resulting in an electrical short.

1.16.4 Boeing thermal propagation modelling

Boeing constructed a computational thermal model of the ELT and its battery, to understand the propagation of failures from cell to cell and the key parameters which govern the propagation. The model simulated a short-circuit at the pinched wire location, resulting in the failure of Cell 2, and then predicted the resulting temperature response of the remainder of the battery and ELT case.

The model treated the five battery cells as five individual isothermal nodes, and the PTC as another node. The remainder of the model's 300 nodes represented the ELT case and chassis walls, with the largest concentration of nodes on the top of the ELT case, in particular the battery compartment cover-plate. The model took account of conductive, convective and radiative

© Crown Copyright 2015

heat transfer between cells and from the cells to the air within the ELT, and to the ELT case.

The following assumptions were used in the model:

- The discharge time for each cell was 50 seconds, assuming a hard short-circuit;
- The exothermic reaction time was 10 minutes;
- The electrical discharge energy of each cell was 127.9 kJ[22]. The model allows for full depletion of this energy in each cell prior to failure of the first cell;
- The trigger temperature at which a cell fails is 170°C, marginally below the 180°C melting point of lithium and consistent with the findings from the Root Cause testing. After triggering the initial event, when the predicted temperature response of an adjacent cell reaches 170°C, that cells releases its energy and the simulation continues;
- The thermal capacitance of a cell is 102.9 J/°C and 44.7 J/°C after it has vented[23].

The high concentration of computational nodes on the battery cover plate was intended to allow simulation of the heat energy released from a short-circuit at the location of the pinched wires. The model assumed that this heat was dissipated in the cover-plate, in order to determine whether this heat load could cause failure of Cell 2 or 3 (closest to the pinched wires), before the PTC reached its trigger temperature of 118°C.

The model was run, and following the Cell 2 failure, it predicted a propagating thermal failure through the cell stack, with cell temperatures peaking at 920°C (Figure 36). The time from the initial cell failure to that of the last cell was 5 minutes. The model provided good correlation with the test results from the Root Cause testing.

22 Refer to Section 1.18.A of this report.
23 Based on data from the battery manufacturer.

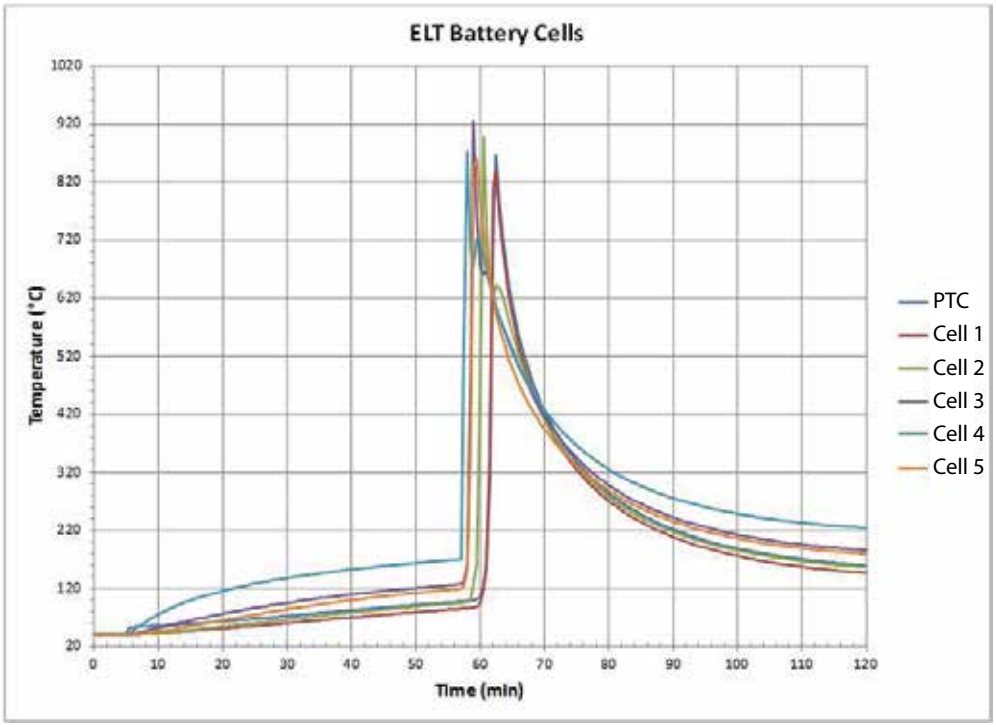

Figure 36

Thermal model prediction of an event initiated by a short-circuit at the location of the pinched wires

Further runs of the model were performed to estimate the possible range of short-circuit resistance values that could lead to a cell failure, prior to the PTC tripping. The results, over a range of possible short currents from 2A to 8.3A (PTC minimum trip current), are shown in Figure 37.

The model predicted that if the short-circuit current was less than approximately 2A, the heat from the short-circuit can conduct through the cell stack and ELT chassis. This would cause the temperature to exceed the PTC switching temperature (118°C). The PTC would therefore trip and protect the battery. (Note: the Capacity and Time-to-fail curves in Figure 37 become asymptotic at 2A).

© Crown Copyright 2015

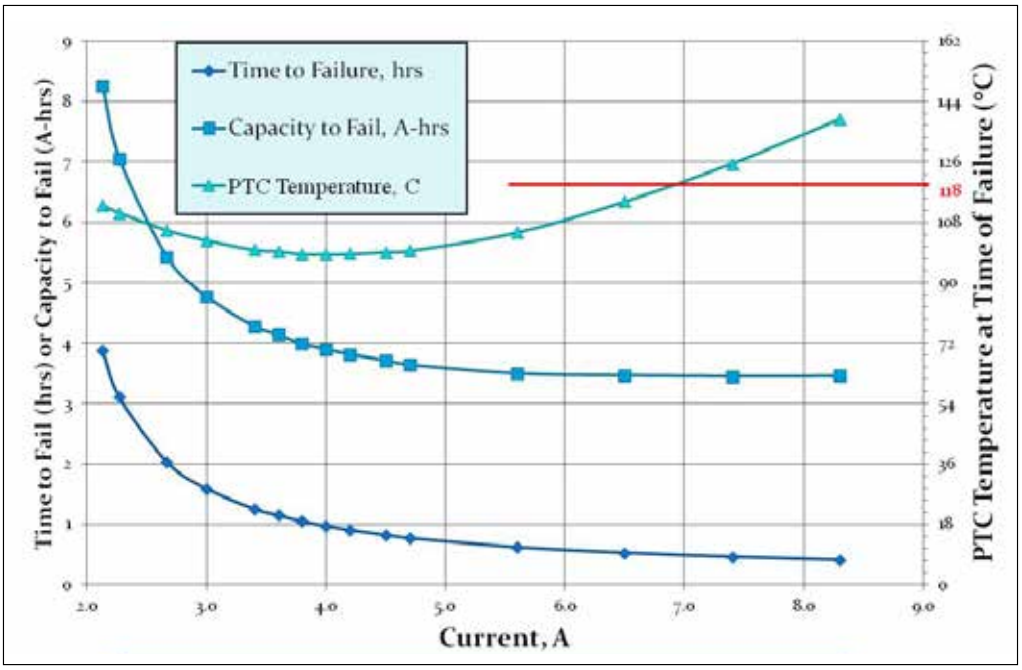

Figure 37

PTC and cell temperature thermal analysis

As the short-circuit current was increased above 2A, the model predicted that Cell 2 could fail when the PTC temperature was below the switching temperature. It showed that the time to failure would drop from 4 hours to 30 minutes as the current increased.

The model showed that the predicted PTC temperature at the time of Cell 2 failure would reach a minimum, at a short-circuit current of approximately 4A. The PTC temperature would then increase as the current increased, due to the dissipated power losses (I^2R) within the PTC.

The model predicted that with a short-circuit current of 7A and above, the PTC temperature would exceed 118°C, causing it to trip and protect the battery.

In summary, a short-circuit current of between 2A and 7A could lead to a cell failure without activation of the PTC. The results of this modelling broadly matched the results of the Root Cause testing, which indicated that a short current below 2A would not result in the PTC tripping.

© Crown Copyright 2015

1.16.5 Calorimeter tests

1.16.5.1 General

The AAIB commissioned a number of tests involving ELT cells and batteries in an Accelerating Rate Calorimeter[24] (ARC). The ARC provides an adiabatic[25] environment, so any heat generated by the cells or battery under the test condition remains in the calorimeter chamber. Calorimeter tests can obtain more accurate data than open or 'free-air' bench tests. The adiabatic environment represents a worst case scenario for heat dissipation and is thus a highly adverse operating environment for cells and batteries. The results of these tests are presented in Appendix B.

1.16.5.2 Specific heat capacity test

In order to understand the heat dissipation requirements of the ELT battery it is necessary to know the specific heat capacity[26] of the individual cells used in the battery. To determine this, three cells from an ELT battery were mounted in the calorimeter and heat was applied directly to the cells in incremental steps via a heating element. The ARC chamber tracked and matched the surface temperature of the cells so that no heat loss occurred. Heating continued until the cells decomposed in thermal runaway.

When heat energy of a known magnitude is transferred to the cells, and no heat loss occurs, then the heat capacity can be calculated from the corresponding increase in cell temperature. However, beyond a certain temperature (approximately 80°C in this case), the internal chemical reaction of the cells will contribute to the cell heating rate and thus the cell heat capacity cannot be correctly measured once this internal reaction begins. Therefore only results up to 80°C were used to calculate the heat capacity.

The average heat capacity of the three cells was determined to be between 0.88 and 0.91 J/gK. The results of this test are presented in Appendix B (i).

1.16.5.3 Battery discharge tests

Three tests were conducted to understand how the ELT battery would behave during discharge in adiabatic conditions. In each test, a cycler applied a 1A

[24] An Accelerating Rate Calorimeter (ARC) is a device which allows exothermic reactions from hazardous and reactive chemicals to be simulated or quantified safely, in a laboratory environment. It is commonly used to evaluate the performance, efficiency and safety of electrochemical cells, which often contain reactive components.

[25] An adiabatic environment is one in which zero heat-loss occurs.

[26] The heat capacity of an object is the amount of energy (measured in Joules (J)) added or subtracted to 1 gram of the material in order to change (increase or decrease) its temperature by 1° Kelvin (K). The specific heat capacity of an object is therefore the heat capacity per unit mass. Specific heat capacity is expressed in units of Joules per gram Kelvin (J/gK).

© Crown Copyright 2015

discharge current to a sample ELT battery. Instrumentation measured the battery pack and cell voltages and thermocouples recorded the individual cell surface temperatures, and the air temperature above the battery.

The heat generated during a battery discharge is a combination of resistive heating due to the discharge current and the chemical reactions within the cells. In these tests, the calorimeter tracked and matched the heat produced by the battery (based on the Cell 3 surface temperature), so that no heat transfer took place between the battery and its surroundings. The thermal data from the discharge tests, together with the specific heat capacity determined in the previous test, allow the heat energy produced by the battery to be calculated. Therefore the energy lost as heat during the battery discharge can be calculated, as well as the energy resulting from the decomposition reaction.

1.16.5.3.1 Battery discharge Test 1

During discharge the battery temperature gradually increased over a period of approximately 8 hrs from an ambient starting temperature of 20°C, until at approximately 98°C, when the battery was 70% discharged, the PTC tripped. The self-heating rate up to this point had been between 0.1 and 0.2°C/min. The test configuration did not allow for measurement of the PTC leakage current or battery pack voltage after the PTC tripped.

After the PTC tripped the battery continued to self-heat. Between 115°C (10 hours) and 122°C (12 ½ hours) the self-heating rate dropped to approximately 0.02°C/min, which is likely to indicate activation of the cell shutdown separators. At around 122°C the Cell 2 voltage began to increase, reaching a maximum of 4.7V, before decreasing again. The self-heating rate began to increase again after the battery temperature reached 132°C (18 hours), exhibiting a very rapid increase at 150°C (22 hours).

At this point the Cell 2 temperature rose sharply, and as the temperature approached the melting point of lithium-metal (180°C) its voltage dropped to zero. This was accompanied by venting and decomposition of the cell under thermal runaway. The failure rapidly propagated to the neighbouring cells in the following order: Cell 1, Cell 3, Cell 4 and Cell 5. The maximum cell temperature measured during the test was 454°C on Cell 2 and the maximum self-heating rate was in excess of 1000°C/min. The results of this test are presented in Appendix B (ii).

Examination revealed that the cell cases were burnt and blackened from the decomposition. However, there was little evidence of carbon powder inside the calorimeter chamber, which indicates that prolonged open flame was not present.

© Crown Copyright 2015

1.16.5.3.2 Battery discharge Test 2

The test configuration for Test 2 was the same as Test 1, except that additional instrumentation was added to record the battery pack total voltage and the PTC leakage current after the PTC trip, and the starting temperature was somewhat higher at 29°C.

As the battery discharged, its temperature gradually increased at a rate of 0.2 to 0.3°C/min until at 113°C (5 ½ hours), when the battery was 50% discharged, the PTC tripped.

The battery continued to self-heat but the self-heating rate dropped to around 0.14°C/min, increasing again only when the battery temperature reached 122°C (6½ hours). Coincident with this, Cell 1 voltage dropped to -9V, making it very resistive and causing the overall pack voltage to drop to 2.15V. The Cell 1 temperature continued to rise at the same rate as the other cells, and approaching 180°C (8¾ hours) the cell temperatures increased rapidly and the remaining cells experienced voltage drops in rapid succession. The cells vented and decomposed under thermal runaway in the following order: Cell 1, Cell 2, Cell 3, Cell 4 and Cell 5. The maximum cell temperature measured during the test was 634°C on Cell 3 and the maximum self-heating rate was in excess of 2,000°C/min. The results of this test are presented in Appendix B (iii).

The cell cases were burnt and blackened and the calorimeter chamber was coated with a layer of carbon, indicating that a significant combustion event had taken place.

1.16.5.3.3 Battery discharge Test 3

The Test 3 configuration was the same as for Test 2. As the battery discharged, its temperature gradually increased at a rate of 0.2 to 0.3°C/min, until at 113°C (6¾ hours), when the battery was 60% discharged, the discharge current dropped to zero. Coincident with the current drop, the Cell 5 voltage dropped to -10V, causing the overall pack voltage to drop to 0.5V. This is indicative of the Cell 5 shutdown separator activating. Once the discharge current dropped to zero, it was not possible to determine whether the PTC subsequently tripped at any point.

Subsequent to this, the self-heating rate dropped to around 0.14°C/min. However, when the temperature reached approximately 120°C (7½ hours), the self-heating rate began to increase steadily. During this time the Cell 5 temperature remained between 6 and 12°C lower than the other cells. A dramatic increase in self-heating rate occurred at approximately 156°C (9½ hours) when

© Crown Copyright 2015

the decomposition sequence began. The cells vented and decomposed in the following order: Cell 1, Cell 2, Cell 3, then Cell 4 and Cell 5 simultaneously.

The maximum cell temperature measured during the test was 562°C on Cell 1 and the maximum self-heating rate was close to 2000°C /min. The results of this test are presented in Appendix B (iv).

The cell cases were burnt and blackened and the calorimeter chamber was coated with a layer of carbon, indicating that a combustion event had taken place, but the level of damage and carbon deposits indicated the decomposition was not as severe as Test 2.

1.16.5.3.4 Thermal and electrical characteristics of the ELT battery

From the results of the specific heat capacity and discharge tests it was possible to determine the heat energy (enthalpy[27]) and the electrical energy generated by the battery during discharge. This provides an indication of the heat dissipation characteristics of the battery. Also, understanding the relationship between the thermal and electrical energy provides an indication of battery efficiency.

Enthalpy and electrical energy calculations, for each of the three discharge tests, are presented in Appendix B (vi). Across the three tests the enthalpy varied between 26.7 and 30.8 kilo-Joules (kJ) and the electrical energy was between 175.7 and 292.3 kJ. Battery efficiency varied between 86.8 and 90.5%, meaning that between 9.5 and 13.2 % of the battery's total energy was released as heat during a 1A discharge. This equated to between 1.8 and 2.6 Watts (W) of heat.

1.16.6 Aircraft structural testing and modelling

1.16.6.1 General

In order to accurately determine the extent of the fire damage to the fuselage structure, in particular how far the structure had been affected beyond the boundary of the visible damage, a test program was developed by Boeing, in conjunction with the AAIB and NTSB. The test program, conducted at Boeing facilities in Seattle, used destructive and non-destructive testing (NDT) to determine the remaining thickness and condition of the resin. The results of these tests were then used to model the residual strength of the structure and provide data to understand the propagation of the fire.

[27] Enthalpy is defined as the thermodynamic potential of a system. The total enthalpy of a system, H, cannot be measured directly, only a change in enthalpy, ΔH, can be measured. ΔH is equal to the change in internal energy of the system, plus the work that the system has done on its surroundings. The unit of enthalpy is Joules (J). In the case of the battery discharge, the change in enthalpy is the heat released by the battery through chemical reaction or external heat transfer.

The principal techniques used on the damaged skin and frame sections, were:

1. 'Ultrasonic pulse-echo': This technique could construct a through-thickness image of the entire test article.
2. 'Through-transmission ultrasonic' (TTU): This technique is normally used for quality control to verify that no delamination is present in new components.
3. X-Ray imaging: This technique provides a quantitative map of resin loss. It requires the use of a sample CFRP 'step wedge' to provide a reference of undamaged structure with known thickness.
4. Computed tomography (CT): Due to limitations on the specimen size, this technique could only be used on small samples to record specific local damage features.

The data generated by NDT techniques 1 and 2 were used to produce damage maps of the crown skin.

After completing the NDT inspections, destructive testing of local areas of the crown panels was undertaken to understand the sub-surface material condition. Fourier-transform infrared (FTIR) spectroscopy was used, in conjunction with microscopy to determine the condition of the resin and the amount remaining in the coupons.

1.16.6.2 Skins and stringers

The results of the ultrasonic pulse-echo and TTU tests on the individual sections of damaged crown skin were combined to produce a mosaic of the skin damage (Figures 38 and 39).

The darker areas in Figure 38 indicate damaged material which does not reflect the ultrasonic wave, including delaminated material not visible to the naked eye.

Figure 39 provides an indication of the depth of undamaged material, measured from the outer face of the skin section. The darker blue areas indicate areas where damage extends through the majority of the skin thickness. The white areas represent areas which have full-thickness delamination. This illustrates that in the region of the ELT, where the fuselage skin has its smallest cross section, all the resin within the CFRP had been consumed. In areas of greater cross section, despite significant visual damage, some resin was still present.

© Crown Copyright 2015

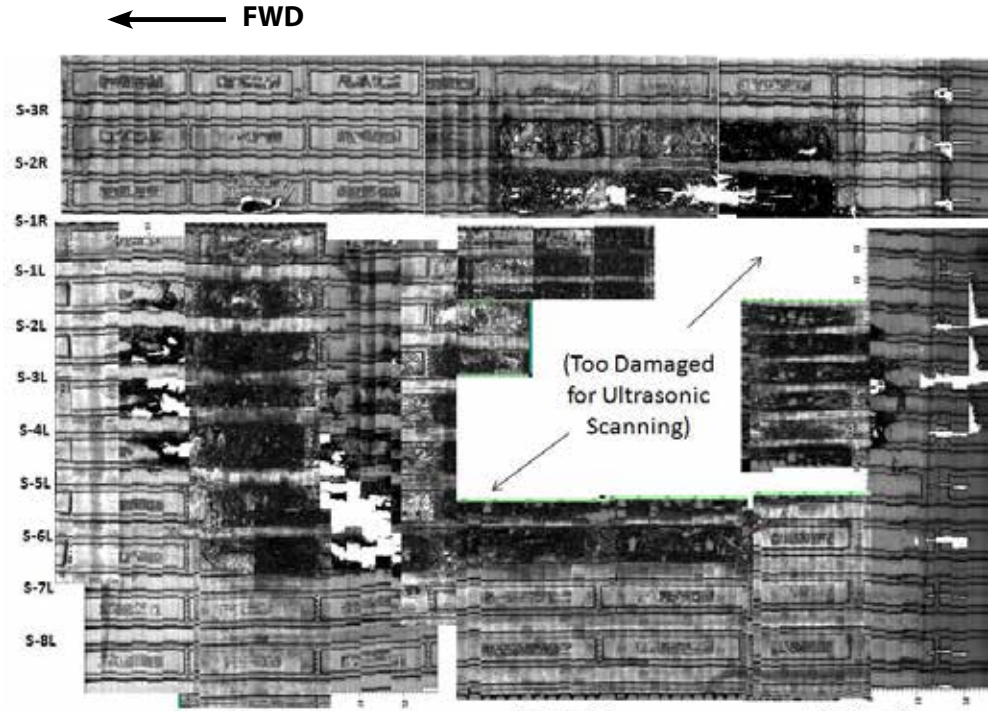

Figure 38

Ultrasonic pulse-echo mosaic of crown skin damage

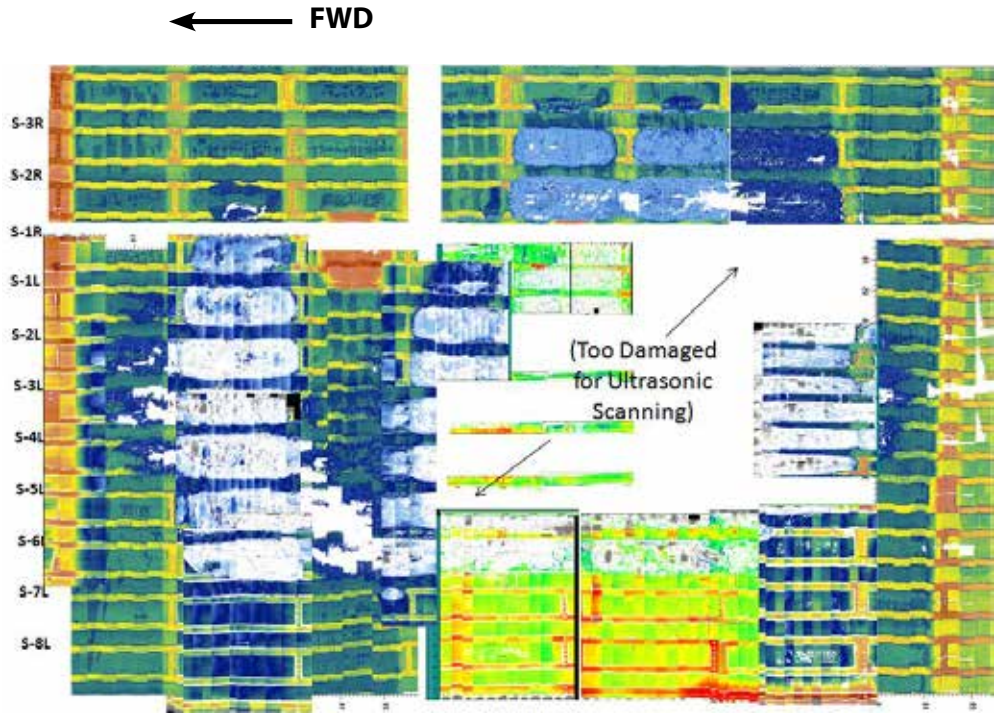

Figure 39

TTU mosaic of crown skin damage

The two sets of results were combined to produce a composite picture of the condition of the crown skin and stringers (Figure 40).

Figure 40

Composite plot of crown skin-stringer ultrasonic test results

1.16.6.3 Frames

A number of frames exhibited evidence of burning on both sides of the frame, yet they still retained some structural integrity. This indicated that despite the visual damage, some resin was present within the CFRP. The use of X-ray examination confirmed that resin was present in the most damaged areas of all frames with the exception of frames 1719, 1744 and 1769, which were the closest frames to the ELT.

All the frames were manually scanned with ultrasonic probes and the damage boundary for each frame was identified. The transition area from heavily burnt sections of the frame to sections with no damage, was typically less than one to two inches.

© Crown Copyright 2015

The data provided by these tests was overlaid on the data obtained during the skin and stringer testing (Figure 40), to produce a combined representation of the delamination of the damaged fuselage structure (Figure 41).

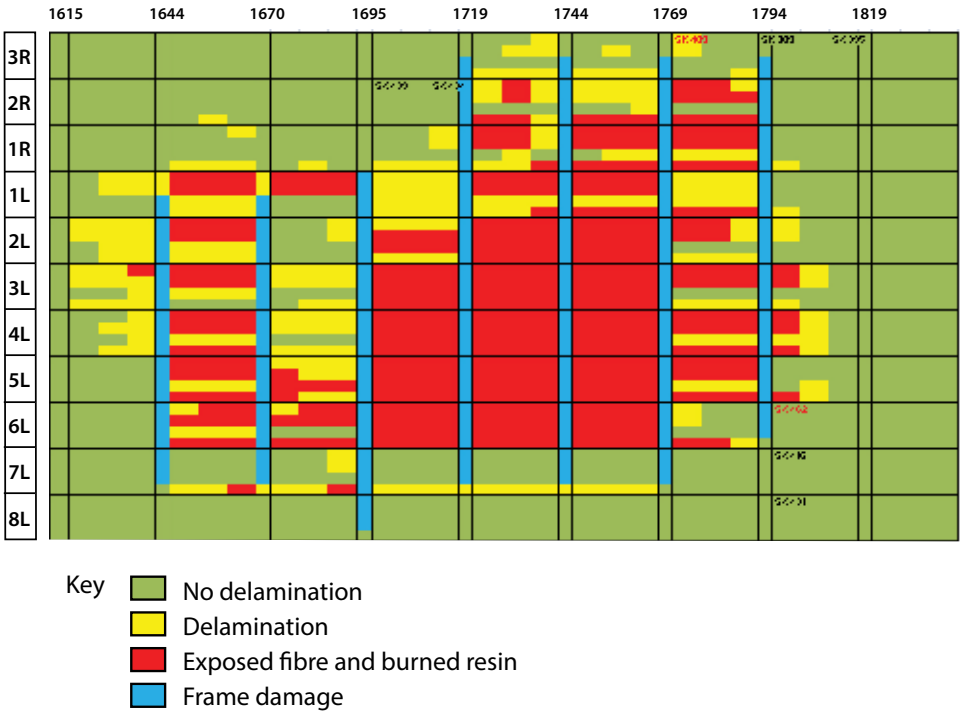

Figure 41

Combined composite plot of skin and frame delamination

1.16.6.4 FTIR test results

The FTIR technique was used to assess the condition of thermally degraded resin beyond the boundary of delamination. The results indicated that within the crown skin, the typical transition zone extended approximately six inches beyond the boundary of any delamination. The FTIR results were superimposed on the composite skin-stringer damage mosaic (Figure 42) to provide an overall image of the damage to the skin panels and the stringer webs (Figure 43).

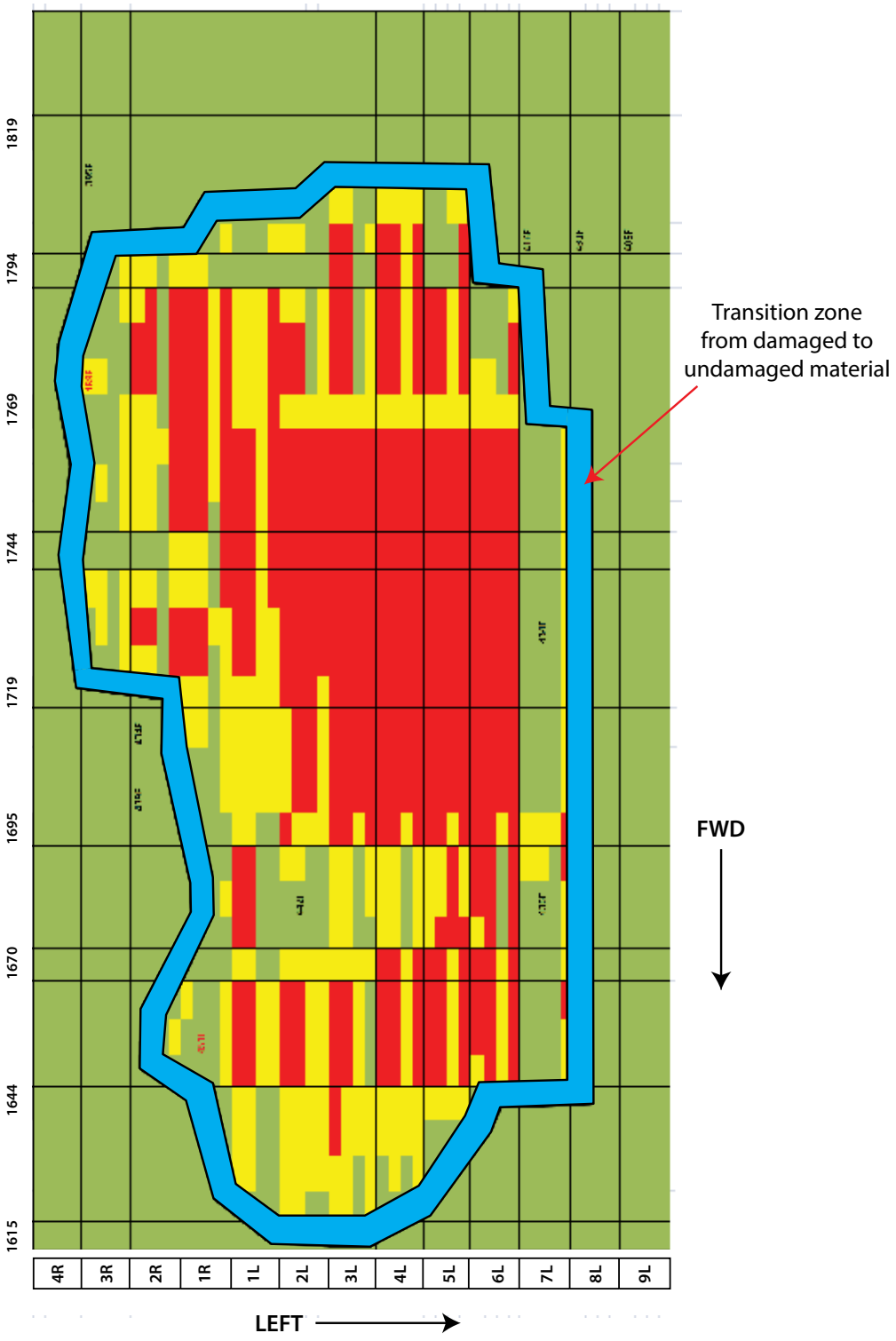

Figure 42

Boundary of damaged skin panel resin

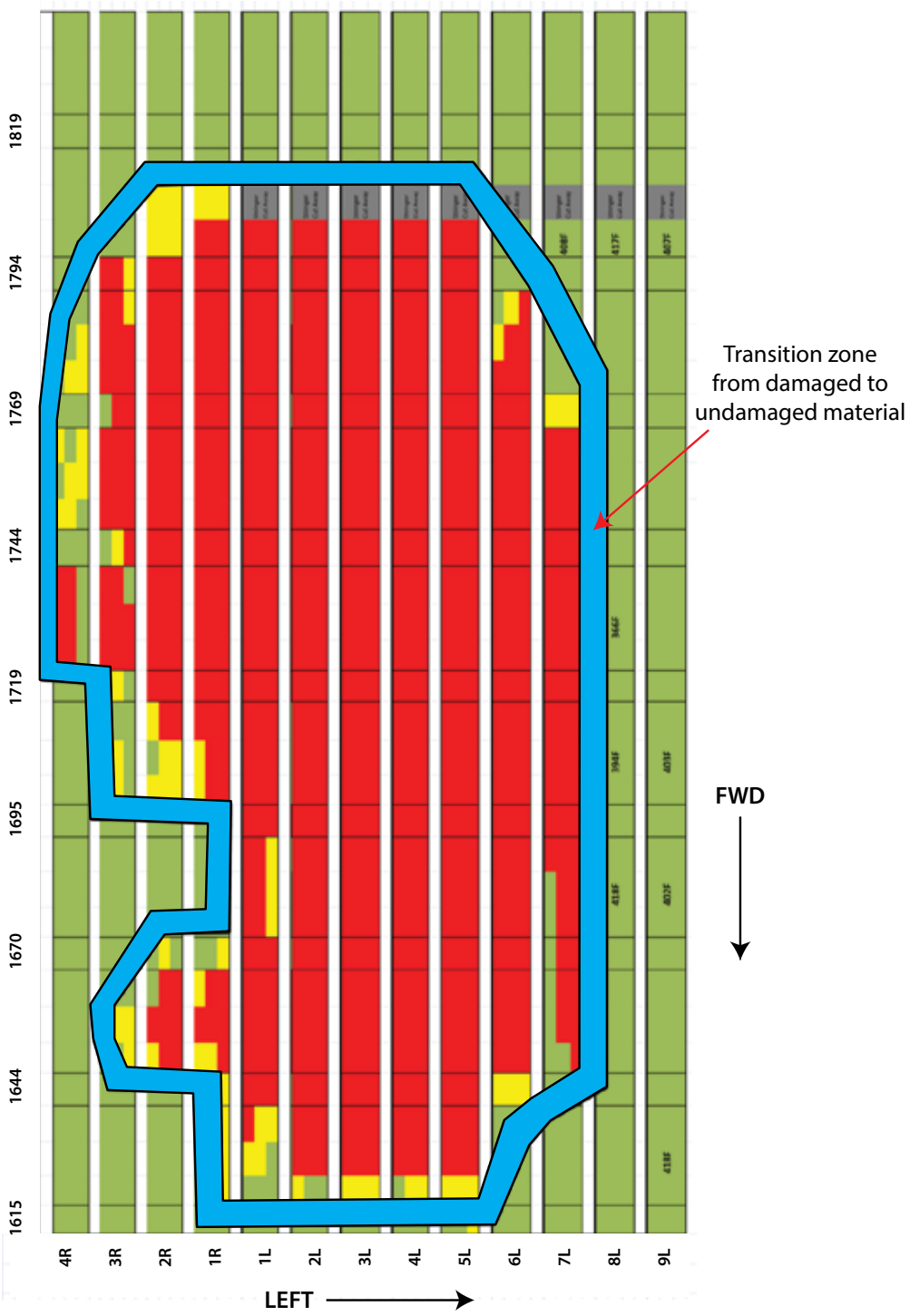

Figure 43

Boundary of thermal damage on stringer webs

1.16.6.5 Thermal modelling

In order to determine if the aircraft would sustain the same level of damage if the ELT fire had occurred in flight, Boeing developed two computational fluid dynamic models to replicate the characteristics of the ground fire. These models used the material properties of the aircraft structure, the predicted ignition energy of the ELT battery failure, the effects of the aircraft's insulation blankets, the assumed temperature in the fuselage crown and the effect of external cooling from airflow. This modelling attempted to examine the factors that would differ between an in-flight and an on-ground event.

FLUENT thermal model

The first model was produced using FLUENT[28] and provided a baseline understanding of the effects of the external air temperatures and velocities, using on-ground and in-flight conditions. This model did not take account of the additional heat that would be produced by the combustion of the CFRP resin and assumed a constant heat source from the ELT battery.

The FLUENT model was designed to replicate the thermal conditions on the ground during the incident and in cruising flight at an altitude of 35,000ft at Mach 0.85. In both cases a constant ELT heat source, a hot gas plume, was assumed. The results of the model are shown in Figures 44 and 45, which provide a side-by-side comparison for the on-ground and in-flight conditions at two arbitrary times, t1 and t2. Time t1 represents a point early in the heating process and t2 late in the process. The comparison between t1 and t2 is used to illustrate the trend in the temperature gradient between the on-ground and in-flight condition.

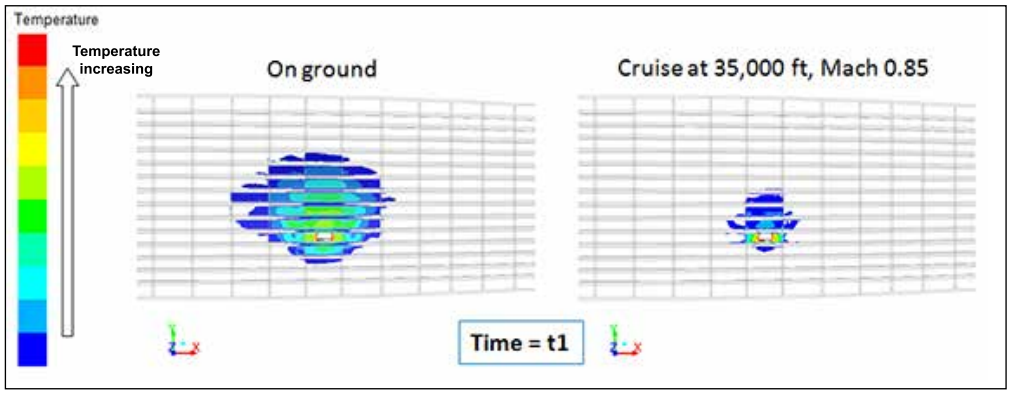

Figure 44

FLUENT model results at time t1

[28] FLUENT http://www.ansys.com/Products/Simulation+Technology/Fluid+Dynamics/Fluid+Dynamics+Products/ANSYS+Fluent

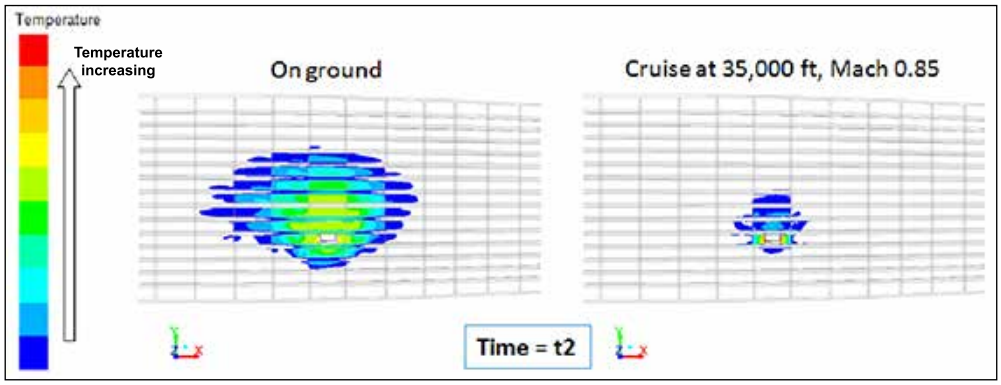

Figure 45

FLUENT model at time t2

The results of the FLUENT model illustrated that, using the on-ground conditions, the temperature of the fuselage skin would continue to increase with time and the heat-affected zone would grow; the in-flight case maintained a nearly constant skin temperature and the elevated temperatures remained local to the heat source.

Fire Dynamics Simulator thermal model

The second thermal model was developed using Fire Dynamics Simulator (FDS)[29]. This simulation used a simplified three-bay model of the fuselage structure to evaluate the interaction of the fuselage and ELT configuration, the thermal properties of the fuselage structure and insulation blankets and the combustion dynamics of the composite structure. This model was first used to produce a qualitative representation of the expected fire propagation during the ET-AOP incident. However, in order for the FDS model to simulate the effects of a hot flame plume on the fuselage skin, it was necessary to introduce an assumed air gap between the skin and the insulation blankets and to remove the insulation blanket adjacent to the ELT within the simulation. This model used an energy release profile for the ELT battery derived from one of the Boeing Root Cause tests (Section 1.16.3).

Due to the variability of the composite combustion process, a worst-case scenario was used, based on a total release of the ELT battery energy and direct flame impingement on the composite structure. The modelling software did not allow the use of typical in-flight cruise conditions, and required the use of a lower heat transfer coefficient than would be likely in-flight. This led to the modelling results being more severe than actual conditions in cruise flight and therefore introduced conservatism into the simulation.

[29] Fire Dynamics Simulator, NIST http://www.nist.gov/el/fire_research/fds_smokeview.cfm

The fire progression in the on-ground and in-flight simulations at four arbitrary times, t1, t2, t3 and t4, are shown in Figure 46. The results show that the effect of external in-flight cooling decreases the flame propagation rate within the structure and limits the damage. It also demonstrates that when the heat transfer rate is high, the fuselage frames become a more effective barrier to fire progression, and the in-flight fire is restricted to a single bay before self-extinguishing. Had the model used a heat transfer rate more representative of cruise conditions, it is likely that this damage would be limited further.

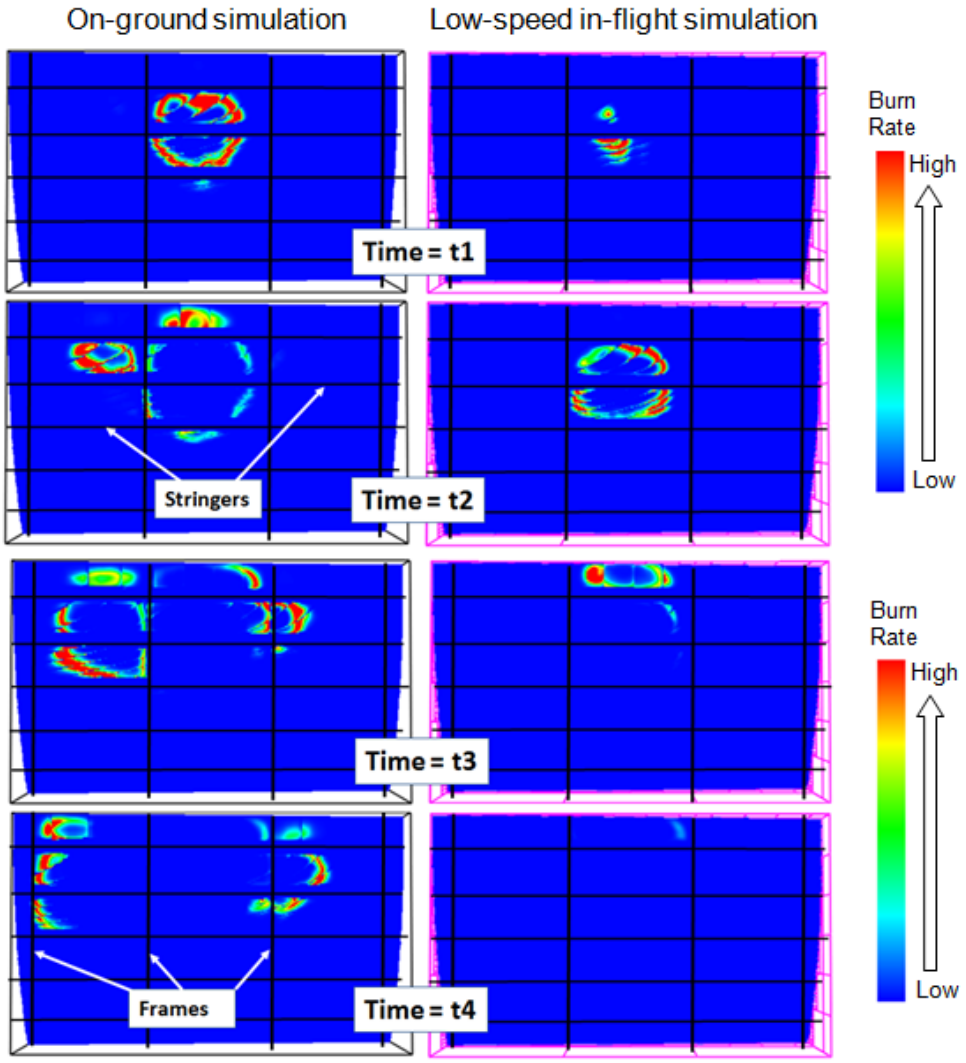

Figure 46

FDS fire model results

It was not possible to produce results which were directly comparable to the ET-AOP incident due to the lack of data regarding the initial state of the fire, the limitations of the FDS software and the assumptions made during the modelling. It did, however, produce a qualitative comparison of the probable flame propagation rates in differing flight conditions.

© Crown Copyright 2015

1.16.6.6 Structural modelling

Actual damage

In order to assess the effect of the actual damage on the fuselage structure's ability to carry load, a number of assumptions were made which allowed Boeing to generate a representative finite element model of the damaged structure.

It was assumed that the areas of the fuselage structure exhibiting delamination and extensive heat damage were incapable of carrying load. The remaining structure was deemed to have full load-carrying capability.

This finite element modelling showed that the structural damage caused by the ground fire would have rendered the aircraft unable to sustain normal flight loads.

In-flight scenario

The thermal modelling of the in-flight scenario had shown that the amount of convective heat loss from the structure would result in significantly different temperatures to the incident ground fire. To understand what the effect would be on the aircraft's structure, the in-flight temperature profile from the thermal modelling was used to identify where the load-carrying capability of the structure would have been reduced or non-existent.

Two different structural damage scenarios were developed within the finite element model to assess the load-carrying capability of the crown skin in the event of an in-flight fire.

The first, a worst-case scenario, assumed that an area of structure equivalent to 18 stringer-frame bays (Figure 47), had no remaining structural strength and the adjoining bays had reduced strength. The results of the finite element modelling indicated that for this scenario cabin pressure would not be maintained but the fuselage would remain capable of carrying flight loads.

© Crown Copyright 2015

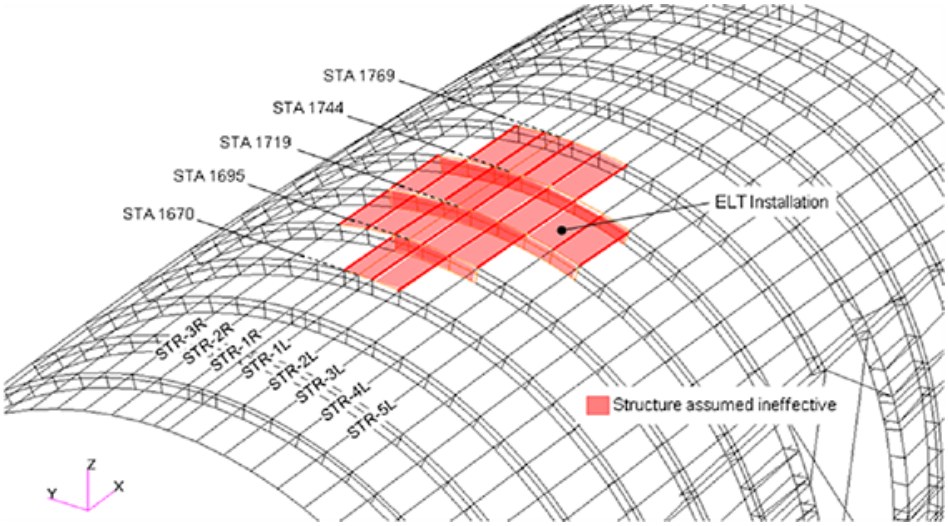

Figure 47

In-flight fire - large area of skin damage

The second scenario, assumed that a smaller area of damage, equivalent to 5 stringer-frame bays, was unable to carry structural loads (Figure 48).

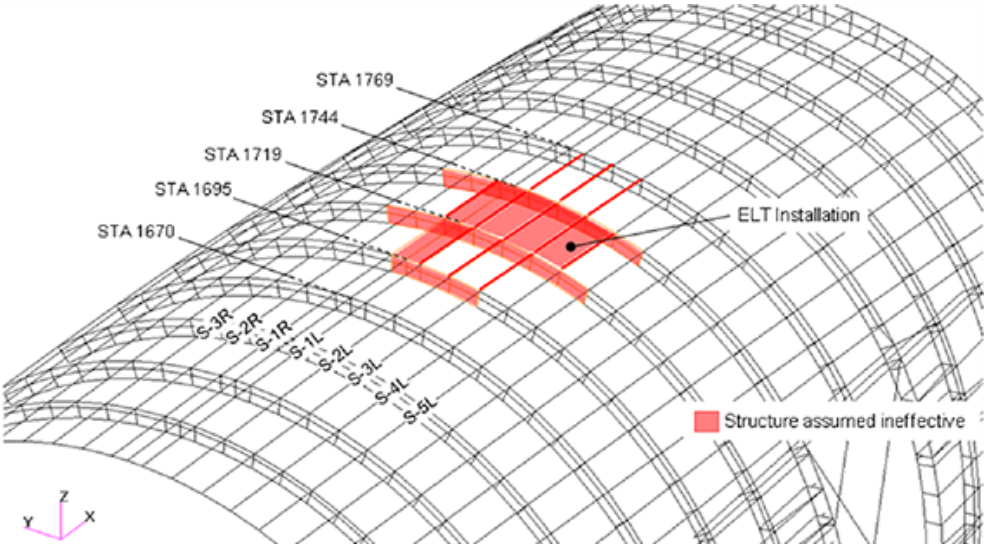

Figure 48

In-flight fire - small area of skin damage

The results of the finite element modelling for this scenario predicted that the fuselage would remain capable of maintaining cabin pressurisation loads and flight loads.

1.17 Organisational and management information

Not applicable.

1.18 Additional information

1.18.1 Failure modes and design considerations of lithium-metal batteries

1.18.1.1 Failure modes of lithium-metal batteries

Lithium is the lightest of all metals, has the highest electrical potential and is highly reactive and flammable. These properties give lithium a very high energy density, making it ideal for use in batteries. Large amounts of energy can be stored in very small volume, lightweight, long-life cells. The energy can be extracted rapidly, with cells capable of delivering high currents.

However, because of the energetic materials used, precautions are necessary in the design, test, utilisation and storage of lithium-metal batteries for use in aircraft applications.

In particular, lithium-metal batteries may be sensitive to thermal, electrical or mechanical abuse. Known failure modes of lithium-metal batteries include:

- external short-circuit in the battery circuit;
- internal short-circuit within the cell, from contact between the electrodes, which can be caused by failure of the separator, manufacturing defect such as an inclusion, or perforation of the separator due to defect, impact or puncture;
- over-discharge, discharging the battery beyond its capacity;
- over-charge; attempting to charge a non-rechargeable battery;
- external heating;
- over-heat (self-heating);

External and internal short-circuits can lead to rapid and uncontrolled discharge and over-discharge of a cell. All of these failure conditions lead to elevated temperature within a cell, resulting in the generation of heat and gas as the electrolyte starts to boil. The pressure within the cell will start to increase. If the cell can adequately dissipate the heat generated, no adverse outcome will occur.

However, if the heat generated by a cell is greater than the heat it can dissipate, the cell temperature will continue to rise. If the temperature

approaches 180°C, the melting point of lithium-metal, the cell will decompose in a highly reactive manner, known as thermal runaway, which can involve violent venting or rupture of the cell, explosion and the release of toxic gas, flammable electrolyte and flames.

1.18.1.2 Design considerations and safety features of lithium-metal batteries

Thermal stability is a key criterion in battery design and installation. Therefore cell and battery designs typically include thermal protection devices and other safety features to mitigate against the risk of thermal runaway. The battery or equipment installation should also ensure that heat generated by the battery can be readily dissipated.

The cells of the battery in the RESCU 406AFN ELT have two safety vents in the base of the cell, intended to provide a controlled release of pressure if a thermal event occurs; the cell separator is designed to become less porous above a certain threshold temperature and shut down the electrochemical reaction within the cell. The PTC is intended to protect the battery from external short-circuits, over-current and over-temperature conditions by limiting the amount of current that can flow under the fault condition.

1.18.1.3 Cell internal resistance

The internal resistance of a cell is dependent on cell size, design, and chemistry. Li-MnO_2 cells tend to have higher relative resistance than conventional cells of the same size and construction, due to the lower conductivity of the organic-solvent based electrolytes used in them. However designs that maximise electrode area and decrease electrode spacing, such as spiral-wound cells, reduce the internal resistance[30].

A cell's resistance increases as it depletes during discharge. Generally, resistance is a mirror image of the voltage profile, remaining fairly constant for most of the discharge and increasing at the end of life[31].

1.18.1.4 Cell imbalance and voltage reversal

Batteries comprised of multiple cells connected in series can be prone to negative effects from cell imbalance, which can result in a slow degradation of the battery. No two cells are identical; there will always be slight differences in the capacity, state-of-charge, self-discharge rate and internal resistance, due to manufacturing variance, even between cells from the same production

[30, 31] '*Linden's Handbook of Batteries*', Fourth Edition, edited by Thomas B. Reddy, Pg 14.59, McGraw Hill (2011), ISBN 978-0-07-162421-3.

© Crown Copyright 2015

lot[32]. Thermal differences across a battery pack can also result in different self-discharge rates of the cells.

In an unbalanced battery pack, the cell with the smallest capacity is a weak point. During discharge, weaker cells tend to have a lower voltage, due either to higher internal resistance or the faster rate of discharge that results from their smaller capacity. Weak cells can therefore be 'over-discharged', while other cells are only partially discharged.

If the weak cell reaches discharge level ahead of the rest, the remaining cells can force current through the discharged cell, driving its voltage below 0V. The cell's internal resistance can create a resistive voltage drop that is greater than the cell's electrical potential. This is known as 'cell reversal' or 'voltage reversal', as the cell experiences a reversal of its polarity.

Cell reversal can result in undesirable and irreversible chemical reactions and elevated cell temperatures, which can cause permanent damage to the cell and lead to a large increase in internal resistance.

Cell reversal is a characteristic event which can precipitate a significant thermal event and violent cell decomposition.

1.18.1.5 Balanced packs

Cell selection is important to achieve a balanced battery pack. Cell capacity is dictated by the amount of reactive materials in the cell and can be controlled by careful metering of the materials during cell production. It is possible to measure internal cell resistance and group cells of similar resistance together. In this way variability between cells can be minimised and batteries can be constructed using matched cells, from the same manufacturing batch. However individual cell variations can still lead to a divergence in cell voltages over time.

Battery balancing is a technique employed in more complex batteries with a Battery Management System (BMS), which transfers energy between individual cells to achieve a balanced pack. However, there is no means to achieve cell balance in the ELT battery, or in any non-rechargeable battery.

[32] '*Cell balancing buys extra run time and battery life'* – Shiua Wen, Analog Applications Journal 1Q 2010, Texas Instruments.

1.18.2 Additional information on the PTC

1.18.2.1 Installation guidance for the PTC

The specification sheet for the PTC includes the following generic installation guidance:

> *'[Polymeric] PTC devices operate by thermal expansion of the conductive polymer. If devices are placed under pressure or installed in spaces that would prevent expansion, they may not properly protect against damage caused by fault conditions. Designs must be selected in such a manner that adequate space is maintained over the life of the product.'*

and:

> *'Twisting bending or placing the PTC device in tension will decrease the ability of the device to protect against damage caused by electrical faults. No residual force should remain on [the] device after installation. Mechanical damage to the PPTC device may affect device performance and should be avoided.'*

1.18.2.2 PTC testing

The LR4-380F PTC meets the standards documented in UL 1434[33]. The associated qualification testing requires that PTC devices are subjected to 6,000 trip events at their rated voltage and current. It also requires that the PTC is subjected to 'trip endurance' testing, where it must operate continuously under power for 1,000 hours after tripping at the rated voltage current. The devices must exhibit expected PTC behaviour after exposure to these conditions.

If a PTC fails, it must fail in the high-resistance mode, with no arcing or burning.

1.18.2.3 Selection of the PTC for the ELT battery

The Ultralife ELT battery was designed as a replacement for an obsolete ELT battery manufactured by a previous supplier to Instrumar (see section 1.18.7.4) which already included a PTC. Instrumar requested that Ultralife produce a similar battery. The intended design function of the PTC was to protect against external short-circuits. During the investigation, Ultralife stated that they did not have documentation relating to the selection criteria for the PTC or the rationale for selecting this particular PTC for use in the ELT battery application. The maximum operating voltage of the PTC is 15V and

[33] Underwriters Laboratories: UL 1434 – Thermistor-type Devices.

Ultralife assumed that in a short-circuit scenario the battery voltage would drop, bringing it within the 15V capability of the PTC.

Published data from the PTC manufacturer[34] suggests that designers of equipment wishing to use a PTC should consider hold and trip currents, the effect of ambient conditions on device performance, device reset time, leakage current in a tripped state and automatic or manual reset conditions. It also suggests that a failure to understand the precise nature of the device's resettable functionality may lead to improper use of the PTC device in a circuit. Lastly, this document also provides guidance on choosing between a fuse[35] and a resettable PTC device for circuit protection. It suggests that in certain circumstances, particularly where restoration of normal circuit operation (after a PTC trip and reset) poses a potential safety hazard or might require maintenance intervention, a fuse may be the preferred form of circuit protection.

1.18.3 Manufacture of the ELT battery

1.18.3.1 General

The AAIB conducted a visit to the Ultralife cell manufacture and battery assembly facilities in Newark, New York. No Li-MnO_2 D-cells were being produced during the visit, however the production of similar Li-MnO_2 cells using the same equipment, materials and processes was observed. The AAIB did not have concerns about the cell production process. There was no ELT battery assembly scheduled during the AAIB visit and this process was not observed.

1.18.3.2 Cathode manufacture

The calendaring, rolling, cutting to size and cleaning operations of the cathode manufacturing process are all automated. The welding of the cathode tab in the centre of the cathode strip is also automated. Throughout the process the cathode material is subject to various weight and thickness checks to ensure consistency and quality. A visual check is also performed for any inclusions, defects or sharp edges which could pierce the separator or any lack of uniformity in the cathode coating, which could affect cell performance. Any cathode strips which do not meet the required criteria are rejected. The cathode material and manufacturing process are selected to optimise the cell capacity and discharge performance.

[34] TE Connectivity Technical Paper: *'Fundamentals of Resettable Functionality in PPTC devices'*, dated 2011

[35] A fuse is on over-current circuit protection device that activates or 'blows' when too much current flows through it. A thin strip of metal wire in the fuse melts, breaking the electrical circuit so that current stops flowing. This results in a permanent open-circuit condition.

Lithium-metal reacts violently with water, so the cathode strips are oven-dried to reduce moisture content and then oven-stored at a lower temperature, until required to be used.

The lithium foil anode is bought pre-assembled on a spool, with the copper current collector strip already embedded.

1.18.3.3 Cell assembly

Cell assembly is conducted in a dry-room. A winding machine is pre-loaded with spools of lithium foil and separator material and the pre-cut cathode strips are manually loaded. A pre-determined length of the electrodes and separator material are auto-wound on a mandrel before being placed inside a cell can. The width of the anode is slightly less than the cathode, to reduce the likelihood of any sharp edges on the cathode protruding through the separator during the winding process. The anode tab is welded to the lithium foil during the winding process. The amount of metallic lithium in each cell dictates the initial cell capacity. Automation of the cell winding process ensures that a consistent amount of lithium-foil goes into each cell.

The cathode tab is then welded to the positive terminal on the cell header, and the anode tab is folded between the cell can and header, before the header is welded to the can. A metered volume of liquid electrolyte is automatically dispensed into each cell under vacuum conditions, via the fill port which is then crimped shut. The quantity of electrolyte in the cell is chosen to allow full saturation of the cathode and the separator. Between each assembly step, electrical checks are performed on each cell. An audible alarm is sounded if any internal short circuit conditions are detected and the cell is then rejected.

1.18.3.4 Cell acceptance testing

All cells are subject to a pre-discharge step immediately after assembly, where a small amount of the cell's total energy is removed at a high rate, using constant current load. This process burns off any impurities in the lithium, removes any residual moisture and ensures the formation of a passivation layer on the surface of the lithium anode, which is essential to obtain good high-rate performance. The cell voltage is monitored to ensure the cell connections can maintain the current.

The cells are also subject to 100% vacuum leakage checks, after which they are examined for any signs of leakage. The cells then undergo an oven recovery step where they recover some of the capacity lost in the pre-discharge step.

© Crown Copyright 2015

Lastly the cells are subject to 100 % OCV and CCV testing. The OCV must be between 3.22 and 3.30V and the CCV must be greater than 2.8V, under a 3 ohm load.

1.18.3.5 Battery assembly

Battery assembly is a manual process. Small insulator discs are placed around the positive terminal of each cell, before the series connection tabs are welded. The battery wiring harness is supplied preassembled with the PTC attached to the negative wire, and the positive tab on the positive wire. These are welded to Cell 5 and Cell 1 respectively and the tabs are then bent at 90^{o} so that the wires run sit in the gap between adjacent cells. Glue is applied, cardboard insulation and foam pads are added before the whole pack is encased in a PVC heat-shrink case.

1.18.3.6 Battery acceptance tests

5% of assembled battery packs are subjected to a check of the external dimensions and the length and orientation of the battery wires. If any batteries fail this check, the entire production lot must be 100% checked.

OCV and CCV checks are performed on 100% of batteries, however only 5% of the results are recorded. OCV must be between 16.1 and 16.5V; CCV must 12.5V or above. Label placement is also checked on all batteries.

No other electrical checks are performed on the assembled battery pack.

1.18.4 ELT battery internal energy

Each lithium cell is designed to deliver a certain amount of electrical energy, assuming it is released at the intended rate. This is governed by depletion of the lithium in the cell. However, in a thermal decomposition event such as that on ET-AOP, all of the components within the cell may be converted into thermal energy. This chemical energy can represent substantially more energy than the available electrical energy.

In a thermal event in which there is sufficient oxygen for the cell components to burn fully, the estimated total energy of an 11.1Ah Li-MnO_2 D-cell will have the following values in kilo-Joules[36]:

[36] Based on data provided by the cell manufacturer.

Component	Energy (kJ)	% of total cell energy
Lithium	32.0	6.15 %
Electrolyte	327.9	62.96 %
Cathode	109.2	20.98 %
Separator	51.6	9.91 %
Total	**520.8**	**100 %**

Table 4

Estimated breakdown of chemical energy in an 11.1Ah Li-MnO_2 D-cell

Under normal discharge conditions the 11.1Ah Li-MnO_2 D-cell can deliver approximately 128kJ (3.2V x 11.1Ah x 3600 secs/hour) of electrical energy.

A fully charged cell in a thermal event will release approximately 521kJ of energy. A depleted cell will release 521kJ minus a portion of the 128kJ of electrical energy removed by depletion.

For the ELT battery pack these figures would be multiplied by the number of cells (5), giving an estimated total energy per pack of 2,605kJ, of which 640kJ (24.5%) is comprised of available electrical energy.

1.18.5 Previous events

1.18.5.1 RESCU 406AFN ELT wiring anomalies

At the time of the incident to ET-AOP there were approximately 3,650 identical batteries in service, installed in RESCU 406AFN and the similar RESCU 406AF ELTs, fitted to numerous aircraft types. There were also approximately 2,900 similar batteries, using the same cell, installed in the Honeywell Portable ELT RESCU 406SE. Honeywell reported that they were not aware of any previous in-service thermal events involving these batteries or cells.

In February 2013 Honeywell became aware of battery wiring anomalies on a RESCU 406AFN ELT returned by an aircraft manufacturer due to a discharged battery. Inspection of the unit found the battery wires trapped under the cover-plate, cuts in the gasket and insulation damage exposing the positive conductor. There was no evidence of thermal damage to the battery.

As a result of these findings Honeywell conducted a quality review, resulting in modification of the Instrumar ELT assembly instructions, to route the wires through the battery pull-tabs, and better contain them within the battery

© Crown Copyright 2015

compartment. This corrective action was introduced in April 2013 on newly manufactured ELTs. No inspections or modifications were recommended for ELTs already delivered. The findings were not communicated to customers / aircraft manufacturers.

Following the ET-AOP incident in July 2013, all in-service RESCU 406AF AFN ELTs were subject to a mandatory one-time inspection as a result of Airworthiness Directives issued by the FAA, EASA and Transport Canada (see Section 1.18.3). While there is no formal means for an equipment manufacturer to track compliance with such inspections, a review of Honeywell and Instrumar ELT returns data for the period July 2013 to mid-July 2014 showed that 360 ELTs had been returned. The units were returned for a variety of reasons including the battery being damaged, expired or requiring upgrade; damaged or pinched battery wires; damage to the gasket or foam; circuit card failures; labelling issues; problems with the switch; and lightning damage. Many of the ELT units were returned with multiple findings.

Of the units exhibiting wire damage, this included pin damage on the connector, tool marks on the wires, minor nicks or other damage to the insulation causing the conductor to be exposed. Trapped wires were observed on 33 of the units.

As of August 2014 a total of 35 ELTs had been identified with trapped wires. Of these, 27 had either the positive, or both wires trapped, ten of which had the positive conductor exposed. Seven of these ten units were returned with fully charged batteries, indicating the exposed conductor had not resulted in a short-circuit.

Of the remaining three units, one was the unit with the depleted battery identified in February 2013. Honeywell concluded that the exposed positive conductor had created a short-circuit, but the PTC had worked as designed, resulting in benign depletion of the battery.

The second unit was from ET-AOP, and the third unit was returned without its battery installed, so the state of charge of that battery is not known. Honeywell assumed that this battery had discharged. However, the unit exhibited no evidence of a thermal event, indicating that any associated battery failure was benign.

Honeywell was unable to determine whether the trapped wires on the returned units had occurred at the time of manufacture, or at a subsequent point. Honeywell does have some previous experience of customers disconnecting the ELT battery upon delivery of the unit and then reconnecting it prior to aircraft delivery, as a means of extending battery life. However, there was no evidence to indicate that this had occurred on the ELT installed in ET-AOP.

© Crown Copyright 2015

1.18.5.2 Other ELT battery events

Following the ET-AOP incident, Boeing, who use a number of different ELT suppliers across their fleet, undertook a review of internal and industry reporting databases to determine whether there had been any previous occurrences of thermal events in ELTs powered by non-rechargeable lithium-metal batteries. The search covered the period between 1994 and 2013 and identified seven events. Four of the events related to odours associated with burning or electrolyte venting on portable ELTs. One event related to a burst D-cell in a portable ELT. Two of the occurrences related to single-cell thermal events in a fixed ELT, resulting in localised burning.

The events described occurred on a variety of aircraft types but none occurred on B787 aircraft and none involved Honeywell fixed or portable ELT products. The reporting databases did not contain sufficient information to identify the exact cell chemistry, battery design and circuit protection features of the ELT batteries involved, or the severity of the thermal events.

Additionally, Transport Canada conducted a review of the Service Difficulty Database, which contains over 1,500,000 reports submitted to Transport Canada, FAA and the Australian Civil Aviation Safety Authority. The review searched for all reports relating to ELTs between 2007 and April 2015. Out of 299 reports relating to ELTs, only two referred to an overheat occurrence. One of these occurred on an ELT installed in a helicopter and was unrelated to the ELT battery; the other occurred on a small aircraft and described a bulged ELT case, signifying that the ELT had been subjected to high temperatures. There were no reports of fire in either case. Neither event involved a Honeywell ELT product.

1.18.6 ELT case resistance

Honeywell made resistance measurements on a sample of 64 ELT TUs, between the J1 shield and a point on the chassis. The J1 shield is directly connected to the battery ground lead. Values ranged from 2.5 to 52 milli-ohms, with the vast majority (96%) of units having a case resistance of less than 20 milli-ohms.

© Crown Copyright 2015

1.18.7 Battery and ELT certification and system safety

1.18.7.1 Technical Standard Orders

A Technical Standard Order[37] (TSO) is an FAA document which describes the minimum performance standards required to be met for specified materials, parts or appliances used on civil aircraft. To obtain a TSO approval an equipment manufacturer must produce a 'Statement of Conformance' declaring that their equipment meets all of the requirements of the relevant TSO and submit supporting documentation to the relevant FAA Aircraft Certification Office (ACO) for review. The TSO approval process relies heavily on self-certification by the applicant.

An aircraft manufacturer wishing to install a TSO-approved item on their aircraft must obtain FAA approval to do so and they must demonstrate that it meets all applicable airworthiness regulations. These include FAR 14 CFR parts 25.1301 'Function and installation', 25.1309 'Equipment, systems and installations' and 25.1353 'Electrical equipment and installations.'

1.18.7.2 ELT certification requirements

At the time of development of the RESCU 406AFN ELT, technical standards for the performance of an ELT as a 'stand-alone' item were specified in FAA TSO-C91a 'Emergency Locator Transmitter (ELT) Equipment' dated April 1985, and FAA TSO-C126 '406 MHz Emergency Locator Transmitter (ELT)' dated December 1992.

1.18.7.3 Battery certification requirements

1.18.7.3.1 TSO-C142 '*Lithium Batteries'*

At the time of development of the RESCU 406AFN ELT, technical standards for lithium cells and batteries intended for use in aircraft equipment were outlined in FAA TSO-C142 'Lithium Batteries', dated April 2000. TSO-C142 referred to RTCA[38] document DO-227 'Minimum Operational Performance Standards for Lithium Batteries', dated 23 June 1995 and in paragraph 3 'Requirements,' specifically stated that batteries approved under this TSO must meet the standards described in Section 2.0 of DO-227.

[37] A Technical Standard Order (TSO) approval is one means for a manufacturer to demonstrate that their equipment complies with applicable airworthiness requirements and it is generally used to obtain approval for equipment which can be installed on multiple aircraft types. A TSO approval is a design and production approval for the specified equipment, but does not constitute approval to install and use the equipment on an aircraft. The FAA TSO process is described in 14 Code of Federal Regulations (CFR) Part 21, Subpart O.

[38] RTCA – The Radio Technical Commission for Aeronautics develops technical guidance and equipment standards for use by regulatory bodies and industry. The RTCA is an advisory body to the FAA.

© Crown Copyright 2015

1.18.7.3.2 RTCA DO-227 'Minimum Operational Performance Standards for Lithium Batteries'

General

RTCA document DO-227 contains both requirements and general guidelines for the design, test, application, handling, storage and disposal of lithium cells and batteries.

DO-227 Section 2.0 (Requirements)

Section 2.0 of DO-227, 'Qualification requirements and test procedures,' describes the required 'cell-level' and 'battery-level' tests that TSO applicants must perform in order to qualify their product for use in aircraft equipment. These tests expose the cells and batteries to environmental conditions (shock-loading, temperature-cycling, altitude, decompression, humidity); electrical conditions (discharge, forced discharge, external short-circuit, load profile); and design-abuse conditions (internal short-circuit and venting).

The pass/fail criteria vary from test to test. In general however, the cells and batteries must not exhibit any leaking or venting of electrolyte, distortion, fire, rupture or a change of more than 2% in Open Circuit Voltage (OCV). Predominantly, the DO-227 tests are conducted on cells and batteries in 'free air', at ambient laboratory conditions or, where a test is required to be conducted at a specific temperature, in an oven.

DO-227 paragraph 2.4.1.2 describes the discharge test which requires cells and batteries to be discharged to zero volts at the rated maximum continuous current, at ambient temperatures of -20°C, +24°C and +55°C. When the samples reach zero volts, the forced discharge test, described in paragraph 2.4.1.3, is immediately commenced. The duration of the test is determined by the rated capacity of the cell/battery and the test current.

Paragraph 2.4.1.4 describes the external short-circuit test required to be performed on individual cells (at 24°C and 55°C) and batteries (at 55°C). The short-circuit is created by connecting the positive and negative terminals with a low-resistance conductor. DO-227 does not specify to what capacity, or for how long, the cells or battery should be discharged under the short-circuit condition.

Further, DO-227 paragraph 2.4.2.1 describes the internal short-circuit test which is only required to be completed at cell-level at 24°C. To induce the short-circuit condition, an electrically isolated sample cell is required to be deformed between a rod and a plate, until the OCV drops by at least two-thirds.

© Crown Copyright 2015

DO-227 guidance material

The remaining sections of DO-227 contain guidance on all aspects of cell and battery chemical composition, design, construction, operation and safety.

In Section 1.5 Design Considerations, paragraph 1.5.7 states the following regarding the use of protective devices in battery design:

> *'Fuses, thermal fuses, thermal switches, diodes and other protective devices are recommended for use in lithium batteries to guard against potential hazards resulting from excessive current drain, force discharge into voltage reversal (for weak cells), charging parallel cells strings or charging of a battery from an external source ... Thermal protective devices are to be located centrally within the assembly of cells where the evolution of heat would be expected to be maximized ….. Under certain cell or battery qualification test conditions, such devices may be bypassed, removed or not installed in the interest of acquiring the necessary safety data.'*

The guidance material also includes advice on battery/equipment integration and the associated effects on battery performance. Specifically in respect of thermal management within batteries, DO-227 paragraphs 1.5.10 and 1.5.12 state:

> *'Thermal management within the battery itself, and when installed within equipment, must also be carefully considered in view of the heat developed within the cells or battery, by the equipment, and by the environment.'*

and:

> *'Thermal management is important in lithium batteries because lithium has a very low melting point: 180°C. At or near this temperature lithium may react vigorously with other cell components, and the results could be catastrophic ..... Therefore, in cell and battery design, it is important to ensure that the temperature is maintained well below the melting point of lithium. Additionally, it must be recognized that under certain discharge conditions, significant heat will be generated within each cell….. Heat is dissipated by radiation, conduction and convection; therefore consideration must be given to any aspect of battery design that will influence these parameters.'*

Paragraphs 1.4 and 1.4.1.4 also state:

> *'Proper integration of lithium cells and batteries into aviation-related equipment requires cooperation between the cell supplier, the battery supplier and the equipment designer. Only through this effective cooperative exchange of the equipment's performance requirements and the cell and battery's capabilities and limitations can an effective pairing of equipment and battery be realized.'*

and:

> *'There must be a safety design review including both the designers of the lithium cells or batteries and of the aircraft equipment that the cells and batteries are intended to power. The manufacturer of the airframe in which lithium-battery-powered equipment is to be used should be included in the safety design review.'*

1.18.7.3.3 TSO-C142 amendments to RTCA DO-227

Appendix 1 of TSO-C142 lists a number of FAA-prescribed enhancements intended to modify the requirements and guidance contained in DO-227. However, Appendix 1 is not specifically adopted as a formal requirement in the 'Requirements' paragraph of the TSO.

The enhancements include a modification to the internal short-circuit test procedure and the following modification to the discharge test, described in paragraph 2.4.1.2:

> *'If the sample contains one or more protective devices, the test current shall be just below (by no more than 10 percent) that at which any protective device will activate during the forced discharge test.'*

The modifications also include the addition of a new paragraph in DO-227 dealing with 'Toxic Gas Venting Procedures,' stating:

> *'Batteries that are capable of venting toxic gases shall not be installed or used in the aircraft cockpit because of an increased probability of immediate flight crew impairment.*
>
> *Batteries that are capable of venting toxic gases may be installed or used in an aircraft passenger compartment if the installer shows that a safety hazard would not be created. Methods of preventing a safety hazard may include any of the following:*

> *a. Installing a system for overboard venting, absorption, or containment; or*
>
> *b. Showing that, if venting occurs, permissible exposure limits that are maintained by organizations such as the Occupational Safety and Health Administration and the American Conference of Governmental Industrial Hygienists, Inc. would not be exceeded.'*

1.18.7.3.4 Current battery certification requirements

In August 2006 TSO-C142 was superseded by TSO-C142a 'Non-rechargeable lithium cells and batteries'. Paragraph 3 'Requirements' of TSO-C142a requires compliance with DO-227 Section 2.0, 'as amended by Appendix 1 of this TSO'. Appendix 1 of TSO-C142a includes as formal requirements all of the items previously addressed in Appendix 1 of TSO-C142, plus some additional items. Of particular note, Appendix 1 of TSO-C142a introduces a new requirement: 'Test Procedures for Installed Equipment Performance,' which states:

> *'(a) Because lithium batteries have ignited, vented gas or exploded, we require additional performance standards governing the use of lithium batteries or equipment incorporating lithium cells or batteries on airplanes. Airplane and equipment manufacturers incorporating lithium cells or batteries must ensure that if there is a fire within a single cell of the battery, the equipment unit will contain the fragments and debris (but not smoke/gases/vapours) from a battery explosion or fire.'*

Further, additional fire safety test criteria are specified in TSO-C142a Appendix 1, which include additional external short circuit, crush, over-discharge, overheat and fire tests.

TSO-C142a was an evolution of TSO-C142, updated to reflect new industry knowledge on lithium batteries. As such, there was no regulatory requirement for the FAA retrospectively to review products previously certified to TSO-C142 standards to determine whether they would meet the new requirements of TSO-C142a.

1.18.7.4 Development and certification history of the RESCU 406AF/AFN ELT and ELT battery

Honeywell/Instrumar began development of the RESCU 406AF ELT in 1999 and Honeywell submitted a certification plan to Transport Canada detailing how they intended to demonstrate compliance with the applicable ELT requirements.

The RESCU 406AF battery (Honeywell P/N 1096449-1) was designed and supplied by FRIWO, Germany under contract from Instrumar and included a PTC device. TSO-C142 was not applicable when the certification plan was approved, therefore there was no requirement to conduct a dedicated battery qualification test programme. However, TSO-C91a and TSO-C126 contained some limited battery guidance. The RESCU 406AF ELT received FAA TSO-C91A and TSO-C126 approval on 6 July 2001.

In 2004 Transport Canada requested Honeywell to upgrade the RESCU 406AF battery to meet the requirements of the now-applicable FAA TSO-C142. Ultralife were engaged by Instrumar to develop a new battery, based on the original FRIWO design and to obtain TSO-142 approval from the FAA NY ACO. Honeywell/Instrumar communicated the design specifications for the battery to Ultralife including dimensions, weight, voltage, current and amp-hour capacity. Ultralife subsequently obtained TSO-C142 approval for the new battery (Honeywell P/N 1096801-1) on 28 November 2005. The modified RESCU 406AF received FAA TSO-C91a and TSO-C126 approval on 10 January 2006.

Development of the RESCU 406AFN ELT as a replacement for the RESCU 406AF began in 2005. The certification plan submitted to Transport Canada in March 2005, specified that the RESCU 406AFN would use the existing TSO-C142-approved battery (Honeywell P/N 1096801-1) from the RESCU 406AF. TSO-C142a was not in existence at this time. The RESCU 406AFN ELT received FAA TSO-C91A and TSO-C126 approval on 9 April 2007.

1.18.7.5 Ultralife qualification tests for TSO-C142 approval

Ultralife performed the TSO-C142 qualification testing programme for the ELT battery and its constituent cells. The results are documented in ‘Ultralife TSO-C142 Test Report for P/N U3356 cell’, dated 2 May 2005 and ‘Ultralife TSO-C142 Test Report for battery P/N S00130’, dated 26 August 2005. These reports state that the cells and the battery met all the evaluation criteria of DO-227 Section 2.0 and that no failure conditions were identified during the test campaign. Both the TSO-C142 qualification test reports for the cells and battery contain a compliance matrix outlining how the cells/battery comply with each individual paragraph of TSO-C142, and another compliance matrix detailing how the cell/battery complies with the relevant individual test requirements of DO-227 Section 2.0. Neither compliance matrix makes reference to the guidance contained in TSO-C142 Appendix 1, nor the amendments it infers on the test requirements of DO-227 Section 2.0.

© Crown Copyright 2015

The results for the external and internal short-circuit tests indicated conformance with the DO-227 criteria, but the maximum temperatures reached by the cells or batteries during the tests were not documented in the reports.

1.18.7.6 Honeywell ELT qualification tests for TSO-C91a and TSO-C126

The qualification testing performed on the RESCU 406AFN ELT for TSO-C126 and TSO-C91a approval contained elements of abuse testing (flame, shock, impact and crush tests) on the ELT. In addition, as the RESCU 406AFN ELT had been selected for use on the B787, Boeing defined additional test requirements relating to vibration, acceleration, temperature and temperature variation. Although not intended as battery design-abuse tests, the battery was installed in the ELT when all of these qualification tests were performed and no battery failures were noted.

1.18.7.7 Boeing ELT certification process for the B787

1.18.7.7.1 General

In March 2003, Boeing applied for a type certificate for the B787-8 aircraft. The FAA's Seattle ACO provided oversight of the certification process, in accordance with 'FAR 14 CFR Part 25'[39]. The B787-8 achieved type certification in August 2011 and this certification was validated by the European Aviation Safety Agency (EASA).

Although Boeing had contracted Honeywell Aerospace to design the Navigation Radio System (NRS), overall responsibility for the integration and certification of the NRS, which included the ELT, remained with Boeing, as the aircraft manufacturer. Therefore Boeing developed a B787 NRS Certification Plan.[40] The first revision of the certification plan was approved by the FAA in December 2005, as were subsequent revisions. The latest revision of the certification plan is Revision F, dated January 2010.

1.18.7.7.2 Boeing 787 Navigation Radio System certification plan

The B787 NRS certification plan included a high-level system overview of the NRS and its constituent radios and defined all of the applicable FAA and EASA requirements, TSOs, RTCA documents, Advisory Circulars, FAA Issue Papers and Boeing internal requirements relevant to the NRS. The certification plan also outlined the proposed means of compliance to obtain FAA certification approval for all elements of the NRS, including the ELT. This document stated that:

[39] US Federal Aviation Regulations, 14 Code of Federal Regulations Part 25 '*Airworthiness Standards: Transport Category Airplanes*'.

[40] Boeing document: '*Certification Plan No. 433, 787 Navigation Radio Systems Certification Plan*', dated 6 January 2010.

> *'Honeywell will submit the application for TSO/ETSO approval for each navigation radio system prior to the 787 type certification …… TSO approval letters will be the evidence of the regulators approvals.'*

1.18.7.7.3 Honeywell Navigation Radio System safety assessment

In order for the NRS to comply with the requirements 14 CFR 25.1309 'Equipment, systems and installations,' Boeing required Honeywell to conduct an NRS System Safety Assessment,[41,42] a Functional Hazard Assessment[43] (FHA) and a Failure Modes and Effects Analysis[44] (FMEA), the results of which were then fed into the overall aircraft-level safety assessment.

The NRS safety assessment presented the safety analysis for all elements of the NRS, including the ELT. It evaluated the NRS design for compliance with all applicable regulatory requirements, issue papers and advisory material. Compliance with applicable requirements for the ELT were demonstrated by reference to the qualification tests previously performed for RESCU 406AFN's TSO-C91a, TSO-C126 and TSO-C142 approvals and the additional testing performed to support the Boeing-defined requirements. The results of these tests were reviewed and approved by Boeing.

The NRS safety assessment for the ELT included the results of an ELT FHA and FMEA.

The ELT FHA listed three hazards associated with loss of ELT output or erroneous ELT output, all of which were classified as having a 'Minor'[45] hazard effect. There were no documented hazards relating to the ELT battery.

The ELT FMEA[46] identified a number of possible failure modes for the ELT battery, which were attributed to either an internal open-circuit or short-circuit. However, the effects of these failures were considered only in respect of their

41 Honeywell document '*System Safety Assessment, Boeing 787 Navigation Radio System*', dated 20 June 2008.

42 A safety assessment is a structured process applied to systems that are critical to flight safety, which aims to identify all significant single-failure conditions and to ensure that all combinations of failures which could result in hazardous or catastrophic aircraft-level effects have been considered and mitigated. The system safety assessment process is described in FAA Advisory Circular AC 25.1309-1A '*System Design and Analysis*'.

43 A Functional Hazard Assessment (FHA) is a systematic examination of a system's functions and purpose to determine potential hazards the system can introduce to the aircraft or its occupants.

44 A FMEA is a systematic technique for failure analysis for each component in a system which aims to identify failure modes, their causes and the effects of those failures at the next higher level of a system.

45 'Minor' failure conditions are defined in FAA AC 25.1309-1A as those which would not significantly reduce aircraft safety, and which would involve crew actions that are well within their capabilities. Minor failure conditions may include, for example, a slight reduction in safety margins or functional capabilities, a slight increase in crew workload, such as, routine flight plan changes, or some inconvenience to occupants.

46 Honeywell document '*Failure Modes and Effects Analysis (FMEA) for the RESCU 406AFN ELT*', dated 29 April 2008.

impact on the provision of electrical power to the ELT; the more hazardous effects of a battery fault were not identified. As a result, no failures relating to battery thermal failure were identified in the FMEA.

The provision of a FMEA for the ELT was a Boeing-defined requirement; this was not required by TSO-C126. Similarly TSO-C142 contained no requirement for a dedicated 'battery-level' FMEA. The battery aspects of the Honeywell ELT FMEA were therefore based, in part, on documentation from Ultralife, but Ultralife did not participate in, or directly contribute to, the FMEA process. The TSO-C142 documentation[47] for the battery provided to Instrumar by Ultralife, did not contain information regarding specific battery failure modes. However, it did contain the following statement on generic lithium battery safety concerns in the 'Installation Procedures and Limitations' section:

> *'The conditions and tests required for this TSO approval of this battery are minimum performance standards. It is the responsibility of those desiring to install this battery in a specific class [of] aircraft to determine that the aircraft installation conditions are within the TSO standards. The battery may be installed only if further evaluation by the applicant documents an acceptable installation and is approved by the Administrator. Lithium battery safety concerns include the possibility of fire, venting violently, and venting toxic gases.'*

The Ultralife Material Safety Data Sheet (MSDS) for the lithium-metal cells within the ELT battery, which was included with each battery shipment to Instrumar and which is reproduced in the Honeywell RESCU 406AF and 406AFN component maintenance manuals (CMM), also contained information on lithium-metal battery safety hazards, handling and storage guidance and fire-fighting measures.

1.18.7.7.4 FAA Issue paper SE-09

The NRS Certification Plan made reference to FAA Issue Paper SE-09 'Special Conditions: Lithium-ion battery installations',[48] dated March 2006. During the B787 certification campaign the FAA had determined that existing regulations did not adequately address failure modes and operational characteristics of the rechargeable large-format lithium-ion integral aircraft batteries, intended for use as the B787's main and APU[49] batteries. Although this document was not applicable to the lithium-metal batteries used in the ELT, recognising the

47 Ultralife '*TSO-C142 Test Report for battery P/N S00130*', dated 26 August 2005.

48 SE-09 was published to address known failure modes and operational characteristics of lithium-ion batteries, in advance of certification of the B787-8 main and APU large format lithium-ion batteries.

49 Auxilliary Power Unit.

fact that both types of lithium battery share many of the same failure modes, Boeing requested that Honeywell review Issue Paper SE-09, to show how the identified concerns were addressed for the ELT battery.

SE-09 listed nine Special Conditions (SC), of which six were of possible relevance to the ELT batteries. In particular, SC-2 stated:

> *'The batteries must be designed to preclude the occurrence of self-sustaining, uncontrolled increases in temperature in pressure.'*

Honeywell advised that the cell shutdown separator and the pressure vents would limit any uncontrolled increase of temperature and pressure.

Also, SC-6 stated:

> *'Each battery installation must have provisions to prevent any hazardous effect on structure or essential systems that may be caused by the maximum amount of heat the battery can generate during a short circuit of the battery or of its individual cells.'*

Honeywell advised that the cell shutdown separator would limit temperature to a safe level, and that the battery was installed within a sealed compartment of the ELT transmitter unit. Boeing accepted the Honeywell position on this and documented the response in the Boeing '787 ELT Certification Summary.[50]'

1.18.7.7.5 Boeing 787 ELT Certification Summary

At the conclusion of the ELT certification effort, the B787 ELT certification summary summarised the activities accomplished specific to the ELT, in support of the overall B787 type certification, and documented how compliance had been achieved with all applicable criteria identified in the NRS certification plan. This document was the final engineering deliverable relating to the ELT certification and the ELT installation was approved by the FAA as part of the B787 type certification.

The certification summary included the following statements in respect of compliance with FAR 14 CFR 25.1309 (d)[51]:

[50] Boeing document '*787 Emergency Locator Transmitter (ELT) System Certification Summary*', dated 14 December 2010.

[51] FAR 14 CFR 25.1309 *'Equipment Systems and Installations'.*

> *'The ground test and the functional failure modes for the ELT were analyzed to ensure that any failure, or combination of failures, which would prevent the continued safe flight and landing of the airplane is extremely improbable. There are no ELT failures which could reduce the capability of the airplane or the ability of the crew to cope with adverse operating conditions.'*

and:

> *'The ELT system design was adapted from Boeing legacy airplane design which has been proven over many decades. The assurance level of the Fixed ELT on Boeing airplanes has long been established to be a Level D system[52].'*

1.18.8 Previous Safety Recommendations and safety actions

1.18.8.1 Safety Recommendations issued in AAIB Special Bulletin S5/2013

On 18 July 2013 the AAIB made the following Safety Recommendations in Special Bulletin S5/2013:

> **Safety Recommendation 2013-016**
>
> It is recommended that the Federal Aviation Administration initiate action for making inert the Honeywell International RESCU 406AFN fixed Emergency Locator Transmitter system in Boeing 787 aircraft until appropriate airworthiness actions can be completed.
>
> **Safety Recommendation 2013-017**
>
> It is recommended that the Federal Aviation Administration, in association with other regulatory authorities, conduct a safety review of installations of Lithium-powered Emergency Locator Transmitter systems in other aircraft types and, where appropriate, initiate airworthiness action.

1.18.8.2 Safety actions by industry

Following the ET-AOP incident on 12 July 2013, on 19 July 2013 Boeing issued a Multi Operator Message MOM-13-0570-01B to all B787 operators, recommending that they remove or inspect the RESCU 406AFN ELT within 10 days and provide feedback. The recommended inspection called for

[52] Level D is a Design Assurance level which is consistent with the 'Minor' hazard effect classification of the ELT, as defined by FAA AC 25.1309-1A. It implies that the ELT presents no risk to the safety of the aircraft or its occupants.

removal of the battery cover-plate, inspection for proper wire routing and any signs of wire damage or pinching, removal of the battery and inspection of the battery compartment for any unusual signs of heating or moisture. Boeing recommended that during reinstallation of the battery that the wires were routed through the pull-tabs used to remove the battery and folding over the pull-tabs, to ensure the wires remained within the battery compartment and were not pinched under the cover plate.

On 28 July 2013 Boeing also issued a number of MOMs to operators of all other Boeing aircraft types equipped with Honeywell RESCU 406AF (part number 1152682-1) and 406AFN (part numbers 1152682-2 or -3) ELTs, containing the same recommendations as MOM-13-0570-01B and requesting feedback on findings by 7 Aug 2013.

On 1 Aug 2013 Honeywell issued Alert Service Bulletin (SB) 1152682-23-A22 for RESCU 406AF/AFN ELTs, revised to Revision 1 on 8 Aug 2013. This instructed operators with aircraft equipped with ELTs with part numbers 1152682-1,-2 or -3 and serial numbers prior to 1152682-06131, to inspect the battery 'at the next possible access' for pinched wires, damage to the wires or battery, deformation of the battery cover plate or damage to the battery cover gasket, which may prevent it from forming a water-tight seal and to correct any anomalies.

As a result of the early investigation findings and feedback from the inspections described in the Boeing MOMs and Honeywell Alert SB, Honeywell modified the battery orientation within the ELT on all new RESCU 406AFN production units. This modification, effective May 2014, and also incorporated on all replacement ELT batteries, routed the wires underneath the battery, thereby preventing the possibility of the wires becoming trapped under the battery cover-plate.

1.18.8.3 Safety actions by regulatory bodies

In response to Safety Recommendation 2013-016 the FAA issued Airworthiness Directive (AD) 2013-15-07 on 26 July 2013, effective immediately, requiring either the removal or inspection of Honeywell RESCU 406AFN ELTs with part number 1152682-2, installed on B787-8 aircraft, within 10 days of the effective date of the AD. Where inspection was chosen as the method of compliance, this was to focus on discrepancies associated with the ELT, ELT battery, and associated wiring, performing corrective action as necessary.

Similarly, on 26 July 2013 the European Aviation Safety Agency (EASA) issued AD 2013-0168, effective 31 July 2013 requiring either the removal or inspection of Honeywell RESCU 406AFN ELTs with part number 1152682-2,

© Crown Copyright 2015

installed on B787-8 aircraft, in accordance with Boeing MOM-13-0570-01B, within 10 days of the effective date of the AD.

On 15 Aug 2013 Transport Canada issued AD CF-2013-25, effective 26 August 2013, mandating the embodiment of Honeywell Alert SB 1152682-23-A22 for all aircraft on which the RESCU 406AF / AFN ELTs are known to be fitted, within 150 days of the effective date of the AD.

On 18 September 2013 the FAA issued AD 2013-18-09, effective 3 October 2013, mandating the embodiment of Honeywell Alert SB 1152682-23-A22 within 120 days of the effective date of the AD.

1.18.8.4 FAA response to Safety Recommendations from AAIB Special Bulletin S5/2013

On 18th April 2014 the FAA responded to Safety Recommendation 2013-017 as follows:

> *'The FAA is currently conducting a safety review of Lithium-powered ELT systems with other regulatory authorities to identify any unsafe conditions in other aircraft types. The FAA expects to provide an update on the status of the safety review by March 31 2015.'*

On the basis of this response and publication of FAA ADs 2013-15-07 and 2013-18-09, the AAIB categorises Safety Recommendations 2013-016 and 2013-017 as '*Adequate - Closed*'.

1.18.8.5 Safety Recommendations issued in AAIB Special Bulletin S4/2014

On 17 June 2014 the AAIB made the following Safety Recommendations in Special Bulletin S4/2014:

> **Safety Recommendation 2014-020**
>
> It is recommended that the Federal Aviation Administration develop enhanced certification requirements for the use of lithium-metal batteries in aviation equipment, to take account of current industry knowledge on the design, operational characteristics and failure modes of lithium-metal batteries.
>
> **Safety Recommendation 2014-021**
>
> It is recommended that the Federal Aviation Administration require that electrical performance and design-abuse certification tests for lithium-metal batteries are conducted with the battery installed in the parent equipment, to take account of battery thermal performance.

Safety Recommendation 2014-022

It is recommended that the Federal Aviation Administration work with industry to determine the best methods to force a lithium-metal cell into thermal runaway and develop design-abuse testing that subjects a single cell within a lithium-metal battery to thermal runaway in order to demonstrate the worst possible effects during certification testing.

Safety Recommendation 2014-023

It is recommended that the Federal Aviation Administration require equipment manufacturers wishing to use lithium-metal batteries to demonstrate (using the design-abuse testing described in Safety Recommendation 2014-022) that the battery and equipment design mitigates all hazardous effects of propagation of a single-cell thermal runaway to other cells and the release of electrolyte, fire or explosive debris.

Safety Recommendation 2014-024

It is recommended that the Federal Aviation Administration review whether the Technical Standard Order (TSO) process is the most effective means for the certification of lithium-metal batteries installed in aircraft equipment, the actual performance of which can only be verified when demonstrated in the parent equipment and the aircraft installation.

1.18.8.6 FAA response to Safety Recommendations (2014-020 to -024) in AAIB Special Bulletin S4/2014

As of June 2015, final response from the FAA is awaited for Safety Recommendations 2014-020 to -024, however in a letter dated 31 October 2014, the FAA provided the following interim comment in respect of Safety Recommendation 2014-022:

'We plan to request that the Radio Technical Commission for Aeronautics (RTCA) task Special Committee 225, 'Rechargeable Lithium Batteries and Battery Systems', to revise and update RTCA Document DO-227, 'Minimum Operational Performance Standards for Lithium Batteries', for non-rechargeable lithium metal batteries. The revision would include methods to force lithium metal cells into thermal runaway and develop design abuse testing that would subject a single cell within a lithium metal battery to thermal runaway conditions.

> *The tasking would include exploring the mitigation of the worst possible effects of this condition during certification testing. We plan to include evaluation criteria to ascertain pass/fail criteria under these conditions.'*

In the same correspondence, the FAA provided the following interim comment in respect of Safety Recommendation 2014-024:

> *'We believe a Technical Standard order (TSO) is effective in approving the design and production of an article to meet the Minimum Performance Standards. A TSO alone is not sufficient for certification approval. In order to complete a certification of a lithium metal battery installed in aircraft equipment, an airworthiness regulation approval is required. The airworthiness regulation must be complied with during Type certification, and Supplemental Type certification (including their respective amendments).*
>
> *I believe the FAA has effectively addressed Safety Recommendation [2014-024] and we do not plan any further action.'*

1.18.8.7 Additional FAA safety actions

Lithium battery safety review

As a direct result of this incident, the FAA Technical Centre in Atlantic City, New Jersey, have undertaken a review of a wide range of lithium battery types currently installed, or proposed to be installed, in transport category aircraft, to characterise the thermal runaway hazard associated with the lithium cells. The review includes lithium-ion, lithium-metal and lithium-polymer cells of various chemistry and cell size combinations, used in aircraft equipment.

Cells have been tested in three configurations: a single cell in thermal runaway; a single cell in thermal runaway in the presence of an ignition source; and a single cell in thermal runaway in a multi-cell pack. For the purposes of the test, thermal runaway is initiated by applying an external heat source.

The tests aimed to understand whether the cells are explosive in failure, if the electrolyte is flammable, if the failure propagates to adjacent cells and whether the temperatures reached are sufficient to ignite or compromise aircraft materials. Data collected in each test includes cell case temperature, test chamber pressure and hydrocarbon concentration.

As of June 2015 the results were being analysed and documented. Significant differences were observed between certain cell chemistries and how they

© Crown Copyright 2015

behave in thermal runaway, for example the temperature needed to induce thermal runaway, the degree of flammability of the electrolyte and the propensity for cell-to-cell propagation. Differences in cell design/construction were also observed, where cells of the same chemistry and similar electrical specifications have exhibited drastically different responses.

The results of the review will be used to inform the RTCA committee charged with amending RTCA document DO-227 (refer to Section 1.18.8.6) and the FAA Draft Issue Paper, discussed below.

Draft FAA Issue Paper: 'Lithium battery safety review'

As of June 2015, the FAA was in the process of compiling an Issue Paper to address potential safety issues associated with the installation of non-rechargeable lithium batteries, for future aircraft certification campaigns.

Although the content is not yet finalised, the Draft Issue Paper indicates that applicants will be expected to identify all battery and battery system failure modes which could lead to a hazardous situation, including: propagation of a single-cell failure to other cells; battery cell or system manufacturing defects, including wiring defects; defects introduced through mishandling, damage or improper storage; defects that could cause a hazardous increase in cell temperature or pressure; explosive or toxic gases that may be emitted in normal operation, or as a result of a failure of the battery systems; and the potential effect of fire, explosion or high temperature due to a battery failure on surrounding structure or adjacent aircraft systems, equipment or electrical wiring.

The Draft Issue Paper also states that, pending the outcome of ongoing research and service investigations, the FAA may propose new or revised standards for future certification programmes that involve non-rechargeable lithium batteries and battery systems.

The content of the Draft Issue Paper is likely to be formalised on a project by project basis.

1.18.9 Aircraft structure certification information

1.18.9.1 Certification requirements

'Post-crash fire' requirements

The structure of the Boeing 787-8 aircraft was certified by the FAA as meeting the requirements of Federal Aviation Requirement FAR 25. In addition to these requirements, Boeing were required to demonstrate that the level of fire safety

in the Boeing 787 was equivalent to a conventional transport aircraft, FAA Issue Paper CS-14, '*Fuselage Post-Crash Fire Survivability of Boeing Model 787 Series Aircraft*'.

Boeing proposed that the burn-through resistance of the Boeing 787 composite fuselage provided an equivalent level of safety to the FAA thermal acoustic insulation burn-through resistance regulation during a survivable post-crash fire (Federal Requirement 45046, dated July 31, 2003). To evaluate this, the FAA developed a small-scale test to expose fuselage constructions representative of the B787 fuselage material, to a simulated post-crash fire and to collect and analyse gas emissions that could affect occupant survival[53]. It was shown that the composite gas emissions produced were actually lower than the emissions from two types of burn-through-resistant insulation materials. The FAA also conducted full-scale post-crash fire tests to develop scaling factors to use in conjunction with the small-scale test, to predict cabin gas concentration levels during a post-crash fire[54].

'In-flight fire' requirements

Traditional metallic aircraft structures do not normally require evaluation for flammability, because they do not contribute to a fire, and have therefore historically not been required to meet the FAA's cabin interior fire test requirements. The use of Special Conditions is currently the only method used by the FAA to certify composite aircraft for flammability. Given the potential flammability of composite material the FAA introduced FAA Special Condition No: 25-07-09-SC: Boeing Model 787-8 Airplane; 'Composite Fuselage In-Flight Fire/Flammability Resistance', which required Boeing to demonstrate that the B787 would provide a level of fire protection equivalent to, or better than, traditional aluminium aircraft against 'hidden' in-flight fires. This required intermediate-scale tests and the B787 met these test requirements. To remove the need for these intermediate-scale tests in future certification programmes, the FAA developed a small-scale fire test method to measure the in-flight fire resistance of composite fuselage structure[55].

The FAA also examined the heat transfer characteristics and integrity of composite and aluminium fuselage skins during a hidden in-flight fire under simulated flight conditions in a wind tunnel. The results showed that airflow-induced cooling allowed both materials to remain intact, although the heat transfer characteristics of aluminium and composite skins were very

53 Marker, T. and Speitel, L: *'Development of a Laboratory-Scale Test for Evaluating the Decomposition Products Generated Inside an Intact Fuselage During a Simulated Postcrash Fire,'* FAA report DOT/FAA/AR-TN07/15, August 2008.

54 Marker, T. and Speitel L: '*Evaluating the Decomposition Products Generated Inside an Intact Fuselage During a Simulated Postcrash Fuel Fire'*, FAA report DOT/FAA/AR-09/58.

55 Ochs, R: '*Development of a Flame Propagation Test Method for Structural Aircraft Composite Materials in Inaccessible Areas,'* FAA report, to be published.

different, the aluminium being a superior conductor in all directions, whereas the composite mainly conducted heat through its thickness[56].

1.18.9.2 Flammability certification tests

The FAA flammability test requirements are laid down in the Aircraft Materials Fire Test Handbook (Report DOT/FAA/AR-00/42). This document contains the fire test requirements that must be satisfied before materials can be approved for use in aircraft. During the design and certification process, Boeing were able to demonstrate to the FAA that the materials used in the B787 met the requirements of the Aircraft Materials Fire Test Handbook as well as FAA Special Conditions Nos. 25-348-SC and 25-07-09-SC and FAA Issue Paper CS-14.

1.18.9.3 Composite flammability testing

Prior to this incident, the FAA Technical Centre had initiated a series of tests to determine the effect of external ambient conditions and material thickness on the flame propagation potential of CFRP fuselage materials, when exposed to a hidden fire. The tests allowed the ambient conditions on the external (non-flame) side of the flat-panel test samples to be varied, to represent different flight conditions. A low heat loss scenario was modelled by insulating the external face of the sample, and a high heat loss scenario used water cooling of the external face.

These tests indicated that the relative flammability of the composite material was dependent upon the rate of heat dissipation from the surface exposed to the flame. The rate of dissipation varied with the thickness of the test panel and the dissipation from the external surface. Thin panels (0.04 to 0.1 inch thick) were found to allow flame propagation under ambient conditions, and the rate of flame progression was strongly influenced by the rate of external cooling. Thicker panels (0.13 to 0.37 inch thick) would not propagate a flame under ambient conditions and were less affected by heat transfer from the external surface. The results of this test program, which are yet to be published[57], provide useful information in assessing the in-flight fire threat for composite fuselage aircraft. However, actual composite constructions will have variable skin thickness and integral structural members such as frames, stringers and shear ties, resulting in different levels of heat conduction from a hidden fire. Consideration must be given to these factors when performing an analysis of in-flight composite material flammability.

56 Webster, H: '*Comparison of Aluminum and Composite Aircraft Hull Materials When Exposed to an In-Flight Fire*', FAA report, to be published.

57 '*Evaluation of Carbon Fiber Composite Flammability: Effect of Sample Thickness and External Ambient Conditions on Inboard Surface Flame Propagation'*, Robert I Ochs, FAA, to be published.

To develop this testing further, and to take account of the fire propagation characteristics observed in the ET-AOP incident, the FAA Technical Centre initiated a programme to procure further test specimens, more representative of actual composite aircraft fuselage sections. These were to be used for tests to simulate more realistic in-flight hidden fire conditions to develop flammability certification requirements. Initial results from this test program were to be available in the first half of 2015.

2. Analysis

2.1 General

Initial examination of the aircraft identified that the area of most severe thermal damage was in the fuselage crown, approximately centred on the location of the ELT. The extent of the heat damage to the ELT, and the absence of any other systems capable of providing an ignition source, in that area, identified the ELT as the source of the fire.

Examination of the ELT identified that a high-energy thermal event had occurred within its battery, consistent with a cascading thermal runaway. The trapped wires indicated the likelihood of an external short-circuit having contributed to the battery failure. The nature and intensity of the battery failure resulted in the cell electrode windings being destroyed or completely consumed. Therefore there was little evidence available which could provide an indication of the pre-incident cell condition and it was not possible to determine whether any other failure mechanism may have contributed to the thermal runaway.

An extensive programme of testing and analysis was therefore undertaken to determine what failure modes could result in the type of damage experienced by the ELT battery in ET-AOP, and in particular whether an external short-circuit could cause this type of failure.

2.2 ELT and battery examination

2.2.1 Identification of external short circuit

Examination of the ELT confirmed that the battery wires were crossed and trapped between the battery cover-plate and the ELT case. Forensic analysis confirmed that there was evidence of metal-to-metal contact between the conductor of the positive wire and the underside of the battery cover-plate.

The surface treatment of the aluminium cover-plate was damaged at the contact locations, indicative of relative movement between the wire and the cover-plate. Had direct contact between the positive wire and cover-plate existed when the ELT was installed in the aircraft, it would have been detected by the ELT self-test. It is therefore likely that the integrity of the insulation on the positive wire degraded over time, eventually exposing the copper conductor to the cover-plate.

Direct contact between the positive conductor and the cover-plate could have provided a path for current to flow through the battery circuit and ELT case, creating a short-circuit condition.

© Crown Copyright 2015

Forensic analysis also confirmed evidence of contact between the positive and negative conductors at the cross-over location and the possible presence of fretting debris, which suggests a degree of relative movement between the wires. Contact between the positive and negative conductors would also create a direct short-circuit, within the battery circuit.

2.2.2 Battery examination and possible failure sequence

The damage sustained by the ELT battery indicated that all five cells had experienced a high-energy thermal event, consistent with a thermal runaway. Much of the battery material was consumed in the failure and that which remained was badly damaged and extremely fragile. Therefore there was little evidence available which could provide an indication of the pre-incident cell condition and, despite extensive forensic examination and CT scanning of the battery and cells, it was not possible to determine whether any pre-existing defects or failures might have contributed to the battery failure.

The degree of damage to the battery indicated a rapid failure and, while all five cells were badly damaged, the damage was not uniform across the battery pack. The external damage, and the differing amounts of remaining electrode material within the cells, indicates that the temperature evolution was not constant through the battery pack. This is consistent with the results of the Root Cause testing, where cells experienced different temperatures during the failure sequence.

Cells 4 and 5 exhibited the least damage, and had the greatest amount of cell winding material remaining. The copper current collector in Cell 4 was almost intact, indicating that temperatures at the mid-point of the cell had been less than 1,085^{o}C. Cells 1 and 2 exhibited the greatest thermal damage, evidenced by the sidewall ruptures, the fusing of the cell cans, and the fact that both cells had less remaining cell winding material than the other cells. Cell 2 in particular had the least amount of identifiable cell components remaining. The fusing of steel cell cans on Cells 1, 2 and 3 indicates that these cells saw localised temperatures in excess of 1,500^{o}C. The absence of any significant damage to the base of Cell 2 indicates that temperatures at the base of the cell were much lower.

At least one vent had operated on four of the cells, however the bulging of the cells indicates that very high internal pressures had developed prior to rupture, showing that the vents were not able to relieve the pressure rapidly enough.

With the exception of Cell 2, the base of all the cells exhibited significantly greater damage than the cell header. The cell header is the thickest part of the cell can, and therefore might be expected to sustain less damage. Due to

© Crown Copyright 2015

the cell orientation, molten electrode material would pool at the bottom of the cell, which could explain the extent of the damage on Cells 1, 3, 4 and 5. The absence of damage to the base of Cell 2 suggests that the failure of this cell was rapid, with the molten battery material ejected through the sidewall rupture rather than pooling at the bottom of the cell.

Cell 2 was out of vertical alignment with the rest of the pack. This must have occurred early in the failure sequence, prior to the sidewall fusing with Cells 1 and 3, and prior to impingement from the bulge in Cell 3. The fact that the Cell 3 bulge extended into Cell 2, indicates that Cell 3 experienced high internal pressure when Cell 2 had already vented, or failed. This strongly suggests that Cell 2 failed before Cell 3.

The Root Cause tests, calorimeter tests and the Boeing battery thermal propagation modelling demonstrated that a thermal runaway failure in a single cell rapidly propagates cell-to-cell through the pack. While it was not possible to determine with certainty the sequence of cell failures within the incident battery, Cell 2 exhibits a number of features which differentiate it from the other cells. This strongly suggests that the thermal failure initiated within Cell 2.

2.3 Pinched wires

Sufficient slack existed in the ELT wires to allow them to become trapped under the cover-plate. The investigation concluded that the wires were probably trapped during ELT production, or when the battery was last accessed, and this condition remained undetected until the incident.

Although previous instances of trapped battery wires had occurred, the worst identified effect was an external short-circuit which resulted in depletion of the battery. Identification of this issue resulted in a change to the ELT assembly procedures for production units, but did not, at that time, result in inspection of in-service ELTs.

Further instances of pinched wires were found during AD compliance inspections prompted by the ET-AOP incident, however this event was the only occurrence identified by Honeywell as having resulted in a battery thermal event.

The mandatory one-time inspections of all in-service RESCU 406AF/AFN ELT units, following the ET-AOP event, and the Honeywell design modification to invert the battery and re-route the battery wires, have mitigated the possibility of trapped wires on in-service and production units. Therefore no further safety action is considered necessary in this area.

© Crown Copyright 2015

2.4 Root Cause testing

2.4.1 General

The manner in which the ELT battery failed and the high temperatures experienced during decomposition meant that much evidence was consumed by the failure. It was thus not possible to draw conclusions from the forensic examination of the battery, and this precluded determination of the precise cell failure mode based on the physical evidence alone.

Fault tree analysis performed by the aircraft, ELT and battery manufacturers identified a number of possible failure modes, and provided direction for the Root Cause test campaign. As it was determined that the pinched wires could create an external short-circuit, the test programme focused on identifying related electrical failure modes which could reproduce the type of damage sustained by the battery during the incident.

2.4.2 External short-circuit tests

The testing concluded that a 'hard' short-circuit, such as might occur if there was direct contact between the conductors of the pinched battery wires, would not in isolation lead to thermal failure of the battery. Instead the high discharge current would cause the PTC to trip and protect the circuit (Boeing DTP-1). The PTC leakage current was insufficient to elevate the cell temperatures to a dangerous level, resulting in benign depletion of the battery.

However, the tests demonstrated that a partial short-circuit, or short-circuit with some degree of electrical resistance, with a discharge current below the PTC hold current of 3.8A, could lead to a greater temperature rise within the battery cells.

Moderate-resistance discharges of 1A and 2A, performed on batteries while they were installed in the ELT, resulted in cell temperatures of around 120°C and voltage reversals of one or more cells. Although the PTC did not trip in either case, the batteries depleted without a thermal event. However a controlled vent of one cell occurred during the 2A discharge (Boeing DTP-3). These tests demonstrated that moderate-resistance short-circuit currents of between 1 and 2A, substantially below the battery maximum rated discharge current of 3.3A, were capable of elevating the cell temperatures high enough, and for long enough, to result in a chemical breakdown of one or more cells, while sufficient electrical energy remained in the battery to fuel a high-energy decomposition. The temperatures experienced in this test were far in excess of the cell maximum operating temperature of 72°C.

© Crown Copyright 2015

Further moderate-resistance discharge tests, where the resistive heating was retained within the ELT, were perhaps more representative of a real-life resistive short-circuit. A 3.1A discharge performed on an intentionally unbalanced battery pack showed that the depleted cell rapidly became resistive and resulted in a cascading thermal failure of the remaining cells (Honeywell Test 31). However, a moderate-resistance discharge of 2.7A performed on a fresh battery pack, resulted in the PTC tripping and subsequent benign depletion of the battery (Honeywell Test 32).

These results demonstrated that resistive heating is an important factor in temperature evolution within the battery.

2.4.3 Cell voltage reversal

In all cases where the discharge tests resulted in violent decomposition of the battery, the final failure was precipitated by the early depletion of one or more cells which then experienced voltage reversals. This is particularly evident in the results of Honeywell Test 10 (Figure 1.16.3A) where a balanced pack was used, and also in Honeywell Test 31 (Figure 1.16.3C) where an intentionally unbalanced pack was used. Single or multiple cell reversals also featured in some discharge tests which did not result in violent decomposition (Boeing DTP-2 and DTP-3).

In order for a voltage reversal to cause a thermal failure, the depleted cell must become sufficiently resistive and the other cells must have sufficient energy remaining to force current through the depleted cell and elevate the cell temperature to the point of failure. The Battery Drain tests determined that the internal resistance of a cell which had experienced a voltage reversal could be in the range of 4 to 32 ohms.

Voltage reversal is a phenomenon often associated with cell imbalance. Cell imbalance can arise due to cell manufacturing variances. Although the reactive materials in the cells are carefully metered during cell manufacture to achieve consistent cell capacity, and steps are taken during post-production testing of the ELT battery cells to ensure that cell OCV and CCV is within a specified range, cells are not specifically matched prior to battery pack assembly to achieve a balanced pack. While the post-production testing can identify cells with similar voltages, unlike rechargeable cells, non-rechargeable cells cannot be cycled to determine their exact capacity. There will always therefore be a ‘weakest’ cell in each pack. This weakness might remain undetected during normal operation and might only be exposed when the battery is subjected to an adverse electrical environment.

© Crown Copyright 2015

Root Cause testing also demonstrated that the presence of moisture on the top of a cell could short the cell terminals and was therefore identified as another mechanism which could explain early depletion of one or more cells, creating an unbalanced pack.

2.4.4 Nature of the short-circuit

The precise characteristics of the pinched wire short-circuit on the ET-AOP ELT battery are unknown, however testing indicated the short could have been hard, resistive or intermittent in nature. Given the low resistance of the battery wiring, a 'hard' short-circuit in isolation was ruled out as a possible cause of the ELT battery thermal event by testing.

There was evidence of contact between the positive wire conductor and the ELT cover-plate. The maximum measured ELT case resistance was 52 milliohms. This suggests that direct contact would have created a 'hard' short-circuit, with a resulting high-rate discharge current. However it is possible that partial connection or 'soft short' between the positive conductor and the cover-plate could arise if for example, there was a remnant of degraded wire insulation or corrosion present at the interface.

The location, orientation and mounting structure of the ELT combined with the specific cabin environment of the B787, mean that the ELT may be subjected to high atmospheric moisture content. Moisture could collect in the lightening hole on the ELT composite intercostal, directly above the battery cover-plate. As the trapped wires on ET-AOP compromised the environmental seal on the battery cover-plate, it is possible that moisture could have entered the ELT. This would have provided a mechanism for corrosion at the location of the trapped wires, or for depletion of one or more cells.

Post-incident examination of the ELT revealed the presence of corrosion on the upper surface of the case, suggesting the presence of moisture. However, the location of the corrosion was coincident with ejected battery decomposition products and large volumes of water had been directed towards the ELT during fire-fighting. It is therefore likely that the corrosion occurred as a result of the conditions to which the ELT had been exposed during and after the incident. There was no evidence to suggest that corrosion existed in this area prior to the incident, however that does not rule out the possibility of moisture collecting in this area.

Airframe vibration, pressurisation cycles or other mechanical force (such as the vertical acceleration at landing) could also have contributed to intermittent electrical contact at the location of the short-circuit.

© Crown Copyright 2015

The root cause testing could not recreate a resistive short-circuit condition. However the effects of a resistive short circuit, simulated by the inclusion of resistors in the battery circuit, were shown to cause a temperature rise within the battery cells and, in some cases, lead to thermal runaway.

2.4.5 Positive Temperature Coefficient device (PTC)

2.4.5.1 General

The intended design function of the PTC is to protect the battery circuit from the adverse effects of external short-circuits by limiting the discharge current to a safe level. Inadequate circuit protection in this event is fundamental to the battery failure and may have occurred either because the discharge current was insufficient to trip the PTC, the PTC was bypassed or shorted, or the PTC tripped and then subsequently reset. These possibilities are discussed in order, in Sections 2.4.5.2 to 2.4.5.4.

2.4.5.2 Discharge current insufficient to trip the PTC

The Root Cause testing concluded that the PTC was generally effective at preventing cell failure under 'hard' or low-resistance short circuit conditions, because the resulting high discharge currents were sufficient to trip the PTC.

Although the average expected continuous current load from the ELT when transmitting is approximately 0.13A, the rated maximum continuous current of the ELT battery is 3.3A. The minimum current at which the PTC might trip in 20°C ambient conditions is 3.8A. The Root Cause testing confirmed that discharge currents below 3.8A could elevate cell temperatures sufficiently to cause thermal failure without the PTC tripping.

Further, the difference between the PTC hold and trip currents means that in ambient conditions, the battery could experience discharge currents up to 8.3A, far in excess of its rated maximum current, before the PTC trips. In normal ambient conditions, it is therefore evident that the switching point of the PTC is too high for this particular application. Ultralife was not able to provide documentation from the battery design stage that detailed the selection criteria for the PTC. The PTC hold and trip currents vary with temperature, as shown in Figure 6, Section 1.6.4.3. The range of temperatures across which the ELT, and therefore the PTC, is required to operate, contributes to the fact that in certain conditions, the switching point of the PTC exceeds the maximum continuous discharge current specified for the battery.

© Crown Copyright 2015

2.4.5.3 PTC bypassed or shorted

The PTC was intentionally bypassed in some Root Cause tests to demonstrate the effects of an external short-circuit, in combination with an absent/failed/shorted/inadequate PTC. Without the PTC in the circuit, a hard or low-resistance short-circuit could result in single-cell voltage reversals and subsequent cascading thermal failure of the battery (Honeywell Tests 10 and 11). However, a moderate resistance short-circuit (3.3 ohms) on an uninstalled battery, resulted in a benign discharge, even without the protection of the PTC (Honeywell Test 9).

It was also demonstrated that a PTC could be electrically shorted, thus bypassing its circuit protection function, by the application of mechanical force, when it was in the tripped or high-resistance state. The PTC was shown to be very resilient to such damage in the un-tripped state.

The PTC is not subject to any direct loading, however its position in the battery pack may make it vulnerable to mechanical stressing, during battery pack assembly or when the battery is installed in the ELT. Any resulting residual stress could cause a short if the PTC subsequently trips. Further, if the battery encountered very high temperatures (e.g. during a thermal event), it could cause the outer shrink-wrap on the battery to contract and possibly induce stress on the PTC.

Reliability of the LR4-380F PTC trip function was demonstrated during UL[1] qualification testing. However, the absence of both post-assembly electrical testing on the battery and post-installation testing of the battery in the ELT, means there is no opportunity to detect a PTC failure once it is installed in the battery circuit.

2.4.5.4 PTC reset

Honeywell Test 33 demonstrated that a fully-charged battery pack could ultimately fail in thermal runaway with a functioning PTC if the PTC experienced a reset. In this test, the PTC was manually reset multiple times to simulate circuit behaviour in the event of PTC reset. In Honeywell Test 35 the PTC reset following voltage reversal of one cell on a battery which had been discharged at low temperatures.

Additionally, subsequent simple-circuit PTC reset tests demonstrated that a PTC reset could occur if the total circuit resistance increased, the discharge current decreased, or the ambient temperature substantially decreased. These tests demonstrated that the power dissipated by the PTC in the tripped

[1] ‘Underwriters Laboratories’.

state was the key parameter governing its reset behaviour. If changes to the electrical circuit or ambient temperature occurred, such that it was no longer possible for the PTC to maintain the required power (regardless of its resistance), it reset.

An increase in the total circuit resistance would cause a reduction in discharge current. In a battery circuit, the increase in resistance necessary to cause a PTC reset could be provided by a depleted/resistive cell. If the discharge current dropped below the PTC hold current, such that the PTC reset, the battery could continue to discharge and excite the depleted cell to failure, without the PTC re-tripping.

Analysis of the reset test results showed that an increase of circuit resistance in the order of 11 to 18 ohms could be sufficient to cause a PTC reset. These values fall within the 4 to 32 ohm range previously calculated for a depleted cell[2]. However, in the Boeing DTP-3 test the PTC successfully tripped after one cell had already experienced a voltage reversal, suggesting that not all depleted cells will develop sufficient resistance to defeat the PTC circuit protection.

While it seems the PTC trip behaviour was relatively well understood during battery design, neither the PTC reset behaviour, nor its impact on circuit protection, was fully understood by the battery or ELT manufacturers. In particular it was not appreciated that the resettable nature of the device would allow continued operation of the circuit and potential recurrence of the fault condition and that the leakage current in the tripped state would allow continued, albeit low-rate, discharge of the battery.

2.4.6 Summary of battery failure scenarios

The Root Cause testing explored many potential failures and combinations of failures which could have caused the ELT battery fire. While it was not possible to identify the precise failure mechanism(s) involved in the incident, five potential failure scenarios have been identified where the battery pack external short circuit protection can be defeated:

- Scenario 1: A hard short-circuit of battery pack combined with a failed/bypassed/shorted PTC.

  While a hard short-circuit in isolation was ruled out as a potential cause, this mechanism in combination with a failed/bypassed/shorted PTC could have resulted in a battery thermal failure. This scenario requires the battery pack discharge response to be unbalanced, such that one cell

[2] From the Battery Drain Tests.

depletes more rapidly than the others and experiences a voltage reversal, while the remaining cells retain sufficient energy to drive current through the depleted cell, leading to a thermal failure. This scenario has been demonstrated by test.

- Scenario 2: A resistive short-circuit with an operable PTC, where the resulting discharge current is below the PTC trip point.

  This scenario requires the short-circuit to have sufficient resistance to allow a discharge current which is below the PTC switching point, but above the value necessary to excite a resistive cell to overheat. It also requires the battery pack discharge response to be unbalanced, leading to a thermal failure. This scenario has been demonstrated by test.

- Scenario 3: A hard short-circuit of the battery pack combined with a PTC reset, caused by the resistive increase of a depleted cell.

  This scenario requires the only failure to be an external short-circuit. When the short occurs, the current will be limited by the PTC. However, the small PTC leakage current will permit a slow discharge of the battery. This scenario also requires the battery to exhibit an unbalanced discharge response. The depleted cell becomes a resistive element in the circuit, reducing the discharge current below the PTC trip point, allowing the PTC to cool and reset. Upon PTC reset, the discharge current will be determined by the resistance of the depleted cell. This current could remain below the PTC trip current yet still provide sufficient energy to the depleted cell to cause a thermal failure. The different elements of this scenario have been demonstrated by a combination of test and analysis; however, the composite scenario has not been demonstrated by test. Specifically, the role of the PTC reset response is based upon Honeywell Test 35 and the PTC reset tests performed in a simulated circuit, together with subsequent analysis of these results.

© Crown Copyright 2015

- Scenario 4: An intermittent short-circuit of the battery pack combined with PTC reset, resulting in high currents through a depleted cell.

  This scenario assumes that the short-circuit has a high current and short duration but is intermittently removed and reinstated (possibly due to vibration). This would initially cause the PTC to trip and the resulting leakage current to slowly discharge the battery. Intermittency of the short-circuit however could cause the short to open and the PTC to cool and reset and this could happen multiple times. This scenario requires the battery to exhibit an unbalanced discharge response. If the short-circuit is reinstated after a cell has been exhausted or experienced a reversal, thereafter the failure sequence would be the same as in Scenario 3. As in Scenario 3, the different elements of this scenario have been demonstrated by a combination of test and analysis; however, the composite scenario has not been demonstrated by test. The intermittent nature of the short-circuit was simulated during test but could not be recreated.

- Scenario 5: Moisture ingress to the ELT depletes a single cell in combination with a short-circuit and operable PTC.

  In this scenario, the presence of moisture in the ELT could lead to one or more cells becoming depleted, independent of interactions with the other cells. If a short-circuit occurs after cell depletion, then all of the elements necessary to excite a thermal runaway in the depleted cell(s) are present. Scenarios 1 to 4 rely on the early depletion of a single-cell; moisture could act as an enabler for cell depletion.

It is important to note that four of these potential scenarios describe ways in which the battery pack external short circuit protection may be ineffective, despite the presence of a fully functional PTC. This indicates that in some circumstances the PTC may not provide the intended level of external short-circuit protection.

2.4.7 External short-circuit protection

Honeywell RESCU 406AFN ELT – safety action

In order to address the five scenarios identified by the Root Cause testing, Honeywell developed a modification to incorporate a non-resettable ‘slow-blow’ thermal fuse in the ELT battery circuit for the RESCU 406AF and AFN. The fuse was set at 1.5A, substantially below the 3.8A trigger threshold of the PTC.

In August 2014 Honeywell submitted a certification plan for the modified ELT to Transport Canada, who confirmed that the proposed modification constituted a 'minor change'[3] to the ELT's existing TSO-C126 approval.

Unlike the PTC, a fuse is a non-resettable circuit protection device which creates a permanent open-circuit when it activates. It would therefore enhance the external short-circuit protection offered by the existing battery design.

The incorporation of a fuse would mitigate failure Scenarios 1, 3, 4 and 5, as the fuse would open immediately upon application of the short-circuit, electrically disabling the battery. For Scenario 2, the trip value of the fuse would limit the current passing through a depleted cell to a level which would prevent excitation of the cell to thermal failure. However, if a single-cell thermal failure occurred for any reason other than an external short-circuit, the fuse would offer no mitigation against thermal runaway and cell-to-cell propagation.

As of June 2015, Honeywell had manufactured a number of ELT units with the fuse installed but they had not incorporated this as standard in RESCU 406AFN production units. As of June 2015, the modified ELT has not been installed on any aircraft.

Since the ET-AOP ELT battery fire event in July 2013, in-service RESCU 406AF and AFN ELTs were subject to a mandatory one-time inspection for trapped or damaged battery wires, as a result of Airworthiness Directives issued by the FAA, EASA and Transport Canada. In addition, since May 2014 all new production RESCU 406AFN units have had the battery inverted, to route the wires underneath the battery. In-service RESCU 406AF and AFN ELTs will also benefit from the inverted battery as ELT batteries are replaced on an attrition basis.

The AD inspections, and the inverted batteries when installed, will reduce the risk of an external short-circuit event occurring due to trapped wires. However with a battery service life of 10 years, it will be many years until all in-service RESCU 406AF and AFN ELTs have the inverted battery installed.

In the intervening period, were an external short-circuit to occur, or another anomaly which resulted in a high discharge current, the existing standard of RESCU 406AF/AFN ELT battery would not benefit from the enhanced level of external short-circuit protection which is available with the optional fuse modification. As of June 2015, this has not been introduced in production units or made available as a modification to in-service units. While the fuse

[3] Federal Aviation Regulation FAR 21.619 *'Design changes'* states that a manufacturer holding a TSO authorisation can make minor design changes without further FAA approval.

does not address, or limit the effects of, all possible battery failure conditions, it does offer an enhanced level of external short-circuit protection and therefore an enhanced level of safety.

Therefore the following Safety Recommendation is made:

Safety Recommendation 2015-014

It is recommended that the Federal Aviation Administration, in conjunction with the European Aviation Safety Agency and Transport Canada, conduct an assessment of the circuit protection offered by the existing Honeywell RESCU 406AF and 406AFN ELT battery, to determine whether the ELT/battery design incorporates an acceptable level of circuit protection to mitigate against external short-circuits and unbalanced discharge.

Other installed equipment

The existing Honeywell RESCU 406AF/AFN ELT battery design relied on a single PTC as the only protective device against an external short-circuit and the investigation has shown that the level of circuit protection offered by the PTC was inadequate for this particular application. While the proposed addition of a fuse addresses the identified failure modes for this particular equipment, PTCs are widely used in batteries for circuit protection, either in isolation or in conjunction with other circuit protection devices. It is therefore possible that other items of installed aircraft equipment, powered by lithium-metal batteries, rely on PTC devices for circuit protection. The following Safety Recommendations are therefore made:

Safety Recommendation 2015-015

It is recommended that the Federal Aviation Administration, in conjunction with the European Aviation Safety Agency and Transport Canada, conduct a review of installed aircraft equipment on transport category aircraft powered by lithium-metal batteries, which have been approved under TSO-C142 /C142A or by equivalent means, to ensure that the design of such batteries incorporates an acceptable level of circuit protection to mitigate against known failure modes including, but not limited to, external short-circuits and unbalanced discharge.

and:

© Crown Copyright 2015

Safety Recommendation 2015-016

It is recommended that the Federal Aviation Administration, in conjunction with the European Aviation Safety Agency and Transport Canada, require equipment manufacturers intending to use lithium-metal batteries in aircraft equipment to demonstrate that the battery design incorporates an acceptable level of circuit protection to mitigate against known failure modes including, but not limited to, external short-circuits and unbalanced discharge.

2.5 Calorimeter tests

In all three calorimeter discharge tests the ELT batteries decomposed as a result of thermal runaway, triggered by excessive temperature rise, due to a combination of resistive and chemical heating from the discharge.

Although each battery was subject to the same calorimeter conditions and the same discharge current, there was considerable variation in the test results. Test 2 exhibited the most energetic decomposition, then Test 3 and Test 1. The batteries were 50%, 60% and 70% discharged respectively at the time of decomposition, indicating that the state-of-charge (SOC) of the battery had an effect of the severity of the final decomposition.

The profile of the self-heating curves showed close correlation between Tests 2 and 3. Despite all of three tests exhibiting similar initial self-heating rates, the heating rate increased much more rapidly in Test 2 and 3, and the onset of thermal runaway therefore occurred much earlier. The time to decomposition in Test 2 and 3 was broadly similar (8¾ and 9½ hours), while in Test 1 this was 22 hours.

Despite the different time profiles for the three tests, key events such as the PTC tripping, the activation of the first cell separator and the onset of thermal runaway happened at broadly similar temperatures.

In Tests 1 and 2 the discharge stopped when the PTC tripped, with activation of the first cell separator occurring some time later. But in Test 3 it was the activation of the cell 5 separator which caused the discharge to stop.

In Tests 2 and 3 the cell decomposition event was preceded by a single-cell voltage reversal a number of hours before final failure. This was markedly different from Test 1, where Cell 2 briefly exhibited a voltage increase some 10 hours before failure, but no polarity reversal. The single-cell voltage reversals in Tests 2 and 3 would have made these cells resistive which may have accelerated the self-heating rate.

© Crown Copyright 2015

The differences in shape of the total voltage curves and the self-heating curves for each battery indicate differences in electrical performance and thermal response that cannot be accounted for by the very minor changes in the test configurations. It is therefore concluded that there is a degree of unpredictability in the exact discharge response of this battery in these conditions. This behaviour could reasonably be expected of other lithium-metal batteries in similar conditions.

2.6 Certification aspects

2.6.1 DO-227 General

RTCA DO-227, written in 1995, forms the basis of the technical standards (TSO-C142 and TSO-C142a) relating to lithium-metal batteries for use in aviation equipment. AAIB Special Bulletin S4/2014 identified that the guidance and requirements of DO-227 were outdated and did not adequately take account of the advances in lithium battery technology or operational feedback since its inception. The increasing prevalence of lithium batteries in aircraft applications dictates the need for a more robust set of technical standards. Consequently, in June 2014 Safety Recommendation 2014-020 was made to the FAA (Section 1.18.8.5).

2.6.2 DO-227 guidance and requirements

General

Although DO-227 contains both requirements and general guidance for lithium-metal batteries, the wording of TSO-C142 is such that it only explicitly requires compliance with Section 2.0 of DO-227. Therefore battery and equipment manufacturers have no obligation to observe the guidance material in DO-227 as long as they can demonstrate that their products meet the criteria defined in Section 2.0.

The qualification test regime outlined in Section 2.0 is aimed at ensuring the safety, reliability and performance of cells and batteries. Yet the associated guidance material strongly emphasises a number of equipment design and integration considerations that are not adequately addressed by the required testing.

Thermal performance

In particular, the DO-227 guidance stresses that a battery may exhibit considerably different performance when installed in equipment, from that which it exhibits in the uninstalled condition, particularly with respect to heat dissipation. For example, the ELT battery's ability to dissipate heat will depend on the battery materials, the ELT case, its mounting structure, the ambient

temperature in the aircraft and the presence of aircraft insulation. Yet despite this emphasis on battery/equipment integration, none of the DO-227 tests are required to be conducted with the battery installed in its parent equipment, nor with the equipment installed in the aircraft. Instead, these tests address only the identified battery-level hazards and do not take account of equipment-level or aircraft-level hazards.

AAIB Special Bulletin S4/2014 identified that in order to properly understand the most severe effects that could occur when a lithium-metal battery is exposed to adverse electrical conditions, the certification tests must take account of the battery and equipment integration. Therefore in June 2014 Safety Recommendation 2014-021 was made to the FAA (Section 1.18.8.5).

The calorimeter discharge tests conducted by the AAIB represented worst-case heat dissipation conditions for the ELT battery and were not representative of the actual battery installation. However the results demonstrated that a cascading thermal runaway is a plausible outcome for a battery subjected to a moderate-rate discharge, substantially below its maximum rated capability, if the equipment installation prevents adequate heat dissipation. Additionally the Root Cause tests, many of which were conducted in conditions representative of the ELT installation, produced cell temperatures far in excess of the cell maximum operating temperature, in response to moderate discharge currents well within the rated capability of the battery. The 'free-air' or 'fixed-temperature' laboratory tests specified in DO-227 represent much more favourable, but not necessarily realistic, conditions for battery heat dissipation. The actual thermal performance of a battery in the installed condition may vary between these conditions. In the calorimeter tests, between 9 and 13% of the battery's total energy was released as heat (over the normal operating temperature range of the battery). Battery and equipment design must ensure that this heat can be adequately dissipated. The following Safety Recommendation is therefore made:

Safety Recommendation 2015-017

It is recommended that the Federal Aviation Administration, in conjunction with the European Aviation Safety Agency and Transport Canada, require manufacturers intending to use lithium-metal batteries in aircraft equipment, to quantify the heat produced by the battery over a range of discharge conditions and demonstrate that the battery and equipment design can adequately dissipate the heat produced.

© Crown Copyright 2015

Electrical performance and design abuse testing

The DO-227 electrical performance and design abuse tests are intended to simulate the most severe effects of adverse electrical conditions to which the cells or battery may be exposed and known failure modes for lithium-metal batteries.

The discharge and forced discharge tests are performed separately on cells and batteries. The tests do not take account of the effect of a single depleted cell within a battery pack. Also, although DO-227 guidance stipulates that circuit protection devices may be bypassed or removed during qualification testing in the interests of acquiring the necessary safety data, there was no associated test requirement in Section 2.0 and none of the qualification tests for the ELT battery were performed with the PTC missing or bypassed.

Early depletion of a single cell and inadequate PTC protection, in addition to the external short-circuit, were key factors in the ET-AOP battery failure. The abuse tests in DO-227 are laboratory tests, performed in a controlled environment, to controlled test conditions. They look at failure modes in isolation and do not deal with possible combinations of failure modes and are not necessarily representative of in-service conditions. It is clear that the most severe effects of an external short-circuit were not demonstrated during the DO-227 certification testing for the RESCU 406AFN ELT battery (the document did not require this).

The DO-227 internal short-circuit test is completed at cell-level but there is no requirement to conduct this test on an electrically connected cell, or on a single cell within a battery pack, where the heat dissipation and propagation characteristics of the abused cell may differ. The internal short-circuit test is terminated when the cell reaches two-thirds OCV[4]. There is no requirement for the cell to be forced into thermal runaway to evaluate the potential for propagation to other cells, or the ability of the equipment to contain the resulting products of the battery failure.

The DO-227 internal short-circuit test uses a rod and plate to deform the cell. However, there are many industry-accepted abuse methods used to induce a thermal runaway in lithium batteries, including nail penetration, crushing, heater mats and indentation. It is important that any certification test demonstrates the worst effects of a thermal runaway for a particular cell or battery design so that battery and equipment mitigations can be effectively assessed.

[4] Open Circuit Voltage – noted earlier.

The enhanced requirements of Appendix 1 of the current TSO-C142a go some way to addressing these concerns. However, in June 2014 the AAIB made Safety Recommendations 2014-022 and 2014-023 to the FAA (Section 1.18.8.5).

2.6.3 TSO process

Ultralife received TSO-C142 approval for the ELT battery, based on the requirements of DO-227. Although DO-227 contains useful guidance and best practice for battery/equipment integration, the TSO-C142 applicant is required only to demonstrate cell-level and battery-level safety. A battery-level technical standard cannot address all the unique aspects of a battery's operation in the parent equipment and aircraft installation. Aircraft and equipment manufacturers therefore need to evaluate whether additional requirements and testing are necessary to ensure aircraft-level safety. Indeed DO-227 recommends a safety review involving battery, equipment and aircraft manufacturers.

The TSO process is a self-contained, discrete process that results in approval being granted on a single article, which can then be marketed with an existing approval. The process is essentially one of self-certification by the applicant and involves minimal independent scrutiny by the FAA ACO. The RESCU 406AF/AFN ELT situation is somewhat unique in that a TSO-approved article is installed within another TSO-approved article, each approved to a discrete process. This compartmentalised approach to certification puts even greater emphasis on the need for vertical integration through the supply chain. It is important to ensure that safety-critical information is promulgated effectively and battery and equipment-level hazards are adequately addressed in the aircraft-level safety assessment.

This incident has highlighted that better coordination is required between battery manufacturers, equipment manufacturers, aircraft manufacturers and regulators to ensure equipment-level and aircraft-level safety. Therefore in June 2014 Safety Recommendation 2014-024 was made to the FAA (Section 1.18.8.5).

2.6.4 System safety assessment

The ELT and battery design were evaluated and approved independently during their respective TSO approval processes, and as part of the B787 type design certification programme. Although the investigation of this incident found that thermal runaway of a cell occurred, most likely due to an external short-circuit in the battery wiring, in combination with early depletion of a single cell and inadequate circuit protection, none of these design vulnerabilities were identified in the Honeywell NRS system safety assessment, or the wider ELT certification processes.

© Crown Copyright 2015

Despite the failure modes of lithium-metal batteries being well documented, the specific threat of a thermal runaway within the cells of the ELT battery was not identified at any point during the certification process for the battery, the ELT, or the installation of the ELT on the aircraft. The Ultralife TSO C-142 qualification test report for the ELT battery did contain a generic statement identifying that safety concerns for lithium batteries include the possibility of fire, venting violently and toxic gases. However this report did not contain any information on specific cell or battery failure modes nor the potential cascading nature of such failures. The qualification report was available to Honeywell and Instrumar but neither the report nor the identified generic safety concerns were communicated to Boeing, and no associated hazards were identified in the Honeywell NRS safety assessment. Similarly the Ultralife MSDS for the cells within the ELT battery, available to Honeywell and Instrumar, contained generic information about lithium-metal battery hazards, handling and storage guidance and fire-fighting measures. Further, the Issue Paper SE-09 review conducted by Honeywell, at the request of Boeing, concluded that the cell shutdown separators and vents would adequately mitigate the known lithium battery failure modes identified in the Issue Paper, in particular with respect to preventing any *'self-sustaining uncontrolled increases in temperature or pressure'*.

Consequently the Honeywell ELT FHA and FMEA conducted as part of the NRS system safety assessment, focused on battery failures which could adversely impact the operational performance of the ELT, but did not identify any battery failure modes which could represent a hazard to the aircraft.

This position was supported by a documented service history of the RESCU 406AF/AFN ELT, which revealed no adverse battery failure modes. The potential for an uncontrolled release of the stored electrical energy in the ELT battery therefore remained unidentified.

Boeing relied on the information contained in the Honeywell NRS system safety assessment, FHA, FMEA and the review of Issue Paper SE-09, to design and certify the ELT installation on the B787. Consequently no consideration was given to the effect of a cascading thermal runaway of the ELT battery on the safety of the aircraft and its occupants. This aspect is not unique to the B787 certification process as the RESCU 406AFN, and other similar equipment using lithium-metal batteries, are installed on multiple aircraft types.

The Honeywell ELT FMEA was an additional Boeing-defined requirement; neither TSO-C126 nor TSO-C142 required such an analysis. In order to ensure that battery-level hazards are appropriately identified and assessed in respect of their impact on aircraft safety, the following Safety Recommendation is made:

© Crown Copyright 2015

Safety Recommendation 2015-018

It is recommended that the Federal Aviation Administration, in conjunction with the European Aviation Safety Agency and Transport Canada, require the manufacturers of lithium-metal batteries and manufacturers of aircraft equipment powered by lithium-metal batteries, to conduct battery-level and equipment-level 'failure mode and effects analyses' to identify failure modes and their effects.

2.6.5 Toxic gas venting precautions

The TSO-C142 Appendix 1 guidance on *'Toxic Gas Venting Precautions'* is intended to prevent batteries capable of venting toxic gases from being installed in an aircraft cockpit, due to the possibility of flight crew impairment. It is also intended to permit the installation of such batteries in an aircraft passenger compartment, if the installer can demonstrate that a safety hazard will not be created. Although the wording of TSO-C142 precludes the adoption of the Appendix 1 guidance as a formal TSO 'requirement', the intent of the guidance is clear. The Ultralife TSO-C142 cell and battery qualification test reports, provided to Instrumar did not include any specific tests relating to the *'Toxic Gas Venting Precautions'.* However, the reports did contain a statement in the *'Installation Procedures and Limitations'* section indicating that lithium battery safety concerns included the venting of toxic gases. Further, this statement also indicated that it was the responsibility of the installer to ensure that the aircraft installation conditions for the battery were within the TSO standards. These installation limitations were not communicated up the supply chain. Consequently neither Boeing nor Honeywell considered these toxicity requirements during the RESCU 406AFN or B787 certification processes, and no testing was performed to demonstrate compliance with this guidance.

The now-applicable TSO-C142a formalises the *'Toxic Gas Venting Precautions'* as a requirement, however neither the TSO nor DO-227 contains a specific performance standard or test by which a manufacturer can demonstrate compliance with permissible toxicity levels. Post-incident testing performed by Boeing and Honeywell, to identify the composition and quantities of gases released during a battery failure, concluded the gases emitted are dependent upon the test method, the type of combustion and the amount of oxygen available to sustain combustion. The following Safety Recommendation is therefore made:

© Crown Copyright 2015

Safety Recommendation 2015-019

It is recommended that the Federal Aviation Administration, in conjunction with the European Aviation Safety Agency and Transport Canada, review all previously-approved aircraft equipment powered by lithium-metal batteries to determine whether they comply with the intent of the *'Toxic Gas Venting Precautions'* described in TSO-C142/ TSO-C142a Appendix 1.

Other portable equipment powered by lithium-metal batteries, such as portable ELTs, may be installed in aircraft cabins or cockpits. Such equipment is generally operator-specified and not categorised as permanently-installed aircraft equipment. It is therefore not required to meet the requirements of airworthiness rules and falls outside the TSO-C142 applicability, however, the '*Toxic Gas Venting Precautions'* guidance in TSO-C142 can be considered relevant. The following Safety Recommendation is therefore made:

Safety Recommendation 2015-020

It is recommended that the Federal Aviation Administration, in conjunction with the European Aviation Safety Agency and Transport Canada, review whether the *'Toxic Gas Venting Precautions'* described in TSO-C142/ TSO-C142a Appendix 1 should be applied to portable aircraft equipment powered by lithium-metal batteries.

2.7 Design of the battery and ELT

Although the ELT battery satisfied the test requirements of DO-227 Section 2.0, there were many elements of the DO-227 battery design guidance that were not incorporated in the battery's design. In particular DO-227 recommends that any thermal protective devices are centrally located within the pack where maximum heat evolution could be expected; on the ELT battery pack the PTC was located at the end of the series string. The positioning and encapsulation of the PTC also made it potentially vulnerable to mechanical loading.

Further, neither the ELT nor its battery contain any design features to prevent propagation of a single-cell thermal runaway to the remaining cells. Notwithstanding the findings of this investigation, thermal runaway is a known risk in all types of lithium battery. The Root Cause tests, the calorimeter tests and the battery thermal modelling performed by Boeing, all demonstrated that the battery pack construction allowed single-cell failures to rapidly propagate to neighbouring cells via direct thermal energy exchange. Cell segregation features can mitigate direct cell-to-cell propagation, reducing the amount of energy released during a thermal event to that produced by the initiating cell.

© Crown Copyright 2015

2.8 Fire and structures

2.8.1 Propagation of the fire through the aircraft structure

The uncontained ELT battery fire provided sufficient thermal energy to ignite a slow-burning fire in the composite structure adjacent to the ELT.

The orientation of the ELT on the mounting plate, and the compromised seal on the battery cover-plate, permitted the escaping gas, flames and battery decomposition products from the ELT battery to be directed towards the aircraft structure. While the structure would initially have been protected by the bay blanket, the ELT mounting plate would have been immediately exposed to the flames and the energy released by the ELT would initially have been confined close to the fuselage skin by the over-blanket. This, coupled with the elevated temperature in the crown due to the high OAT and the absence of cooling airflow on the external skin surface, produced temperatures sufficient to initiate vaporisation and combustion of the CFRP resin. While the insulation blankets remained intact there would have been only limited heat release from the area of the fire, and limited cooling airflow from the cabin.

Examination of the fuselage structure, the remains of the insulation blankets and the acoustic dampers showed that the fire progressed outwards from the ELT location, through the air spaces between the inner surface of the fuselage skin and the outer face of the bay blankets. This mechanism was confirmed by the damage being severe where there was a large air gap between the insulation blankets and the fuselage skin, and noticeably less severe where this gap was smaller. The damage to the upper ends of the cabin interior tie-rods further illustrated that the fire remained close to the fuselage skin, and was not sufficiently vigorous to progress inward beyond the depth of the insulation blankets.

Overall, the damage to the structure was consistent with a low-energy fire in the composite material and there was no evidence that the rate of combustion was accelerating or that a flashover fire had occurred.

2.8.2 Thermal and structural modelling

Thermal modelling

To understand the mechanism of the ground fire in ET-AOP, and assess the likely effects of such a fire in cruising flight, the aircraft manufacturer undertook a programme of thermal modelling.

This form of computational modelling, attempting to replicate a complex physical process, is limited in its absolute accuracy but is useful for showing the effect of physical variables. In this case, the modelling of the ground fire was effective, particularly in demonstrating the effects of the air gap between the outer surfaces of the insulation blankets and the aircraft skin.

The thermal modelling showed the strong effects of external cooling, which would be present during flight conditions, in mitigating the extent and intensity of the fire in the composite structure after the initial ELT fire was exhausted. Thus the modelling suggested that these conditions would have prevented flame propagation beyond the localised ELT ignition zone, and slowed the propagation rate to a point where the composite fire might self-extinguish. The results of the modelling appear consistent with the findings of the B787 flammability certification tests and the assessment of the actual fire propagation characteristics in the ET-AOP incident. During the climb and descent portions of flight, conduction and convection heat loss conditions, although different from those at cruise altitude, would also reduce the potential for fire propagation.

It is therefore concluded that, in the event of localised ignition of the composite structure in flight, the rate of convective heat loss would reduce the extent and intensity of fire propagation, and may be sufficient to cause the fire to self-extinguish.

Structural modelling

Finite element modelling of structural loads showed that the damage sustained by the fuselage crown skin during the ground fire in ET-AOP compromised the ability of the aircraft structure to carry flight loads. However the structural modelling for the in-flight fire scenario, based on two outcomes from the thermal modelling, predicted that the fuselage would remain capable of carrying flight loads, and, in one scenario, fuselage pressurisation loads.

2.8.3 Toxicity and flammability

During the design and certification process, Boeing demonstrated that materials used in the B787 met the applicable airworthiness requirements (FARs) and Special Conditions relating to flammability and combustion product toxicity.

CFRP combustion products can vary significantly depending on the nature, temperature and intensity of the fire, and the configuration of the installation. It has therefore not been possible to assess the concentration of combustion products produced during the ground fire.

© Crown Copyright 2015

Safety action taken

Boeing is reviewing their current test methodology to determine whether additional tests can be introduced to more accurately assess combustion products.

The FAA has also initiated a re-evaluation of the current flammability and toxicity testing of composite aircraft materials, to ensure the test methodology remains appropriate and they are investigating new test methods to produce more representative data for aircraft certification. The results of this investigation, and the re-evaluation of existing test methods, will be used to amend the current test and certification requirements.

The Boeing Environmental Control System group is developing airflow models to evaluate how the combustion products produced by the ELT battery would be dispersed through the cabin, in an aircraft with an operating ECS system. The results of this evaluation may influence future design and certification standards.

Therefore, the following Safety Recommendation is made:

Safety Recommendation 2015-021

It is recommended that Boeing expedite the modelling of the B787 Environmental Control System, to examine the distribution of ELT battery combustion products through the aircraft cabin, and demonstrate the results of this modelling to the Federal Aviation Administration.

2.9 Cabin fire fighting

This event occurred on the ground to an unoccupied and unpowered aircraft. However, the ELT battery fire could also have ignited during flight. In such a case, the ECS is likely to distribute the odour and fumes of a fire throughout the cabin. This may hinder the cabin crew in locating the source of the fire.

In the case of a lithium battery fire, if the location of the fire can be identified, the FAM states that a Halon, Halon-replacement, or water fire extinguisher, should be used to extinguish the fire and prevent the spread of the fire to adjacent battery cells and materials. After extinguishing the fire, the device should be doused with water or other non-alcoholic liquids to cool the device and prevent additional battery cells from reaching thermal runaway.

© Crown Copyright 2015

If the ELT battery was identified as the source of a cabin fire, gaining access to the ELT, which may require the removal of cabin ceiling panels, and getting close enough to make the use of a fire extinguisher effective, would be challenging. Without specific training it is unrealistic for a member of the cabin crew to perform this task. Further, opening ceiling panels or the access panel in the OFAR could feed the fire with oxygen and invigorate it.

In the event of smoke, fire or fumes a priority is to remove aircraft electrical power from the ignition source. This would not be possible in the event of an ELT battery fire, or a battery fire in any other installed device powered by non-rechargeable lithium batteries.

Water fire extinguishers are effective at extinguishing lithium battery fires and, in particular, cooling the battery to prevent further propagation. On aircraft equipped solely with Halon extinguishers this option would not be available. Given the location of the ELT it would be difficult to cool the ELT battery with anything other than a water fire extinguisher.

Safety action

At the time of the incident, the published ARFF information for the B787 did not indicate the location of the ELT battery, or other lithium battery-powered devices. This meant that the Heathrow Airport RFFS were not aware that there was a lithium-metal battery above the ceiling panels that could have been the source of the fire. By the time the RFFS were alerted to the fire on ET-AOP, the lithium fire in the battery would have been exhausted, leaving a slower-burning fire in the composite structure. However as the fire was hidden behind the ceiling panels, knowledge of a possible ignition source in this area may have facilitated the RFFS in locating the source of the fire. Boeing have since updated the ARFF information for the B787 showing the location of the ELT as a component containing a lithium battery.

2.10 Summary

The ground fire on ET-AOP was initiated by the uncontrolled release of stored energy from the lithium-metal battery in the ELT. It was identified early in the investigation that the ELT battery wires, crossed and trapped under the battery compartment cover-plate, probably created a potential short-circuit current path which could allow a rapid discharge of the battery. Root Cause testing performed by the aircraft and ELT manufacturers supported this latent fault as the most likely cause of the ELT battery fire, most probably in combination with the early depletion of a single cell.

© Crown Copyright 2015

Neither the cell-level nor battery-level safety features were able to prevent this single-cell failure, which then propagated to adjacent cells, resulting in a cascading thermal runaway, rupture of the cells and consequent release of smoke, fire and flammable electrolyte.

The trapped battery wires compromised the environmental seal between the battery cover-plate and the ELT, providing a path for flames and battery decomposition products to escape from the ELT. The flames directly impinged on the surrounding thermo-acoustic insulation blankets and on the composite aircraft structure in the immediate vicinity of the ELT. This elevated the temperature in the fuselage crown to the point where the resin in the composite material began to decompose, providing further fuel for the fire. As a result of this a slow-burning fire became established in the fuselage crown, which continued to propagate from the ELT location at a slow-rate, even after the energy from the battery thermal runaway was exhausted.

© Crown Copyright 2015

3. Conclusions

(a) Findings

General

1) The fire in ET-AOP initiated while the aircraft was parked, unpowered and unoccupied.

2) The extent of the damage to the ELT and the absence of other systems in the vicinity of the ELT capable of providing an ignition source, identified the ELT as the source of the fire.

ELT battery failure

3) The ELT fire resulted from the uncontrolled release of the stored energy within the battery cells.

4) The battery failure most likely resulted from an external short-circuit, in combination with the early depletion of a single cell, leading to thermal runaway which propagated to adjacent cells.

5) The ELT battery failure did not result from external heating, mechanical damage or environmental conditions within the aircraft.

6) The external short-circuit was created by the battery wires being crossed and trapped under the ELT battery compartment cover-plate when the ELT battery was last accessed.

7) The trapped wires remained undetected until the incident.

8) The PTC protective device did not provide the level of external short-circuit protection intended in the battery design.

9) The trapped wires compromised the environmental seal of the battery cover-plate, allowing the escape of hot gas, flames and battery decomposition products.

10) The location and orientation of the ELT within the aircraft, and the compromised seal on the battery cover-plate, allowed the hot gas, flames and battery decomposition products to impinge directly on the composite fuselage structure, providing sufficient thermal energy to initiate a slow-burning fire in the rear fuselage crown.

© Crown Copyright 2015

Battery design

11) The range of temperatures across which the PTC is required to operate means that in certain conditions, the switching point of the PTC exceeds the rated maximum continuous discharge current for the battery.

12) The PTC reset behaviour was not well understood during the battery design.

13) The absence of cell segregation features in the battery or ELT design contributed to the severity of the incident, as the initial cell thermal runaway was able to propagate rapidly to the remaining cells.

Battery and ELT certification

14) The ELT battery held a valid TSO-C142 approval.

15) The guidance and requirements of RTCA DO-227, invoked by TSO-C142, were outdated and did not adequately take account of advances in lithium battery technology since the inception of DO-227 in 1995.

16) The NRS system safety assessment, conducted in support of the B787 certification campaign, did not identify any battery failure modes which could represent a hazard to the aircraft, and as a result, the ELT battery was not identified as a potential ignition source.

Structural fire

17) The location of the fuselage insulation blankets in the region of the ELT allowed sufficient heat to be retained close to the skin to allow the fire to become self-sustaining.

18) The fire progressed outward from the location of the ELT, in the space between the insulation blankets and the fuselage skin, moving between frame bays through the stringer cut-outs in the shear ties.

19) There was no evidence that a flash-over fire occurred, or was about to occur, nor that the rate of progression of the structural fire was increasing.

© Crown Copyright 2015

20) Structural loads modelling, based on the damage sustained during the ground fire, determined that the aircraft's ability to carry flight loads had been compromised.

21) Thermal modelling, conducted to assess the likely effects of a similar fire occurring in-flight, predicted that the increased rate of convective cooling, from the external airflow and lower air temperatures, would substantially reduce the progression of such a fire.

22) Boeing's structural loads modelling, based on the predicted damage from the thermal modelling of an in-flight ELT fire, predicted that the fuselage would remain capable of carrying flight loads but might experience a depressurisation if the damage were extensive.

Fire detection and firefighting

23) The location of the ELT in the fuselage crown made it difficult for the Heathrow Airport RFFS to locate the source of the fire.

24) At the time of the incident, the published ARFF information for the B787 did not indicate the location of ELT battery and the Heathrow Airport RFFS were not aware that there was a lithium-metal battery above the ceiling panels that could be the source of the fire.

25) In the event of an in-flight ELT battery fire, detecting the fire and locating its source would be challenging for cabin crew, due to the inaccessible location of the ELT in the cabin.

26) In the event of an in-flight ELT battery fire, fighting the ELT fire and any subsequent structural fire would be challenging for cabin crew due to the inaccessible location of the ELT in the cabin.

Toxicity

27) It has not been possible to determine accurately the composition and quantity of the combustion products produced by the structural fire.

Aircraft certification aspects

28) At the time of the B787 certification the ELT battery was not identified as a possible ignition source close to the aircraft skin, so the composite flammability tests did not take this into account as a specific source of ignition.

© Crown Copyright 2015

(b) Causal factors

The following causal factors were identified in the ground fire:

a) A thermal runaway failure of the lithium manganese dioxide battery in the ELT resulted in the uncontrolled release of stored energy within the battery cells.

b) The location and orientation of the ELT, and the compromised seal on the battery cover-plate, allowed the resulting hot gas, flames and battery decomposition products to impinge directly on the aircraft's composite fuselage structure, providing sufficient thermal energy to initiate a fire in the rear fuselage crown.

c) The resin in the composite material provided fuel for the fire, allowing a slow-burning fire to become established in the fuselage crown, which continued to propagate from the ELT location even after the energy from the battery thermal runaway was exhausted.

d) The Navigation Radio System safety assessment conducted in support of the ELT certification did not identify any ELT battery failure modes which could represent a hazard to the aircraft and therefore these failure modes were not mitigated in the ELT design or the B787 ELT installation.

The following factors most likely contributed to the thermal runaway of the ELT battery:

a) The trapped ELT battery wires created a short-circuit condition, providing a current path for an unplanned discharge of the ELT battery.

b) The ELT battery may have exhibited an unbalanced discharge response, resulting in the early depletion of a single cell which experienced a voltage reversal, leading to a thermal runaway failure.

c) The Positive Temperature Coefficient protective device in the battery did not provide the level of external short-circuit protection intended in the design.

© Crown Copyright 2015

d) There was no evidence that the reset behaviour and the implications of the variable switching point of the PTC, had been fully taken into account during the design of the ELT battery.

e) The absence of cell segregation features in the battery or ELT design meant the single-cell thermal runaway failure was able to propagate rapidly to the remaining cells.

© Crown Copyright 2015

4 Safety Recommendations

4.1 Safety Recommendation 2013-016 issued on 18 July 2013

Safety Recommendation 2013-016: It is recommended that the Federal Aviation Administration initiate action for making inert the Honeywell International RESCU 406AFN fixed Emergency Locator Transmitter system in Boeing 787 aircraft until appropriate airworthiness actions can be completed.

In response to Safety Recommendation 2013-016, the FAA issued Airworthiness Directive (AD) 2013-15-07 on 26 July 2013 requiring, within 10 days, either the removal, or inspection and corrective action as necessary, of Honeywell RESCU 406AFN ELTs installed on B787-8 aircraft[1].

Honeywell subsequently issued an Alert Service Bulletin (SB) instructing operators of all aircraft types equipped with specified RESCU 406AF / AFN ELTs, to perform an inspection of the ELT and its battery and to correct any anomalies. Embodiment of this SB was mandated by Transport Canada AD CF-2013-25 issued 15 Aug 2013 and FAA AD 2013-18-09 issued 18 September 2013.

This Safety Recommendation has been assessed by the AAIB as '*Adequate – Closed*'.

4.2 Safety Recommendation 2013-017 issued on 18 July 2013

Safety Recommendation 2013-017: It is recommended that the Federal Aviation Administration, in association with other regulatory authorities, conduct a safety review of installations of lithium-powered Emergency Locator Transmitter systems in other aircraft types and, where appropriate, initiate airworthiness action.

In April 2014 the FAA provided the following response:

> *'The FAA is currently conducting a safety review of Lithium-powered ELT systems with other regulatory authorities to identify any unsafe conditions in other aircraft types. The FAA expects to provide an update on the status of the safety review by March 31 2015.'*

This Safety Recommendation has been assessed by the AAIB as '*Adequate – Closed*'.

[1] On 26 July 2013 the European Aviation Safety Agency (EASA) issued AD 2013-0168, with the same intent.

4.3 Safety Recommendations 2014-020 to 2014-024

The following Safety Recommendations were issued on 18 June 2014.

Safety Recommendations 2014-020: It is recommended that the Federal Aviation Administration develop enhanced certification requirements for the use of lithium-metal batteries in aviation equipment, to take account of current industry knowledge on the design, operational characteristics and failure modes of lithium-metal batteries.

Safety Recommendation 2014-021: It is recommended that the Federal Aviation Administration require that electrical performance and design-abuse certification tests for lithium-metal batteries are conducted with the battery installed in the parent equipment, to take account of battery thermal performance.

Safety Recommendation 2014-022: It is recommended that the Federal Aviation Administration work with industry to determine the best methods to force a lithium-metal cell into thermal runaway and develop design-abuse testing that subjects a single cell within a lithium-metal battery to thermal runaway in order to demonstrate the worst possible effects during certification testing.

Safety Recommendation 2014-023: It is recommended that the Federal Aviation Administration require equipment manufacturers wishing to use lithium-metal batteries to demonstrate (using the design-abuse testing described in Safety Recommendation 2014-022) that the battery and equipment design mitigates all hazardous effects of propagation of a single-cell thermal runaway to other cells and the release of electrolyte, fire or explosive debris.

Safety Recommendation 2014-024: It is recommended that the Federal Aviation Administration review whether the Technical Standard Order (TSO) process is the most effective means for the certification of lithium-metal batteries installed in aircraft equipment, the actual performance of which can only be verified when demonstrated in the parent equipment and the aircraft installation.

As of June 2015, final response from the FAA is awaited for Safety Recommendations 2014-020 to 024. However, in a letter dated 31 October 2014, the FAA provided the following interim comment in respect of Safety Recommendation 2014-022:

© Crown Copyright 2015

> *'We plan to request that the Radio Technical Commission for Aeronautics (RTCA) task Special Committee 225, 'Rechargeable Lithium Batteries and Battery Systems', to revise and update RTCA Document DO-227, 'Minimum Operational Performance Standards for Lithium Batteries', for non-rechargeable lithium metal batteries. The revision would include methods to force lithium metal cells into thermal runaway and develop design abuse testing that would subject a single cell within a lithium metal battery to thermal runaway conditions.*
>
> *The tasking would include exploring the mitigation of the worst possible effects of this condition during certification testing. We plan to include evaluation criteria to ascertain pass/fail criteria under these conditions.'*

In the same correspondence, the FAA provided the following interim comment in respect of Safety Recommendation 2014-024:

> *'We believe a Technical Standard order (TSO) is effective in approving the design and production of an article to meet the Minimum Performance Standards. A TSO alone is not sufficient for certification approval. In order to complete a certification of a lithium metal battery installed in aircraft equipment, an airworthiness regulation approval is required. The airworthiness regulation must be complied with during Type certification, and Supplemental Type certification (including their respective amendments).*
>
> *I believe the FAA has effectively addressed Safety Recommendation [2014-024] and we do not plan any further action.'*

4.4 Safety Recommendations 2015-014 to 2015-021

The following additional Safety Recommendations are made in this report:

Safety Recommendation 2015-014: It is recommended that the Federal Aviation Administration, in conjunction with the European Aviation Safety Agency and Transport Canada, conduct an assessment of the circuit protection offered by the existing Honeywell RESCU 406AF and 406AFN ELT battery, to determine whether the ELT/battery design incorporates an acceptable level of circuit protection to mitigate against external short-circuits and unbalanced discharge.

Safety Recommendation 2015-015: It is recommended that the Federal Aviation Administration, in conjunction with the European Aviation Safety Agency and Transport Canada, conduct a review of installed aircraft equipment on transport category aircraft powered by lithium-metal batteries, which have been approved under TSO-C142 /C142A or by equivalent means, to ensure that the design of such batteries incorporates an acceptable level of circuit protection to mitigate against known failure modes including, but not limited to, external short-circuits and unbalanced discharge.

Safety Recommendation 2015-016: It is recommended that the Federal Aviation Administration, in conjunction with the European Aviation Safety Agency and Transport Canada, require equipment manufacturers intending to use lithium-metal batteries in aircraft equipment to demonstrate that the battery design incorporates an acceptable level of circuit protection to mitigate against known failure modes including, but not limited to, external short-circuits and unbalanced discharge.

Safety Recommendation 2015-017: It is recommended that the Federal Aviation Administration, in conjunction with the European Aviation Safety Agency and Transport Canada, require equipment manufacturers intending to use lithium-metal batteries in aircraft equipment, to quantify the heat produced by the battery over a range of discharge conditions and demonstrate that the battery and equipment design can adequately dissipate the heat produced.

Safety Recommendation 2015-018: It is recommended that the Federal Aviation Administration, in conjunction with the European Aviation Safety Agency and Transport Canada, require the manufacturers of lithium-metal batteries and manufacturers of aircraft equipment powered by lithium-metal batteries, to conduct battery-level and equipment-level 'failure mode and effects analyses' to identify failure modes and their effects.

Safety Recommendation 2015-019: It is recommended that the Federal Aviation Administration, in conjunction with the European Aviation Safety Agency and Transport Canada, review all previously-approved aircraft equipment powered by lithium-metal batteries to determine whether they comply with the intent of the *'Toxic Gas Venting Precautions'* described in TSO-C142/ TSO-C142a Appendix 1.

Safety Recommendation 2015-020: It is recommended that the Federal Aviation Administration, in conjunction with the European Aviation Safety Agency and Transport Canada, review whether the *'Toxic Gas Venting Precautions'* described in TSO-C142/ TSO-C142a Appendix 1 should be applied to portable aircraft equipment powered by lithium-metal batteries.

© Crown Copyright 2015

Safety Recommendation 2015-021: It is recommended that Boeing expedite the modelling of the B787 Environmental Control System, to examine the distribution of the ELT battery combustion products through the aircraft cabin, and demonstrate the results of this modelling to the Federal Aviation Administration.

Appendix A

LR4-380F PTC SPECIFICATION

PolySwitch Resettable Devices
Strap Battery Devices

TE Circuit Protection, a pioneer of polymeric positive temperature coefficient (PPTC) resettable devices, offers several material platforms to help protect battery applications. Each of these material platforms offers different performance characteristics that allow the engineer greater design flexibility. PolySwitch devices for battery protection include SRP, LR4, VTP, VLP, VLR and MXP series, disc and special application strap devices.

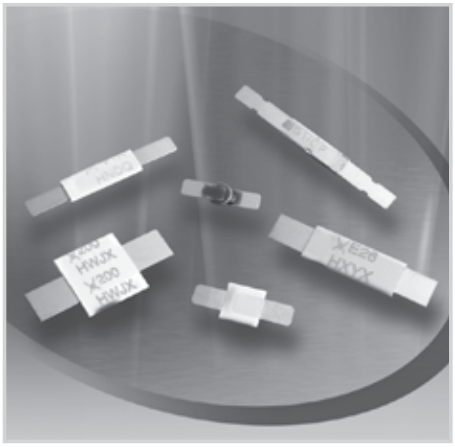

Benefits

- Many material platforms and device form factors help provide engineers more design flexibility
- Compatible with high-volume electronics assembly
- Assists in meeting regulatory requirements
- Low-resistance devices increase battery operating time

Features

- RoHS compliant
- Lead-free versions of all devices are available
- Broad range of resettable devices available
- Current ratings from 1.1A to 13A
- Voltage ratings from 6V to 30V
- Agency recognition: UL, CSA, TÜV
- Fast time-to-trip
- Low resistance

Applications

- Mobile phone and smart phone battery packs
- Tablet PC battery packs
- Mobile radio battery packs
- Computer battery packs
- Digital camera battery packs
- Portable media player battery packs
- Power tools (charge line)

RoHS Compliant, ELV Compliant

© Crown Copyright 2015

Appendix A (cont)

TE connectivity

Application Selection Guide for Strap Battery Devices

The guide below lists PolySwitch strap battery devices which are typically used in applications.
The following pages contain the specifications for the part numbers recommended below.
Once a device is selected, the user should evaluate and test each product for its intended application.

		PolySwitch Resettable Devices — Key Device Selection Criteria		
Protection Application	**Additional Comments**	**Installation Method**	**Lowest Resistance**	**Lowest Thermal Cut-off**
Mobile Phone Battery Packs	Li-ion	Surface-mount	Refer to Surface-mount Section of this Catalog	
		Prismatic	MXP370BD	VLR175F
Cordless Phone Battery Packs	NiMH	Cylindrical	VLP210F	—
			SRP175F	
Mobile Radio Battery Packs	NiMH	Cylindrical	LR4-380F	—
			SRP350F	
Computer Battery Packs	NiMH	Cylindrical	LR4-900F	—
	Li-ion	Cylindrical	LR4-1300SSF	—
		Prismatic	Consult Local Rep	Consult Local Rep
Camcorder Battery Packs	NiMH or Li-ion	Prismatic	VLP270F	VTP210GF
			LR4-380F	—
PDA Battery Packs	Li-ion	Prismatic	VLP220F	VLR175F
Power Tools (Charge Line)	NiCd, NiMH or Li-ion	Cylindrical	Custom LR4	Custom VTP

Table B1 Product Series: Current Rating, Voltage Rating / Typical Resistance for Strap Battery Devices

	VLR	VLP	VTP	MXP	SRP	LR4
	Typical Activation Temperature					
Hold Current (A)	**85°C**	**90°C**	**90°C**	**120°C**	**125°C**	**125°C**
1.10	—	—	16V/0.054Ω	—	—	—
1.20	—	16V/0.053Ω	—	—	15V/0.123Ω	—
1.70	12V/0.025Ω	—	16V/0.041Ω	—	—	—
1.75	12V/0.024Ω	16V/0.032Ω	16V/0.040Ω	—	15V/0.070Ω	—
1.80	—	—	—	6V/0.0105Ω	—	—
1.90	—	—	—	6V/0.011Ω	—	15V/0.056Ω
2.00	—	—	—	—	30V/0.045Ω	—
2.10	—	16V/0.024Ω	16V/0.024Ω	—	—	—
2.20	—	16V/0.023Ω	—	—	—	—
2.30	12V/0.015Ω	—	—	—	—	—
2.50	—	—	—	6V/0.011Ω	—	—
2.60	—	—	—	—	—	15V/0.031Ω
2.70	—	16V/0.015Ω	—	6V/0.0105Ω	—	—
3.10	—	—	—	6V/0.0075Ω	—	—
3.50	—	—	—	—	30V/0.024Ω	—
3.70	—	—	—	6V/0.007Ω	—	—
3.80	—	—	—	—	—	15V/0.020Ω
4.20	—	—	—	—	30V/0.018Ω	—
4.50	—	—	—	—	—	20V/0.016Ω
5.50	—	—	—	—	—	20V/0.013Ω
6.00	—	—	—	—	—	20V/0.011Ω
7.30	—	—	—	—	—	20V/0.009Ω
9.00	—	—	—	—	—	20V/0.008Ω
13.00	—	—	—	—	—	20V/0.006Ω

11

234 RoHS Compliant, ELV Compliant

Appendix A (cont)

Table B2 Thermal Derating for Strap Battery Devices [Hold Current (A) at Ambient Temperature (°C)]

Part Number	Maximum Ambient Temperature -40°C A	-20°C	0°C	20°C	25°C	40°C	50°C	60°C	70°C	80°C	85°C
85°C Typical Activation VLR*											
VLR170F	3.5	2.9	2.4	1.84	1.70	1.2	1.0	0.7	0.3	—	—
VLR175F	3.5	2.9	2.4	1.87	1.75	1.3	1.0	0.8	0.3	—	—
VLR175LF	3.5	2.9	2.4	1.87	1.75	1.3	1.0	0.8	0.3	—	—
VLR230F	5.0	4.2	3.4	2.52	2.30	1.7	1.3	0.9	0.4	—	—
90°C Typical Activation VLP*											
VLP120UF	2.4	2.1	1.8	1.30	1.20	1.0	0.7	0.6	0.3	0.2	0.1
VLP175UAF	3.2	2.7	2.3	1.70	1.75	1.2	1.0	0.9	0.5	0.2	0.1
VLP210F	4.3	3.6	2.9	2.31	2.10	1.6	1.3	1.0	0.6	0.3	0.1
VLP220F	4.5	3.8	3.0	2.45	2.20	1.7	1.4	1.1	0.7	0.3	0.1
VLP270F	5.6	4.7	4.0	3.05	2.70	2.2	1.7	1.4	0.9	0.4	0.1
VTP*											
VTP110F	2.0	1.7	1.4	1.12	1.10	0.85	0.75	0.7	0.4	0.2	0.1
VTP170F	3.2	2.7	2.2	1.80	1.70	1.3	1.0	0.8	0.5	0.3	0.1
VTP170XSF	3.2	2.7	2.2	1.80	1.70	1.3	1.0	0.8	0.5	0.3	0.1
VTP175F	3.2	2.7	2.2	1.84	1.75	1.3	1.0	0.8	0.5	0.3	0.1
VTP175LF	3.2	2.7	2.2	1.84	1.75	1.3	1.0	0.8	0.5	0.3	0.1
VTP210GF	4.1	3.5	2.9	2.26	2.10	1.6	1.3	1.0	0.7	0.4	0.1
VTP210SF	4.1	3.5	2.9	2.26	2.10	1.6	1.3	1.0	0.7	0.4	0.1

Part Number	Maximum Ambient Temperature -40°C A	-20°C	0°C	20°C	25°C	40°C	50°C	60°C	70°C	75°C	80°C	85°C	90°C
120°C Typical Activation MXP*													
MXP180	-	-	2.45	-	1.8	-	-	0.80	-	-	-	-	-
MXP190BB	-	-	2.6	-	1.9	-	-	0.85	-	-	-	-	-
MXP250K	-	-	3.6	-	2.5	-	-	1.3	-	-	-	-	-
MXP270	-	-	3.8	-	2.7	-	-	1.4	-	-	-	-	0.3
MXP310	-	-	5.0	-	3.1	-	-	1.9	-	1.0	-	-	-
MXP370BD	-	-	5.0	-	3.7	-	-	1.9	-	-	-	-	-

Part Number	Maximum Ambient Temperature -40°C A	-20°C	0°C	20°C	25°C	40°C	50°C	60°C	70°C	80°C	85°C
125°C Typical Activation SRP											
SRP120F	1.9	1.7	1.5	1.20	1.17	1.0	0.9	0.8	0.6	0.5	0.4
SRP175F	2.5	2.2	2.0	1.75	1.68	1.4	1.3	1.2	1.0	0.9	0.8
SRP200F	3.1	2.8	2.5	2.00	1.97	1.7	1.5	1.4	1.2	1.0	0.9
SRP350F	5.3	4.8	4.3	3.50	3.44	3.0	2.7	2.5	2.1	1.8	1.7
SRP420F	6.3	5.7	5.1	4.20	4.11	3.6	3.3	3.0	2.6	2.2	2.1
LR4											
LR4-190F	2.8	2.5	2.3	1.9	1.86	1.6	1.5	1.4	1.2	1.1	1.0
LR4-260F	3.8	3.4	3.1	2.6	2.54	2.2	2.0	1.9	1.7	1.4	1.3
LR4-380F	5.4	4.9	4.4	3.8	3.64	3.3	3.0	2.8	2.5	2.3	2.1
LR4-380XF	5.4	4.9	4.4	3.8	3.64	3.3	3.0	2.8	2.5	2.3	2.1
LR4-450F	6.5	5.8	5.3	4.5	4.38	3.9	3.6	3.3	2.9	2.6	2.4
LR4-550F	7.6	6.9	6.2	5.5	5.32	4.7	4.3	4.0	3.6	3.2	3.0
LR4-600F	8.7	7.8	7.1	6.0	5.86	5.2	4.7	4.4	3.9	3.4	3.2
LR4-600XF	8.7	7.8	7.1	6.0	5.86	5.2	4.7	4.4	3.9	3.4	3.2
LR4-730F	10.5	9.5	8.6	7.3	7.13	6.3	5.7	5.4	4.7	4.2	4.0
LR4-900F	12.7	11.4	10.0	9.0	8.50	7.5	6.8	6.2	5.5	4.9	4.5
LR4-1300SSF	17.9	16.2	14.5	13.0	12.40	11.1	10.3	9.5	8.6	7.7	7.2

* Product electrical characteristics determined at 25°C.

RoHS Compliant, ELV Compliant

© Crown Copyright 2015

Appendix A (cont)

TE connectivity

Figure B1 Thermal Derating Curve for Strap Battery Devices

A = LR4
B = SRP
C = VTP, VLP, MXP
D = VLR

Figure B1

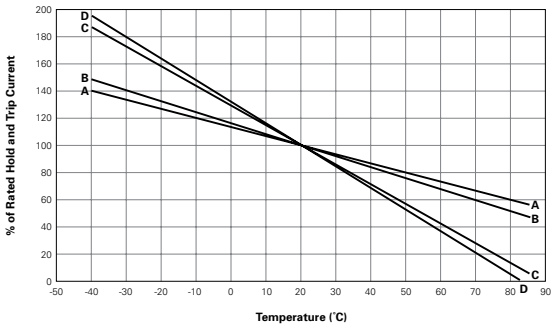

Table B3 Electrical Characteristics for Strap Battery Devices

Part Number	I_H (A)	I_T (A)	V_{MAX} (V_{DC})	I_{MAX} (A)	$P_{D\ MAX}$ (W)	Max Time-to-trip (A)	Max Time-to-trip (s)	R_{MIN} (Ω)	R_{MAX} (Ω)	R_{1MAX} (Ω)	Figure for Dimension
85°C Typical Activation VLR*											
VLR170F	1.70	4.1	12	100	1.4	8.50	5.0	0.018	0.032	0.064	B3
VLR175F	1.75	4.2	12	100	1.4	8.75	5.0	0.017	0.031	0.062	B3
VLR175LF	1.75	4.2	12	100	1.4	8.75	5.0	0.017	0.031	0.062	B3
VLR230F	2.30	5.0	12	100	2.5	10.00	5.0	0.012	0.018	0.036	B3
90°C Typical Activation VLP*											
VLP120UF	1.20	3.6	16	60	1.6	7.00	5.0	0.039	0.067	0.134	B5
VLP175UAF	1.75	3.9	16	60	1.8	8.75	5.0	0.023	0.041	0.082	B5
VLP210F	2.10	5.0	16	60	1.8	10.50	5.0	0.018	0.030	0.060	B2
VLP220F	2.20	5.3	16	60	1.8	11.00	5.0	0.017	0.029	0.058	B3
VLP270F	2.70	6.5	16	60	2.5	13.50	5.0	0.012	0.018	0.036	B3
VTP*											
VTP110F	1.10	2.7	16	100	1.3	5.50	5.0	0.038	0.070	0.140	B5
VTP170F	1.70	3.4	16	100	1.4	8.50	5.0	0.030	0.052	0.105	B2
VTP170XSF	1.70	3.4	16	100	1.4	8.50	5.0	0.030	0.052	0.105	B4
VTP175F	1.75	3.6	16	100	1.4	8.75	5.0	0.029	0.051	0.102	B3
VTP175LF	1.75	3.6	16	100	1.4	8.75	5.0	0.029	0.051	0.102	B3
VTP210GF	2.10	4.7	16	100	1.5	10.00	5.0	0.018	0.030	0.060	B3
VTP210SF	2.10	4.7	16	100	1.5	10.00	5.0	0.018	0.030	0.060	B4
120°C Typical Activation MXP*											
MXP180	1.80	5.2	6	50	1.0	9.00	5.0	0.007	0.014	0.024	B10
MXP190BB	1.90	4.9	6	50	1.0	9.50	2.0	0.007	0.015	0.024	B9
MXP250K	2.50	6.2	6	50	1.0	13.50	2.0	0.006	0.016	0.028	B10
MXP270	2.70	6.2	6	50	1.0	13.50	2.0	0.006	0.015	0.026	B10
MXP310	3.10	9.0	6	50	1.3	17.50	5.0	0.003	0.012	0.018	B10
MXP370BD	3.70	9.0	6	50	1.3	18.50	5.0	0.004	0.010	0.016	B10

* Product electrical characteristics determined at 25°C.

11

RoHS Compliant, ELV Compliant

© Crown Copyright 2015

Appendix A (cont)

Table B3 Electrical Characteristics for Strap Battery Devices Cont'd

Part Number	I_H (A)	I_T (A)	V_{MAX} (V_{DC})	I_{MAX} (A)	$P_{D\ MAX}$ (W)	Max Time-to-trip (A)	Max Time-to-trip (s)	R_{MIN} (Ω)	R_{MAX} (Ω)	R_{1MAX} (Ω)	Figure for Dimensions
125˚C Typical Activation SRP											
SRP120F	1.20	2.7	15	100	1.2	6.00	5.0	0.085	0.160	0.220	B6
SRP175F	1.75	3.8	15	100	1.5	8.75	5.0	0.050	0.090	0.120	B6
SRP200F	2.00	4.4	30	100	1.9	10.00	4.0	0.030	0.060	0.100	B6
SRP350F	3.50	6.3	30	100	2.5	20.00	3.0	0.017	0.031	0.050	B6
SRP420F	4.20	7.6	30	100	2.9	20.00	6.0	0.012	0.024	0.040	B6
LR4											
LR4-190F	1.90	3.9	15	100	1.2	9.5	5.0	0.0390	0.0720	0.102	B7
LR4-260F	2.60	5.8	15	100	2.5	13.0	5.0	0.0200	0.0420	0.063	B7
LR4-380F	3.80	8.3	15	100	2.5	19.0	5.0	0.0130	0.0260	0.037	B7
LR4-380XF	3.80	8.3	15	100	2.5	19.0	5.0	0.0130	0.0260	0.037	B7
LR4-450F	4.50	8.9	20	100	2.3	22.5	5.0	0.0110	0.0200	0.028	B7
LR4-550F	5.50	10.5	20	100	2.8	27.5	5.0	0.0090	0.0160	0.022	B7
LR4-600F	6.00	11.7	20	100	2.8	30.0	5.0	0.0070	0.0140	0.019	B7
LR4-600XF	6.00	11.7	20	100	2.8	30.0	5.0	0.0075	0.0140	0.019	B7
LR4-730F	7.30	14.1	20	100	3.3	30.0	5.0	0.0060	0.0120	0.015	B7
LR4-900F	9.00	16.7	20	100	3.8	45.0	5.0	0.0060	0.0100	0.014	B7
LR4-1300SSF	13.00	21.2	20	100	4.5	50.0	10.0	0.0035	0.0065	0.009	B8

* Product electrical characteristics determined at 25°C.

Notes:

I_H : Hold current: maximum current device will pass without interruption in 20°C still air unless otherwise specified.
I_T : Trip current: minimum current that will switch the device from low-resistance to high-resistance in 20°C still air unless otherwise specified.
V_{MAX} : Maximum voltage device can withstand without damage at rated current.
I_{MAX} : Maximum fault current device can withstand without damage at rated voltage.
P_D : Power dissipated from device when in the tripped state in 20°C still air unless otherwise specified.
R_{MIN} : Minimum resistance of device as supplied at 20°C unless otherwise specified.
R_{MAX} : Maximum resistance of device as supplied at 20°C unless otherwise specified.
R_{1MAX} : Maximum resistance, measured at 20°C unless otherwise specified, of device one hour after being tripped the first time.

Figures B2-B10 Dimension Figures for Strap Battery Devices

Figure B2

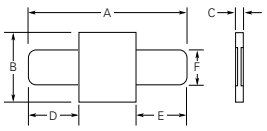

Figure B3

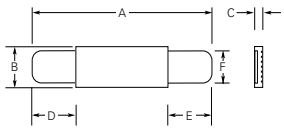

Figure B4

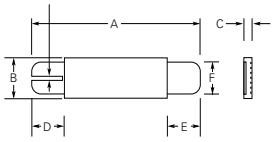

RoHS Compliant, ELV Compliant

© Crown Copyright 2015

Appendix A (cont)

Figures B2-B10 Dimension Figures for Strap Battery Devices Cont'd

Figure B5

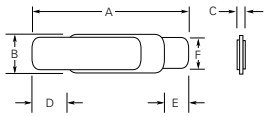

Figure B6

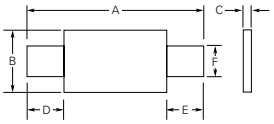

Figure B7

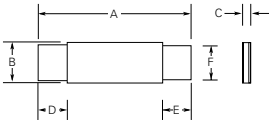

Figure B8

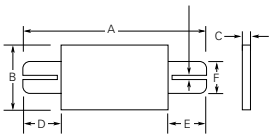

Figure B9

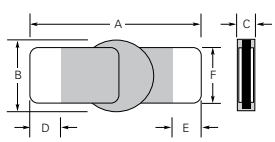

Figure B10

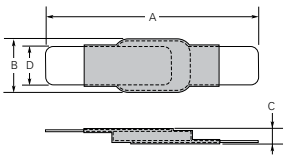

Table B4 Dimensions for Strap Battery Devices in Millimeters (Inches)

Part Number	A Min	A Max	B Min	B Max	C Min	C Max	D Min	D Max	E Min	E Max	F Min	F Max	Figure
85°C Typical Activation VLR													
VLR170F	20.8 (0.832)	23.2 (0.928)	3.5 (0.140)	3.9 (0.156)	— —	0.8 (0.032)	4.5 (0.180)	6.5 (0.260)	4.5 (0.180)	6.5 (0.260)	2.4 (0.096)	2.6 (0.104)	B3
VLR175F	23.0 (0.920)	24.5 (0.980)	2.9 (0.116)	3.3 (0.132)	0.5 (0.020)	0.8 (0.032)	4.7 (0.188)	7.2 (0.288)	3.8 (0.152)	5.4 (0.216)	2.4 (0.096)	2.6 (0.104)	B3
VLR175LF	29.3 (1.172)	31.7 (1.268)	2.9 (0.116)	3.3 (0.132)	— —	0.8 (0.032)	5.2 (0.208)	6.8 (0.272)	10 (0.400)	12.5 (0.500)	2.4 (0.096)	2.6 (0.104)	B3
VLR230F	20.9 (0.836)	23.1 (0.924)	4.9 (0.196)	5.3 (0.212)	— —	0.8 (0.032)	4.1 (0.164)	5.8 (0.232)	4.1 (0.164)	5.8 (0.232)	3.9 (0.156)	4.1 (0.164)	B3
90°C Typical Activation VLP													
VLP120UF	10.9 (0.430)	11.8 (0.460)	4.4 (0.170)	4.6 (0.180)	— —	0.7 (0.028)	5.5 (0.220)	6.5 (0.260)	1.65 (0.065)	1.9 (0.075)	2.3 (0.091)	2.5 (0.098)	B5
VLP175UAF	23.6 (0.944)	25.6 (1.024)	2.7 (0.108)	2.9 (0.116)	— —	0.7 (0.028)	7.0 (0.280)	8.0 (0.320)	7.0 (0.280)	8.0 (0.320)	2.3 (0.092)	2.5 (0.100)	B5
VLP210F	15.4 (0.616)	17.5 (0.700)	6.9 (0.276)	7.3 (0.292)	0.6 (0.024)	0.8 (0.032)	4.0 (0.160)	6.2 (0.248)	4.0 (0.160)	6.2 (0.248)	3.9 (0.156)	4.1 (0.164)	B2
VLP220F	21.1 (0.844)	23.3 (0.932)	3.5 (0.140)	3.9 (0.156)	0.6 (0.024)	0.8 (0.032)	5.1 (0.204)	6.8 (0.272)	5.1 (0.204)	6.8 (0.272)	2.9 (0.116)	3.1 (0.124)	B3
VLP270F	20.9 (0.836)	23.1 (0.924)	4.9 (0.196)	5.3 (0.212)	0.6 (0.024)	0.8 (0.032)	4.1 (0.164)	5.8 (0.232)	4.1 (0.164)	5.8 (0.232)	3.9 (0.156)	4.1 (0.164)	B3

11

© Crown Copyright 2015

Appendix A (cont)

Table B4 Dimensions for Strap Battery Devices in Millimeters (Inches) Cont'd

Part Number	A Min	A Max	B Min	B Max	C Min	C Max	D Min	D Max	E Min	E Max	F Min	F Max	Figure
VTP													
VTP110F	23.6 (0.944)	25.6 (1.024)	2.7 (0.108)	2.9 (0.116)	— —	0.7 (0.028)	7.0 (0.280)	8.0 (0.320)	7.0 (0.280)	8.0 (0.320)	2.3 (0.092)	2.5 (0.100)	B5
VTP170F	15.4 (0.616)	17.5 (0.700)	7.0 (0.280)	7.4 (0.296)	0.5 (0.020)	0.8 (0.032)	4.0 (0.160)	6.2 (0.248)	4.0 (0.160)	6.2 (0.248)	3.9 (0.156)	4.1 (0.164)	B2
VTP170XSF	20.9 (0.836)	22.9 (0.916)	4.9 (0.196)	5.3 (0.212)	0.5 (0.020)	0.8 (0.032)	6.0 (0.240)	8.6 (0.344)	6.0 (0.240)	8.6 (0.344)	3.9 (0.156)	4.1 (0.164)	B4
VTP175F	21.2 (0.848)	23.2 (0.928)	3.5 (0.140)	3.9 (0.156)	— —	0.8 (0.032)	4.6 (0.184)	6.6 (0.264)	4.6 (0.184)	6.6 (0.264)	2.9 (0.116)	3.1 (0.124)	B3
VTP175LF	25.8 (1.032)	28.2 (1.128)	3.5 (0.140)	3.9 (0.156)	— —	0.8 (0.032)	5.7 (0.228)	7.3 (0.292)	8.7 (0.348)	10.3 (0.412)	2.4 (0.096)	2.6 (0.104)	B3
VTP210GF	20.9 (0.836)	23.1 (0.924)	4.9 (0.196)	5.3 (0.212)	— —	0.8 (0.032)	4.1 (0.164)	5.8 (0.232)	4.1 (0.164)	5.8 (0.232)	3.9 (0.156)	4.1 (0.164)	B3
VTP210SF	20.9 (0.836)	23.1 (0.924)	4.9 (0.196)	5.3 (0.212)	0.6 (0.024)	0.8 (0.032)	4.1 (0.164)	5.8 (0.232)	4.1 (0.164)	5.8 (0.232)	3.9 (0.156)	4.1 (0.164)	B4
120°C Typical Activation MXP													
MXP180	9.4 (0.37)	10.0 (0.39)	2.3 (0.09)	2.6 (0.10)	0.7 (0.02)	1.1 (0.04)	1.9 (0.07)	2.1 (0.08)	— —	— —	— —	— —	B10
MXP190BB	9.2 (0.36)	10.8 (0.43)	2.96 (0.12)	3.26 (0.13)	0.7 (0.03)	1.1 (0.04)	1.6 (0.06)	3.1 (0.12)	1.6 (0.06)	3.1 (0.12)	2.2 (0.09)	2.4 (0.10)	B9
MXP250K	11.75 (0.46)	12.35 (0.49)	2.3 (0.09)	2.7 (0.11)	0.7 (0.03)	1.1 (0.04)	2.4 (0.09)	2.6 (0.10)	— —	— —	— —	— —	B10
MXP270	10.3 (0.40)	11.5 (0.45)	2.3 (0.09)	2.7 (0.10)	0.7 (0.02)	1.1 (0.04)	2.1 (0.08)	— —	2.1 (0.08)	— —	1.9 (0.07)	2.1 (0.08)	B9
MXP310	14.5 (0.57)	16.5 (0.65)	2.96 (0.11)	3.26 (0.13)	0.65 (0.03)	0.95 (0.04)	4.6 (0.18)	— —	4.6 (0.18)	— —	2.2 (0.09)	2.4 (0.10)	B9
MXP370BD	10.5 (0.41)	11.3 (0.44)	2.96 (0.11)	3.26 (0.12)	0.7 (0.02)	1.1 (0.04)	2.0 (0.07)	— —	2.0 (0.07)	— —	2.2 (0.08)	2.4 0.09)	B9
125°C Typical Activation SRP													
SRP120F	19.9 (0.796)	22.1 (0.884)	4.9 (0.196)	5.2 (0.208)	0.6 (0.024)	1.0 (0.040)	5.5 (0.220)	7.5 (0.300)	5.5 (0.220)	7.5 (0.300)	3.9 (0.156)	4.1 (0.164)	B6
SRP175F	20.9 (0.836)	23.1 (0.924)	4.9 (0.196)	5.2 (0.208)	0.6 (0.024)	1.0 (0.040)	4.1 (0.164)	5.5 (0.220)	4.1 (0.164)	5.5 (0.220)	3.9 (0.156)	4.1 (0.164)	B6
SRP200F	21.3 (0.852)	23.4 (0.936)	10.2 (0.408)	11.0 (0.440)	0.5 (0.020)	1.1 (0.044)	5.0 (0.200)	7.6 (0.304)	5.0 (0.200)	7.6 (0.304)	4.8 (0.192)	5.4 (0.216)	B6
SRP350F	28.4 (1.136)	31.8 (1.272)	13.0 (0.520)	13.5 (0.540)	0.5 (0.020)	1.1 (0.044)	6.3 (0.252)	8.9 (0.356)	6.3 (0.252)	8.9 (0.356)	6.0 (0.240)	6.6 (0.264)	B6
SRP420F	30.6 (1.224)	32.4 (1.296)	12.9 (0.516)	13.6 (0.544)	0.5 (0.020)	1.1 (0.044)	5.0 (0.200)	7.5 (0.300)	5.0 (0.200)	7.5 (0.300)	6.0 (0.240)	6.7 (0.268)	B6

RoHS Compliant, ELV Compliant

© Crown Copyright 2015

Appendix A (cont)

Table B4 Dimensions for Strap Battery Devices in Millimeters (Inches) Cont'd

Part Number	A Min	A Max	B Min	B Max	C Min	C Max	D Min	D Max	E Min	E Max	F Min	F Max	Figure
LR4													
LR4-190F	19.9 (0.796)	22.1 (0.884)	4.9 (0.196)	5.5 (0.220)	0.6 (0.024)	1.0 (0.040)	5.5 (0.220)	7.5 (0.300)	5.5 (0.220)	7.5 (0.300)	3.9 (0.156)	4.1 (0.164)	B7
LR4-260F	20.9 (0.836)	23.1 (0.924)	4.9 (0.196)	5.5 (0.220)	0.6 (0.024)	1.0 (0.040)	4.1 (0.164)	5.5 (0.220)	4.1 (0.164)	5.5 (0.220)	3.9 (0.156)	4.1 (0.164)	B7
LR4-380F	24.0 (0.960)	26.0 (1.040)	6.9 (0.276)	7.5 (0.300)	0.6 (0.024)	1.0 (0.040)	4.1 (0.164)	5.5 (0.220)	4.1 (0.164)	5.5 (0.220)	4.9 (0.196)	5.1 (0.204)	B7
LR4-380XF	32.2 (1.288)	35.8 (1.432)	4.9 (0.196)	5.5 (0.220)	0.6 (0.024)	1.0 (0.040)	5.5 (0.220)	7.5 (0.300)	5.5 (0.220)	7.5 (0.300)	3.9 (0.156)	4.1 (0.164)	B7
LR4-450F	24.0 (0.960)	26 (1.040)	9.9 (0.396)	10.5 (0.420)	0.6 (0.024)	1.0 (0.040)	5.3 (0.212)	6.7 (0.268)	5.3 (0.212)	6.7 (0.268)	5.9 (0.236)	6.1 (0.244)	B7
LR4-550F	35.0 (1.400)	37.0 (1.480)	6.9 (0.276)	7.5 (0.300)	0.6 (0.024)	1.0 (0.040)	5.3 (0.212)	6.7 (0.268)	5.3 (0.212)	6.7 (0.268)	4.9 (0.196)	5.1 (0.204)	B7
LR4-600F	24.0 (0.960)	26.0 (1.040)	13.9 (0.556)	14.5 (0.580)	0.6 (0.024)	1.0 (0.040)	4.1 (0.164)	5.5 (0.220)	4.1 (0.164)	5.5 (0.220)	5.9 (0.236)	6.1 (0.244)	B7
LR4-600XF	40.5 (1.620)	42.7 (1.708)	6.9 (0.276)	7.5 (0.300)	0.6 (0.024)	1.0 (0.040)	5.2 (0.208)	6.8 (0.272)	5.2 (0.208)	6.8 (0.272)	4.9 (0.196)	5.1 (0.204)	B7
LR4-730F	27.1 (1.084)	29.1 (1.164)	13.9 (0.556)	14.5 (0.580)	0.6 (0.024)	1.0 (0.040)	4.1 (0.164)	5.5 (0.220)	4.1 (0.164)	5.5 (0.220)	5.9 (0.236)	6.1 (0.244)	B7
LR4-900F	45.4 (1.816)	47.6 (1.904)	7.9 (0.316)	8.5 (0.340)	0.9 (0.036)	1.3 (0.052)	4.6 (0.184)	6.2 (0.248)	4.6 (0.184)	6.2 (0.248)	5.9 (0.236)	6.1 (0.244)	B7
LR4-1300SSF	61.5 (2.460)	66.5 (2.660)	9.4 (0.376)	10.0 (0.400)	0.9 (0.036)	1.3 (0.052)	5.0 (0.200)	7.5 (0.300)	5.0 (0.200)	7.5 (0.300)	5.9 (0.236)	6.1 (0.244)	B8

Figures B11-B16 Typical Time-to-Trip Curves at 20°C for Strap Battery Devices

VLR (data at 25°C)
A = VLR170F
B = VLR175F
C = VLR230F

Figure B11

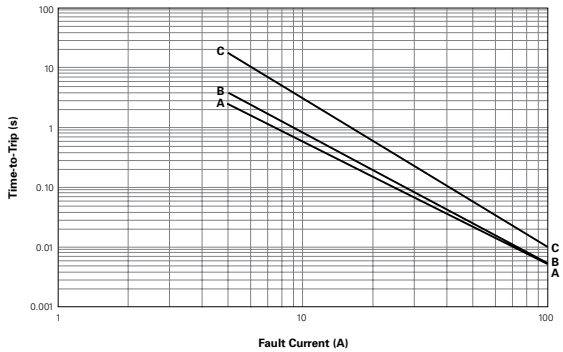

11

240 RoHS Compliant, ELV Compliant

© Crown Copyright 2015

Appendix A (cont)

Figures B11-B16 Typical Time-to-Trip Curves at 20°C for Strap Battery Devices Cont'd

VLP (data at 25°C)
A = VLP120UF
B = VLP175UAF
C = VLP210F
D = VLP220F
E = VLP270F

Figure B12

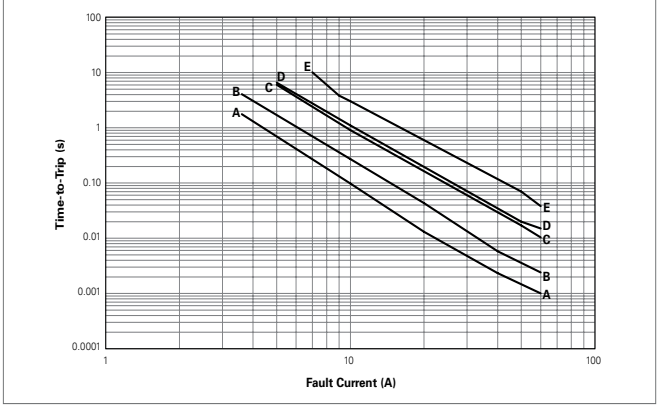

VTP (data at 25°C)
A = VTP110F
B = VTP170F
C = VTP175F
D = VTP210GF

Figure B13

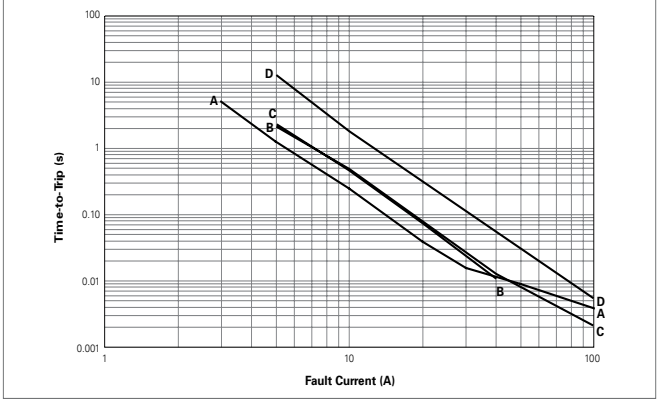

MXP (data at 25°C)
A = MXP180
B = MXP190BB
C = MXP250K
D = MXP270
E = MXP310
F = MXP370BD

Figure B14

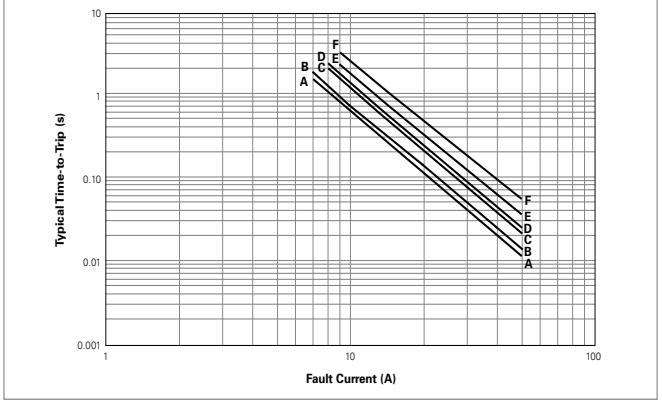

RoHS Compliant, ELV Compliant

11

241

Appendix A (cont)

Figures B11-B16 Typical Time-to-Trip Curves at 20°C for Strap Battery Devices Cont'd

SRP

A = SRP120F
B = SRP175F
C = SRP200F
D = SRP350F
E = SRP420F

Figure B15

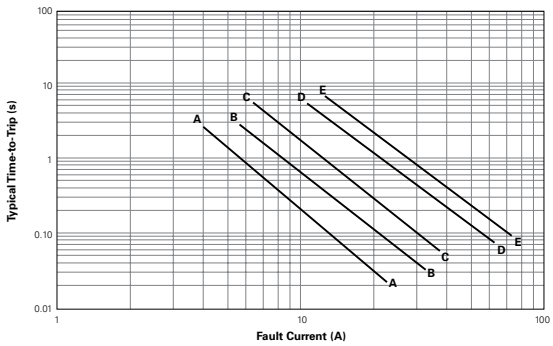

LR4

A = LR4-190F
B = LR4-260F
C = LR4-380F
D = LR4-450F
E = LR4-550F
F = LR4-600F
G = LR4-730F
H = LR4-900F
I = LR4-1300SSF

Figure B16

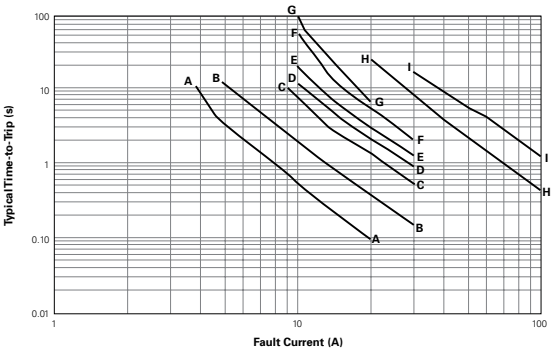

Table B5 Physical Characteristics and Environmental Specifications for Strap Battery Devices

VLR

Physical Characteristics

Lead Material	0.125mm Nominal Thickness, Quarter-hard Nickel
Tape Material	Polyester

Environmental Specifications

Test	Conditions	Resistance Change
Passive Aging	-40°C, 1000 hrs	±5% typ
	60°C, 1000 hrs	±20% typ
Humidity Aging	60°C/95% RH, 1000 hrs	±30% typ
Thermal Shock	85°C, -40°C (10 Times)	±5% typ
Vibration	MIL-STD-883D, Method 2026	No Change

242 RoHS Compliant, ELV Compliant

© Crown Copyright 2015

Appendix A (cont)

Table B5 Physical Characteristics and Environmental Specifications for Strap Battery Devices Cont'd

VLP and VTP

Physical Characteristics

Lead Material	0.125mm Nominal Thickness, Quarter-hard Nickel
Tape Material	Polyester

Environmental Specifications

Test	Conditions	Resistance Change
Passive Aging	-40°C, 1000 hrs	±5% typ
	60°C, 1000 hrs	±10% typ
Humidity Aging	60°C/95% RH, 1000 hrs	±10% typ
Thermal Shock	85°C, -40°C (10 Times)	±5% typ
Vibration	MIL-STD-883D, Method 2026	No Change

MXP

Physical Characteristics

Lead Material	0.1mm Nominal Thickness,Half-hard Nickel
Coating Material	Epoxy

Environmental Specifications

Test	Conditions	Resistance Change
Passive Aging	-40°C, 1000 hrs	±5% typ
	60°C, 1000 hrs	±20% typ
Humidity Aging	60°C/95% RH, 1000 hrs	±30% typ
Thermal Shock	85°C, -40°C (10 Times)	±5% typ
Vibration	MIL-STD-883D, Method 2026	No Change

SRP

Physical Characteristics

Lead Material	0.125mm Nominal Thickness, Quarter-hard Nickel
Tape Material	Polyester

Environmental Specifications

Test	Conditions	Resistance Change
Passive Aging	70°C, 1000 hrs	±10% typ
Humidity Aging	85°C/85% RH, 7 Days	±5% typ
Vibration	MIL-STD-883C, Test Condition A	No Change

LR4

Physical Characteristics

Lead Material	0.125mm Nominal Thickness, Quarter-hard Nickel
Tape Material	Polyester

Environmental Specifications

Test	Conditions	Resistance Change
Passive Aging	70°C, 1000 hrs	±10% typ
Humidity Aging	85°C/85% RH, 7 Days	±5% typ
Vibration	MIL-STD-883D, Method 2026	No Change

Note: Storage conditions: 40°C max., 70% RH max.; devices should remain in original sealed bags prior to use. Devices may not meet specified values if these storage conditions are exceeded.

RoHS Compliant, ELV Compliant

© Crown Copyright 2015

Appendix A (cont)

TE connectivity

Table B6 Packaging and Marking Information/Agency Recognition for Strap Battery Devices

Part Number	Bag Quantity	Tape and Reel Quantity	Standard Package Quantity	Part Marking	Agency Recognition
85°C Typical Activation VLR					
VLR170F	1,000	—	10,000	R17	UL, CSA,TÜV
VLR175F	1,000	—	10,000	R1X	UL, CSA,TÜV
VLR175LF	1,000	—	10,000	R1X	UL, CSA,TÜV
VLR230F	1,000	—	10,000	R23	UL, CSA,TÜV
90°C Typical Activation VLP					
VLP120UF	1,000	—	10,000	—	UL, CSA, TÜV
VLP175UAF	1,000	—	10,000	—	UL, CSA, TÜV
VLP210F	1,000	—	10,000	W21	UL, CSA, TÜV
VLP220F	1,000	—	10,000	W22	UL, CSA, TÜV
VLP270F	1,000	—	10,000	W27	UL, CSA, TÜV
VTP					
VTP110F	1,000	—	10,000	—	UL, CSA, TÜV
VTP170F	1,000	—	10,000	V17	UL, CSA, TÜV
VTP170XSF	1,000	—	10,000	V17	UL, CSA, TÜV
VTP175F	1,000	—	10,000	V1X	UL, CSA, TÜV
VTP175LF	1,000	—	10,000	V1X	UL, CSA, TÜV
VTP210GF	1,000	—	10,000	V21	UL, CSA, TÜV
VTP210SF	1,000	—	10,000	V21	UL, CSA, TÜV
120°C Typical Activation MXP					
MXP180	2,000	—	4,000	—	UL, CSA, TÜV
MXP190BB	4,000	—	8,000	—	UL, CSA, TÜV
MXP250K	2,000	—	4,000	—	UL, CSA, TÜV
MXP270	2,000	—	4,000	—	UL
MXP310	2,000	—	4,000	—	UL
MXP370BD	2,000	—	4,000	—	UL, CSA, TÜV
125°C Typical Activation SRP					
SRP120F	1,000	—	10,000	120	UL, CSA, TÜV
SRP175F	2,000	—	10,000	175	UL, CSA, TÜV
SRP200F	1,000	—	10,000	200	UL, CSA, TÜV
SRP350F	500	—	10,000	350	UL, CSA, TÜV
SRP420F	500	—	10,000	420	UL, CSA, TÜV
LR4					
LR4-190F	2,000	—	10,000	E19	UL, CSA, TÜV
LR4-260F	1,000	—	10,000	E26	UL, CSA, TÜV
LR4-380F	1,000	—	10,000	E38	UL, CSA, TÜV
LR4-380XF	1,000	—	10,000	E38	UL, CSA, TÜV
LR4-450F	1,000	—	10,000	E45	UL, CSA, TÜV
LR4-550F	1,000	—	10,000	E55	UL, CSA, TÜV
LR4-600F	1,000	—	10,000	E60	UL, CSA, TÜV
LR4-600XF	1,000	—	10,000	E60	UL, CSA, TÜV
LR4-730F	1,000	—	10,000	E73	UL, CSA, TÜV
LR4-900F	500	—	10,000	E90	UL, CSA, TÜV
LR4-1300SSF	250	—	10,000	EX3	UL, CSA, TÜV

11

RoHS Compliant, ELV Compliant

© Crown Copyright 2015

Appendix A (cont)

Agency Recognition for Strap Battery Devices

UL	File # E74889
CSA	File # 78165C
TÜV	Certificate Number Available on Request

Installation Guidelines for the Strap Family

- PPTC devices operate by thermal expansion of the conductive polymer. If devices are placed under pressure or installed in spaces that would prevent thermal expansion, they may not properly protect against damage caused by fault conditions. Designs must be selected in such a manner that adequate space is maintained over the life of the product.
- Twisting, bending, or placing the PPTC device in tension will decrease the ability of the device to protect against damage caused by electrical faults. No residual force should remain on device after installation. Mechanical damage to the PPTC device may affect device performance and should be avoided.
- Chemical contamination of PPTC devices should be avoided. Certain greases, solvents, hydraulic fluids, fuels, industrial cleaning agents, volatile components of adhesives, silicones, and electrolytes can have an adverse effect on device performance.
- PPTC strap devices are intended to be resistance welded to battery cells or to pack interconnect straps, yet some precautions must be taken when doing so. In order for the PPTC device to exhibit its specified performance, weld placement should be a minimum of 2mm from the edge of the PPTC device, weld splatter must not touch the PPTC device, and welding conditions must not heat the PPTC device above its maximum operating temperature.
- PPTC strap devices are not intended for applications where reflow onto flex circuits or rigid circuit boards is required.
- The polyester tape on PPTC strap devices is intended for marking and identification purposes only, not for electrical insulation.
- The coating on MXP devices is intended to prevent oxidization/aging of the devices. Damaging the coating or causing the coating to delaminate can have negative effects on device performance and should be avoided.
- MXP devices have a small PPTC chip size and therefore have weaker peel strength between the polymer and Ni-foil of the chip. Excessive mechanical force to the device may cause delamination of Ni-foil from the polymer.

Part Numbering System for Strap Battery Devices

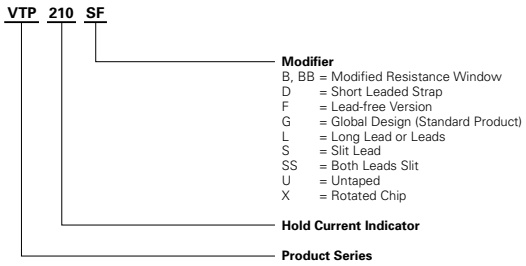

⚠ Warning :

- Users should independently evaluate the suitability of and test each product selected for their own application.
- Operation beyond the maximum ratings or improper use may result in device damage and possible electrical arcing and flame.
- These devices are intended for protection against damage caused by occasional overcurrent or overtemperature fault conditions and should not be used when repeated fault conditions or prolonged trip events are anticipated.
- Contamination of the PPTC material with certain silicone-based oils or some aggressive solvents can adversely impact the performance of the devices.
- Device performance can be impacted negatively if devices are handled in a manner inconsistent with recommended electronic, thermal, and mechanical procedures for electronic components.
- PPTC devices are not recommended for installation in applications where the device is constrained such that its PTC properties are inhibited, for example in rigid potting materials or in rigid housings, which lack adequate clearance to accommodate device expansion.
- Operation in circuits with a large inductance can generate a circuit voltage (Ldi/dt) above the rated voltage of the device.

RoHS Compliant, ELV Compliant

© Crown Copyright 2015

Appendix B

CALORIMETER TEST RESULTS

(i) Specific Heat Capacity Test

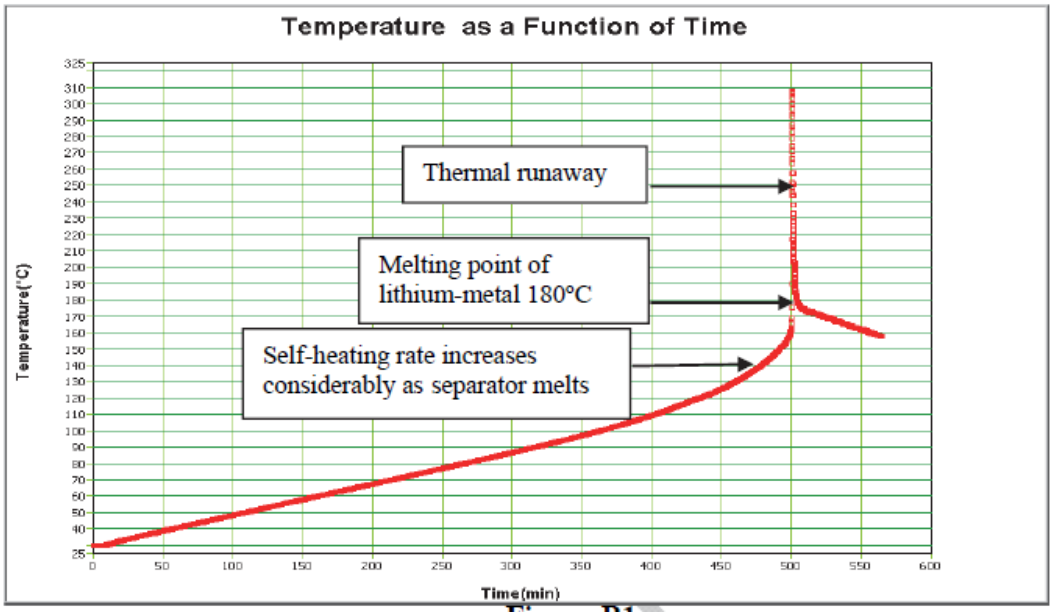

Figure B1

Temperature (°C) versus time (min) for Specific Heat Capacity Test

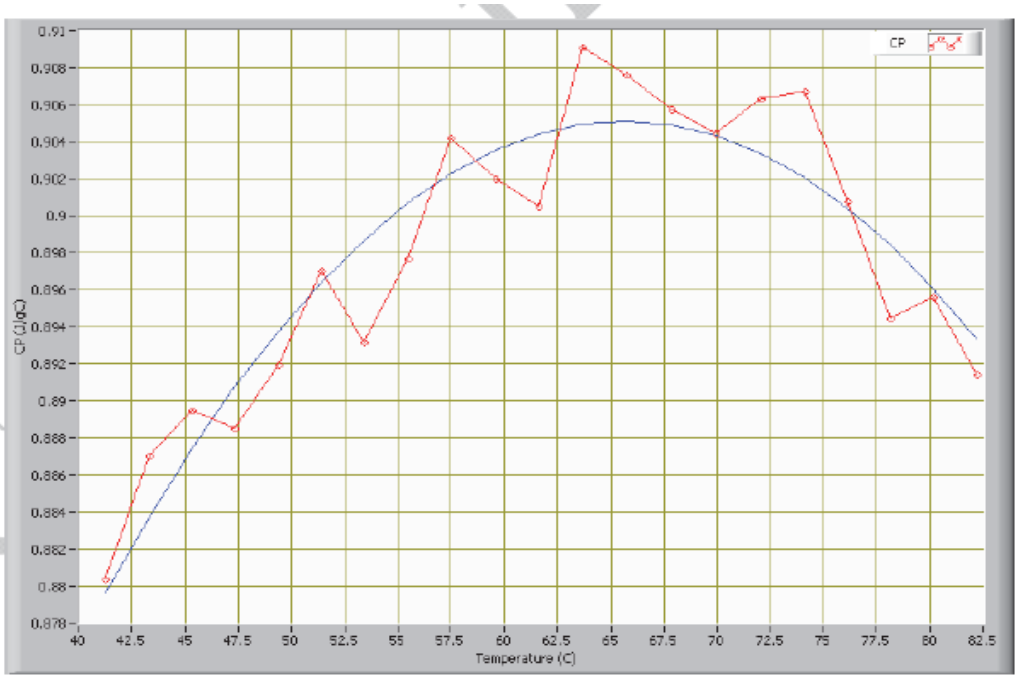

Figure B2

Specific Heat Capacity (Cp) vs temperature (°C)

© Crown Copyright 2015

Appendix B (cont)

(ii) Battery discharge tests – Test 1

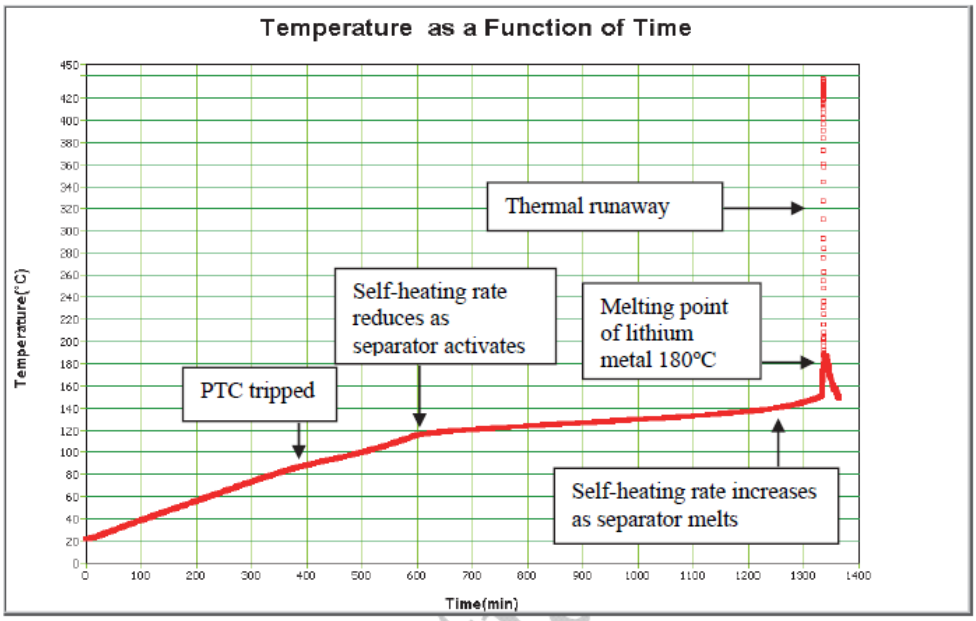

Figure B3

Temperature (°C) versus time (min) for Battery Discharge Test 1

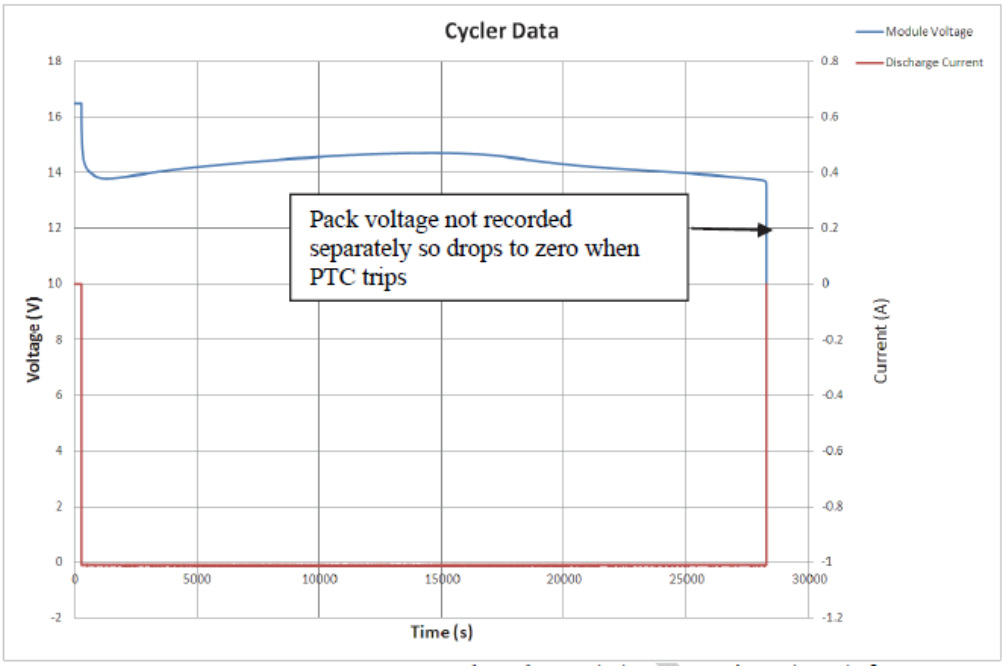

Figure B4

Battery pack voltage (V) versus time (secs) for Battery Discharge Test 1

© Crown Copyright 2015

Appendix B (cont)

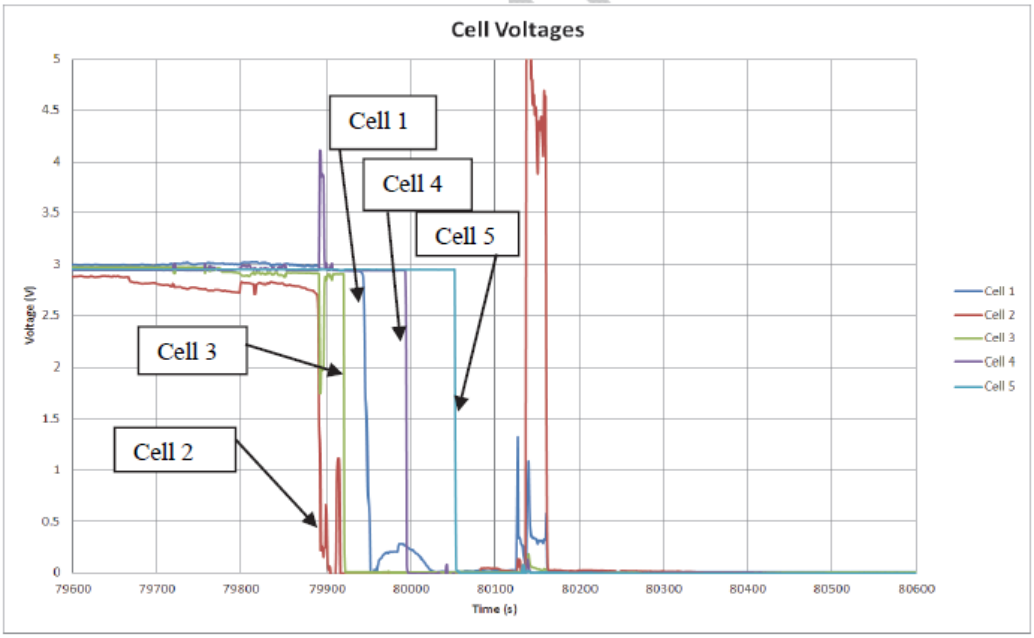

Figure B5

Cell voltages (V) versus time (secs) for Battery Discharge Test 1, expanded view

iii) Battery discharge tests – Test 2

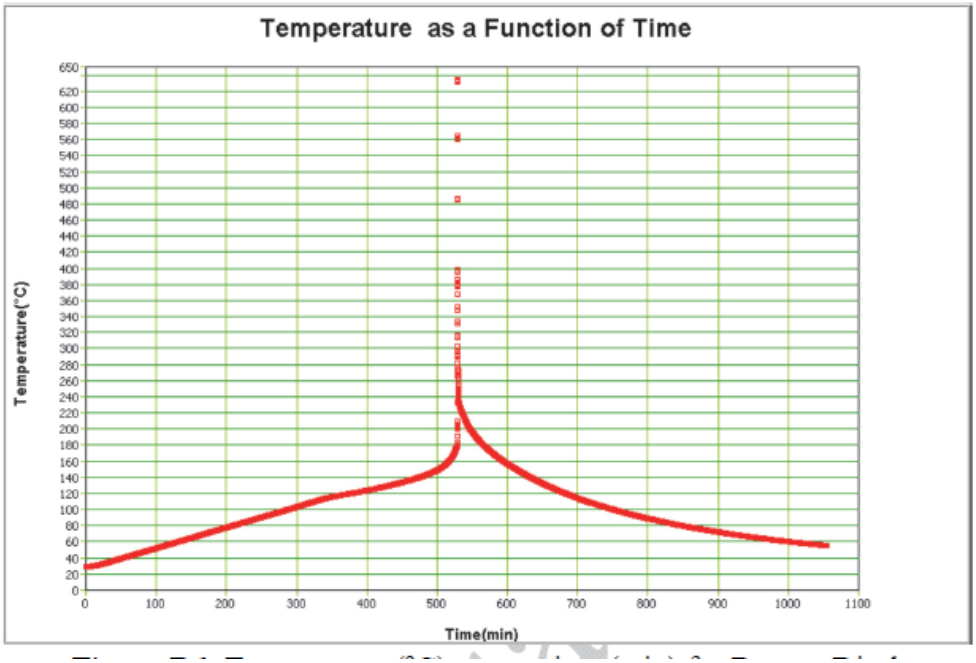

Figure B6

Temperature (°C) versus time (min) for Battery Discharge Test 2

© Crown Copyright 2015

Appendix B (cont)

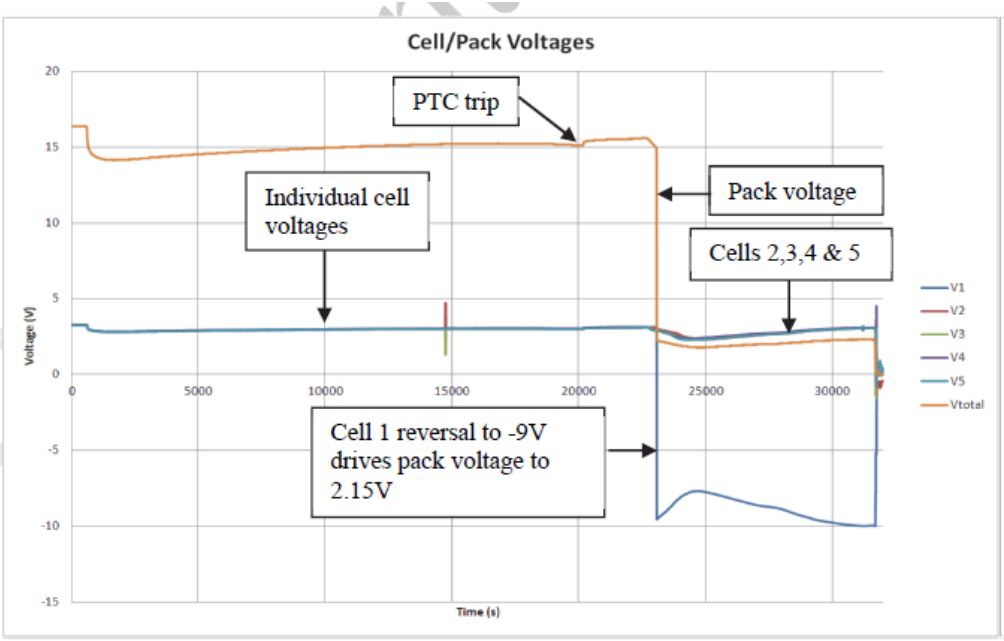

Figure B7

Cell and pack voltages (V) versus time (secs) for Battery Discharge Test 2

(iv) Battery discharge tests – Test 3

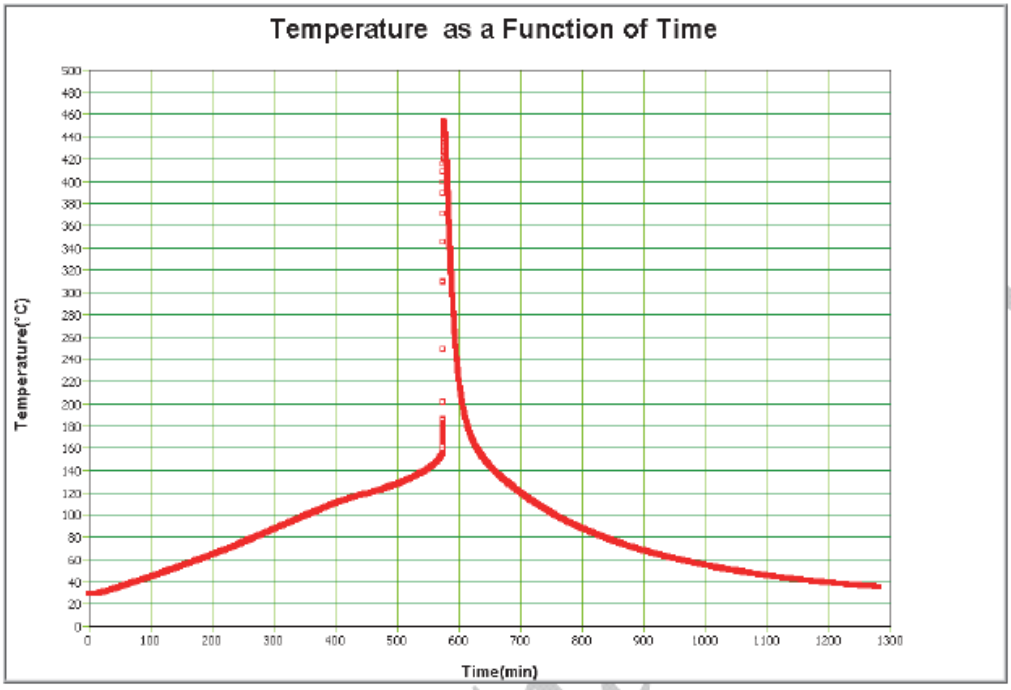

Figure B8

Temperature (°C) versus time (min) for Battery Discharge Test 3

© Crown Copyright 2015

Appendix B (cont)

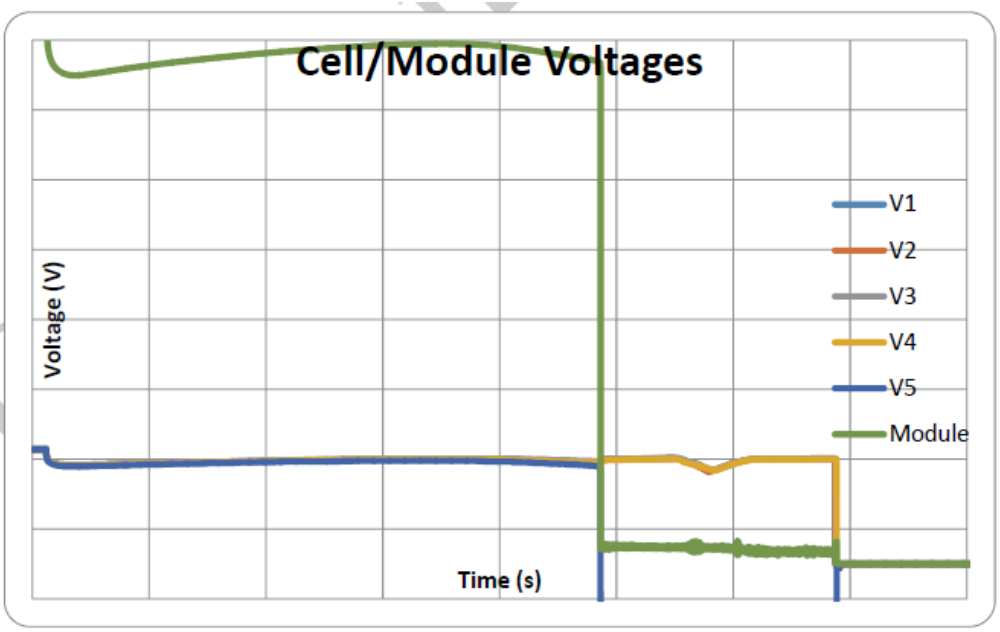

Figure B9

Cell and pack voltages (V) versus time (secs) for Battery Discharge Test 3

(v) Battery discharge tests – Comparison between Discharge Test 1, 2 and 3

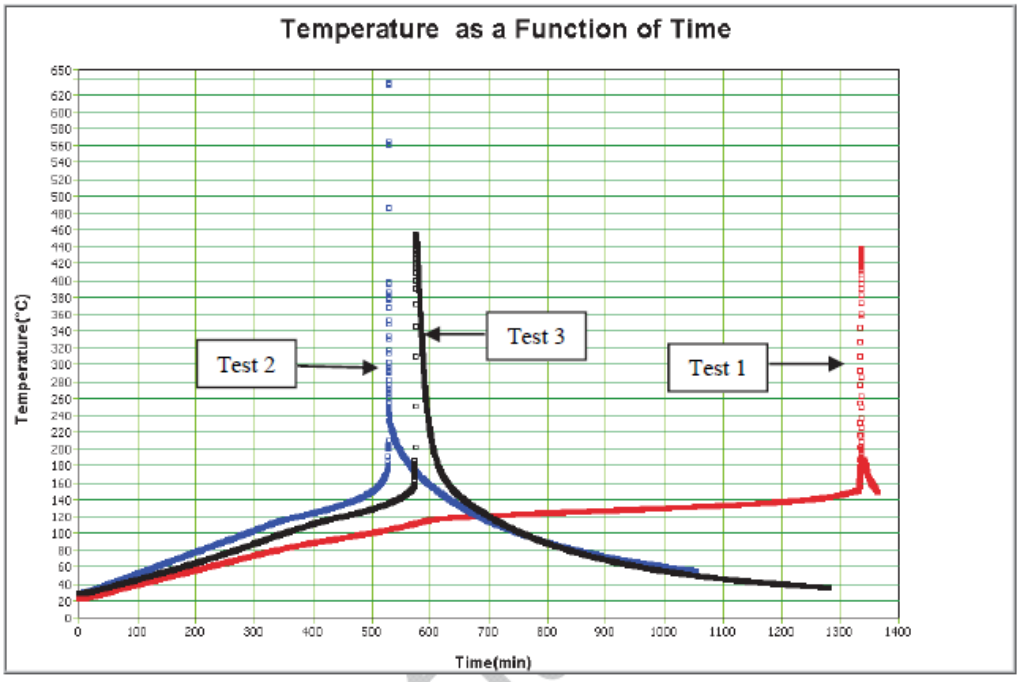

Figure B10

Temperature (°C) versus time (min) for Battery discharge Tests 1, 2 and 3

© Crown Copyright 2015

Appendix B (cont)

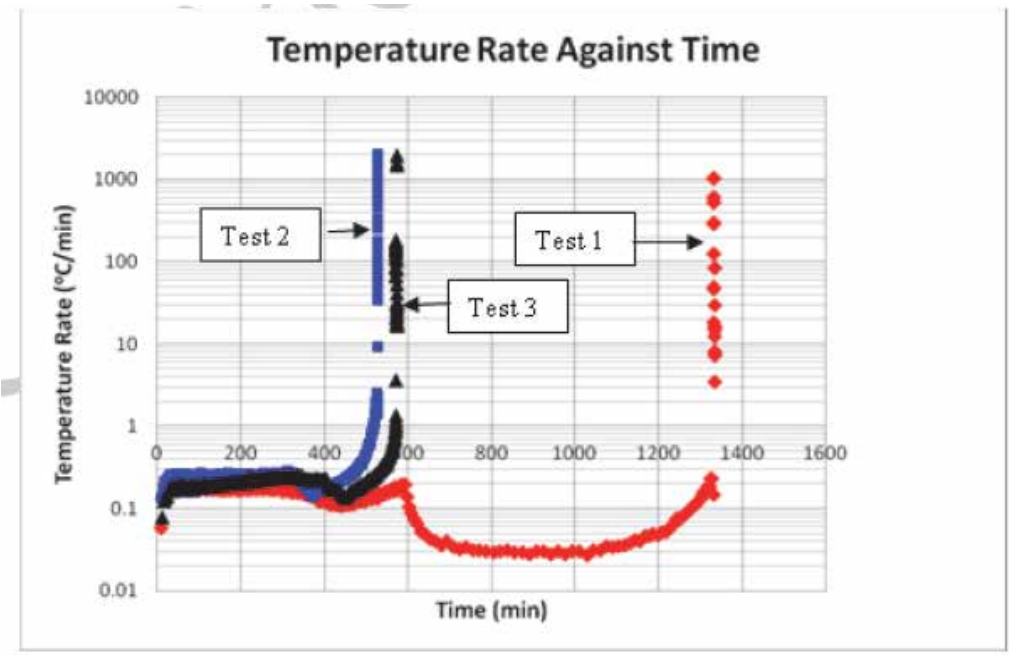

Figure B11

Temperature rate (°C/min) versus time (min) for Battery discharge Tests 1, 2 and 3

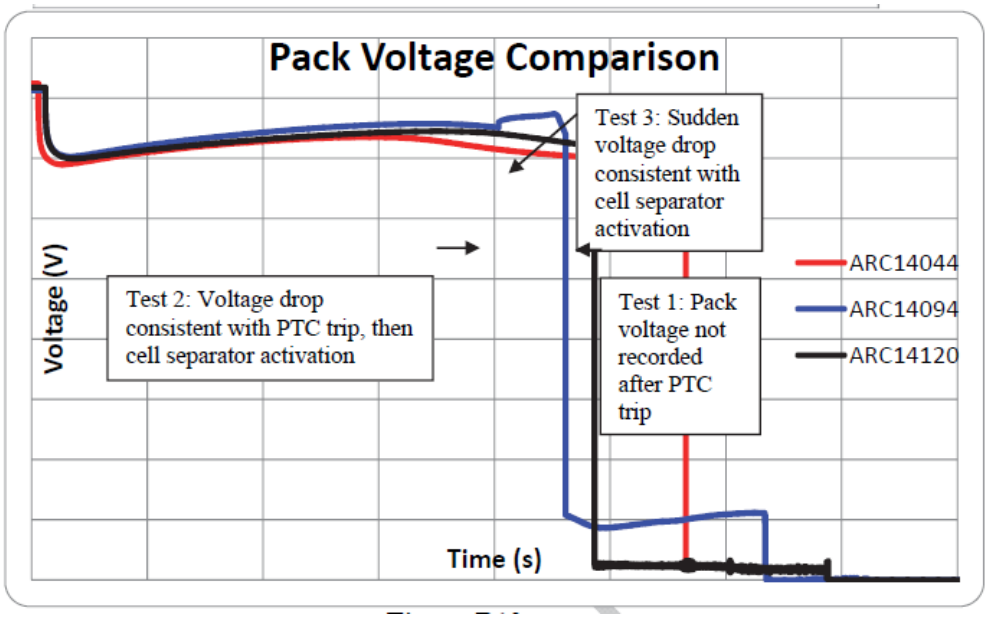

Figure B12

Battery pack voltage (V) versus time (secs) for Battery discharge Tests 1, 2 and 3

© Crown Copyright 2015

Appendix B (cont)

(vi) ELT Battery thermal and electrical performance

From the results of the specific heat capacity and discharge tests it is possible to determine the thermal energy (or enthalpy) and the electrical energy generated by the battery during discharge. This provides an indication of the heat dissipation requirements of the battery. Also understanding the relationship between the thermal and electrical energy provides an indication of battery efficiency.

Enthalpy

In order to calculate the enthalpy (ΔH) in Joules (J) arising from heating during the battery discharge test, under normal conditions up to 80°C, the following formula is used:

$$\Delta H = m \times Cp \times \Delta T$$

Where *m* is the mass of the battery in grams (g) weighed before the calorimeter test, *Cp* is the specific heat capacity of the cells in Joules per gram Kelvin (J/gK) determined in the calorimeter and ΔT is the adiabatic temperature rise resulting from the 1 Amp discharge in Kelvin (K).

Electrical energy

In order to calculate the electrical energy ΔG generated during the discharge the following formula is used:

$$\Delta G = V \times I \times \Delta t$$

Where *V* is the average voltage during the discharge, *I* is the average discharge current in Amps during the discharge and Δt is the discharge time in seconds (up to 80°C).

Efficiency

The battery efficiency can be expressed in terms of enthalpy and electrical energy as follows:

$$\text{Efficiency} = \Delta G / \Delta H + \Delta G * 100\ \%$$

© Crown Copyright 2015

Appendix B (cont)

Efficiency results for discharge Test 1, 2 and 3 up to 80°C

	Discharge Test 1	Discharge Test 2	Discharge Test 3
ΔT[1]	80-22.25 = **57.75 °C**	80-29.836 = **50.164 °C**	80-29.30 = **50.70 °C**
Cp[2] @ 50°C	0.894 J/gK	0.894 J/gK	0.894 J/gK
m	596g	596g	596g
ΔH	57.75 * 0.894 * 596 = **30.8 kJ**	50.164 * 0.894 * 596 = **26.7 kJ**	50.70 * 0.894 * 596 = **27.0 kJ**
V	14.41 V	14.57 V	14.58 V
I	1.011 A	1.010 A	1.013 A
ΔG	14.41 * 1.011 * 60 * 334.5 = **292.4 kJ**	14.57 * 1.010 * 60 * 199[4] = **175.7 kJ**	14.58 * 1.013 * 60 * 258[4] = **228.8 kJ**
Eff.	292.4 /323.0 * 100 = **90.5 %**	175.7/202.4 * 100 = **86.8 %**	228.8/255.8 * 100 = **89.4 %**
Capacity	1.011 * 5.58 = **5.64 Ah**	1.010 * 5.44 = **5.49 Ah**	1.013 * 6.59 = **6.68 Ah**
dT/dt_{max}[3]	0.215°C/min	0.293°C/min	0.273°C/min
P_{max}[4]	0.215/60 * 0.894 * 596 = **1.81 W**	0.293/60 * 0.894 * 596 = **2.60 W**	0.273/60 * 0.894 * 596 = **2.42 W**

Where:

1. ΔT is the temperature change between the start of the discharge and 80°C (above this point chemical reactions contribute to cell heating)

2. Cp is the Specific Heat Capacity of the cells at 50°C (approximate mid temperature range) determined from the Specific Heat Capacity Test

3. dT/dt_{max} is the maximum heating rate up to 80°C

4. P_{max} is the heat in Watts (W) generated by the battery

© Crown Copyright 2015

Unless otherwise indicated, recommendations in this report are addressed to the appropriate regulatory authorities having responsibility for the matters with which the recommendation is concerned. It is for those authorities to decide what action is taken. In the United Kingdom the responsible authority is the Civil Aviation Authority, CAA House, 45-49 Kingsway, London WC2B 6TE or the European Aviation Safety Agency, Postfach 10 12 53, D-50452 Koeln, Germany.